Universität für Bodenkultur Wien

Physical Protein Degradation Mechanisms: Fundamentals for the Design of Small-Scale Models for Formulation, Fill and Finish Operations of Biopharmaceuticals

Dissertation zur Erlangung des Doktorgrades an der Universität für Bodenkultur Wien

Department für Biotechnologie

Institut für angewandte Mikrobiologie

Vorstand: Reingard Grabherr, Ao. Univ. Prof. Dipl.-Ing. Dr. rer. nat.

Betreuer: Rainer Hahn, Assoc. Prof. Dipl.-Ing. Dr. nat. techn.

Eingereicht von **Lukas Brückl, Dipl.-Ing.**

Wien, Oktober 2016

DANKSAGUNG

Ganz herzlich bedanken möchte ich mich bei Corinna Sonderegger, stellvertretend für die Firma Sandoz, welche mir die Möglichkeit für diese eng mit der Industrie verbundene Arbeit geöffnet hat. Corinna, Du hast mir nicht nur freie Hand bei der Gestaltung der Dissertation gelassen, sondern hast auch immer den Überblick über das Projekt bewahrt, konstruktive Ideen eingebracht und mich mit deiner unglaublich schnellen Auffassungsgabe und gründlich durchdachten sowie zeitgerechten Reviews überrascht. Danke!

Weiters bin ich allen Kollegen bei Sandoz dankbar für die vielen Diskussionen und Anregungen. Besonders erwähnen möchte ich hier Thomas Schröder, der mich vor allem am Anfang unterstützt hat, Reinhard Schipflinger, der mein Leben durch pragmatisch einfache Lösungen und seine unzähligen Kontakte vereinfacht hat, sowie Mauro Sergi, der (un)gemein kritische Fragen Stellen konnte und relevante Faktoren von Nebensächlichkeiten in der Planung zu unterscheiden wusste. Zu tiefstem Dank verpflichtet bin ich Stefan Scheler, der viele Stunden seiner Zeit in Diskussionen mit mir investiert hat. Stefan, Du hast mir nicht nur Hilfe beim Verfassen der Publikationen geleistet und viele Ideen im Zuge unserer Unterhaltungen geliefert, sondern Du hast mir vor allem mit deinem persönlichen Interesse an der Arbeit gezeigt, dass man auch als Industrieangestellter die Wissenschaft und Forschung nicht unbedingt aus den Augen verlieren muss. Danke dafür!

Danken will ich auch Prof. Rainer Hahn, der als mein Betreuer an der Universität immer das Telefon griffbereit hatte und mir wissenschaftliche Unterstützung bei unseren Besprechungen in Wien leistete. Danke für deine Zeit!

Ein herzliches Dankeschön für die Unterstützung möchte ich auch zur biophysikalischen Charakterisierungsgruppe nach Oberhaching senden, insbesondere an Otmar Hainzl, Alexander Bepperling, Andreas Hoffmann und Kerstin Grassl.

Ein besonderer Dank gilt meiner Freundin Agnes, welche nie an mir gezweifelt hat und mir das „harte Leben in den Bergen“ versüßt hat.

Schlussendlich möchte ich noch meinen Eltern danken, welche mich auf meinem Lebensweg immer unterstützt haben.

Danke!

ZUSAMMENFASSUNG

Am Ende der Produktion von Biopharmazeutika befinden sich Formulierungs-, Füll- und Endschritte. Im Zuge dieser Prozesse treten verschiedene Stressfaktoren auf. Im Falle einer nicht ausreichenden Stabilität des Wirkstoffes im Formulierungspuffer oder eines nicht optimierten Herstellungsprozesses kann die Produktqualität negativ beeinflusst werden. Die Durchführung von Experimenten für Formulierungsentwicklung, Prozessentwicklung, Optimierung oder Charakterisierung ist aufgrund von großen Arbeitsvolumina und Kapazitätslimitierungen meist nicht im Produktionsmaßstab möglich. Daraus ergibt sich die Notwendigkeit, die Produktion in Form von Modellen im kleinen Maßstab nachzubilden, wodurch Experimente im Labormaßstab durchgeführt werden können. Im Zuge dieser Arbeit wurden potentielle prozessbedingte Stressfaktoren ermittelt und ihre Auswirkung auf therapeutisch genutzte Proteine untersucht. Dabei wurde gezeigt, dass der Effekt von Scherung auf Proteine in freier Lösung vernachlässigt werden kann. Weiters wurde der Abtrag von adsorbierten Proteinen als vorherrschender Mechanismus für Partikelbildung in Reibungsbereichen identifiziert. Anhand dieser Erkenntnisse wurde ein Modell im kleinen Maßstab etabliert, mit dessen Hilfe Formulierungen bezüglich reibungsinduzierter Proteinschädigung unter extremen Bedingungen untersucht werden können. Schließlich wurde ein Miniaturmodell eines Ansatzkessels aus der Produktion entworfen. Dabei wurde ein spezielles Design gewählt, welches es ermöglicht, qualitätsrelevante Einflussfaktoren der Produktion im kleinen Maßstab zu simulieren.

ABSTRACT

At the end of the various manufacturing steps of biopharmaceuticals are the formulation, fill and finish operations. During these steps, various stress factors can occur, which might have a negative impact on the quality of the final drug product administered to the patient, in case the active ingredient is not stable enough in its formulation buffer or if the manufacturing process is not optimized. It is not feasible to perform all experiments for formulation development, process development, optimization or characterization at production-scale due to high working volumes and capacity limitations. Thus, there is the need of so called small-scale models which enable to perform experiments at lab-scale. In the course of this work, potential production-related stress factors were identified and their impact on therapeutic proteins was evaluated. Thereby, it was shown that the effect of shear on proteins in free solution was negligible. Furthermore, abrasion of adsorbed proteins was identified as predominant mechanism during friction-related particle formation. Based on these findings, a worst-case small-scale model for friction-related protein degradation was established that can be used as a tool for formulation screening. Finally, a miniaturized full-scale model of a compounding vessel from production was developed, which was designed to simulate at small-scale the impact on product quality during production.

TABLE OF CONTENTS

INTRODUCTION

1. The Importance of Biopharmaceuticals

In the mid-1970s, a breakthrough in recombinant protein (rDNA) technology and molecular genetics paved the way for the innovation and development of many following recombinant biopharmaceuticals.[1] In 1982, the recombinant human insulin (Humulin®) was approved by drug regulatory agencies as the first biopharmaceutical in the United Kingdom, the Netherlands, West Germany and the United States.[2] Other eight products followed in the 80s including hormones, such as the recombinant human growth hormone (rhGH)[3], cytokines and antibodies. The emergence of monoclonal antibodies (mAbs), a more and more important and successful class of therapeutic biological drugs was enabled by the discovery of continuous culture of hybridoma cells, which secrete antibodies of predefined specificity.[4] Administration of early monoclonal antibodies caused immune responses in patients as they consist of purely murine sequences. Therefore, a second generation of mAbs was developed that is represented by chimeric or humanized antibodies, having reduced or no immunogenicity. Another advantage of the second generation mAbs is their ability to mediate Fc functions via their human Fc region, which was later also used in the generation of fusion proteins.[5] However, also changes to other classes of biopharmaceuticals were introduced to obtain a superior stability, pharmacokinetics or pharmacodynamics over the native protein. Such engineered proteins can be created for example by optimization of the amino acid sequence by site-directed mutagenesis.[5] Further development of biopharmaceuticals is still ongoing. Examples of so called next generation formats are antibody-drug conjugates (ADCs), where toxins are coupled to antibodies to ensure directed delivery, release and effect, or fully functional antibodies lacking light chains, which have been discovered in camels and llamas.[4]

Up to date, almost 400 recombinant produced proteins are approved as biopharmaceuticals with 1300 other candidates waiting in the pipelines of pharmaceutical companies around the world. In 2015, about 50 % of potentially new drugs were in pre-clinical and 33 % in the clinical trial stage.[6] Besides the therapeutic areas of metabolic disorders and hematological disorder, oncology has with 15 % the highest percentage of approved and marketed recombinant proteins. The market share of cancer drugs is currently growing, especially as there is a trend in approvals towards mAb-based products and oncology accounted roughly half of the sales of mAbs in 2010.[4,6] In general, mAbs and other recombinant proteins made up to 17 % of the global market for pharmaceuticals in 2010, which was a total of $597 billion.[7] Since then, the market value of

biopharmaceuticals has been steadily rising.[8] Humira®, the top selling biopharmaceutical generated a sale of $12.5 billion in the year 2014.[6]

The loss of patent protection of more and more first-generation innovator products now clears the way for "generic" substitutes for the original biologics. As inherently variable cell cultures are used during production of biologics or their substitutes, it is impossible to create an exact copy as it can be achieved in a defined chemical synthesis method of a small molecule drug. Thus, the substitutes are "*similar but not the same*" to the originator and are referred to as biosimilars.[9] The big advantage of these biosimilars is that they can be offered at a lower price due to reduced development effort and costs.[8] Omnitrope® (Sandoz GmbH), a recombinant human growth hormone, has gained the European marketing authorization within EU as the very first biosimilar product in the year 2006. Europe's first biosimilar mAb (infliximab, Celltrion, Inc. and Hospira, Inc.) was approved in the year 2013.[8] The first approval of a biosimilar in the US by the Food and Drug Administration (FDA) was achieved in 2015 by the biosimilar product filgrastim-sndz (Zarxio®, Sandoz GmbH).[10]

2. Manufacturing of Biopharmaceuticals

The production of a biopharmaceutical starts with so called upstream processes, where recombinant cell factories, such as bacteria, yeasts or mammalian cells, are used for the expression of the protein of interest.[6] In course of the following downstream processing steps the protein is initially harvested from the cell medium by centrifugation or cross-flow microfiltration. If the proteins are expressed in the cytoplasm, the cells have to be chemically or mechanically destructed. Subsequently, the protein is usually purified by a combination of chromatographic steps resulting in a removal of process related impurities such as host cell proteins, DNA, viruses or endotoxin and of product related impurities such as higher or lower molecular weight variants. Furthermore, viral clearance can be achieved by an additional filtration step and/or inactivation at low pH. Finally, the downstream steps are completed by an ultrafiltration/diafiltration step in which the active pharmaceutical ingredient is buffer exchanged and its concentration is adjusted to a predefined value.[11] The resulting highly pure solution of the active pharmaceutical ingredient is now called drug substance (DS).[12] In order to gain operational flexibility for the following processing steps, the drug substance is commonly frozen and stored at low temperatures until needed. During storage of the protein molecule in a frozen state product quality is maintained best. Degradation reactions are reduced

at low temperatures and diffusive collisions that could lead to aggregation of the product are minimized in a frozen matrix.[13]

The series of processing steps which are required to turn a purified drug substance into its final dosage form for the pharmaceutical market are called "formulation, fill and finish" operations (see Figure 1).[13] The formulation-fill-finish unit operations either begin with the freezing or the subsequent thawing of the drug substance, depending on what is defined as the starting point. Large scale freezing of bulk drug substance is performed in cryovessels, which can bring the disadvantage of cryoconcentration-related effects, such as crystallization of solutes or buffer salts or pH changes that could lead to aggregation of the product.[14] Alternatively, the drug substance can be aliquoted into disposable plastic bottles or bags, if a better heat transfer fluid temperature profile is needed. However, as plastic shows a different robustness, permeability, interaction with the product and a different level of leachables, an impact of the container on product quality has to be considered and characterized.[13] Cryoconcentration-related effects can be reduced by gentle mixing during thawing.

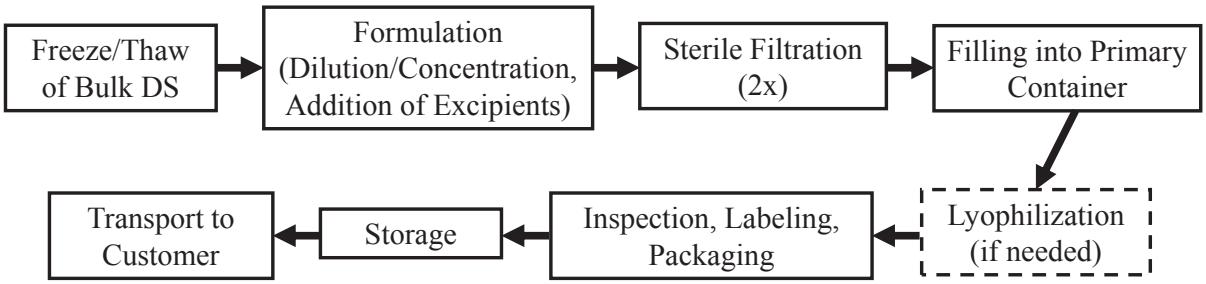

Figure 1: *Overview of the formulation, fill and finish operations during the production of biopharmaceuticals.*

After the drug substance is completely thawed, it is mixed with the appropriate excipients and its concentration is adjusted to a target value. This step is referred to as formulation step and the final buffer in which the protein is formulated is called formulation buffer. Usually, the drug substance is higher concentrated than the formulated form and therefore diluted with concentrated buffer, which simultaneously adds missing excipients that contribute to product stability during subsequent processing and handling processes.[12] The homogenization is commonly performed in stainless steel mixing vessels, which can be equipped with a top entering stirrer or a magnetically coupled bottom mounted stirrer. The advantage of magnetic bottom type stirrers is the absence of mechanical shaft seals that can fail, leading to a contamination of the product, and the ability to operate the vessel at smaller filling volumes.[15] Thereby, the mixing head is kept in its position by a sliding bearing. The bearing consists of a male part, which is fixed to the bottom of the tank (stator) and a female part (rotor), which is

embedded inside the rotating mixing head (see Figure 2). The engineering fit between these two mating parts is in the range of some hundredths of a millimeter. High wear and corrosion resistance of the bearing is enabled by the use of very hard ceramics such as silicon carbide or zirconium dioxide.[16] As the bearing is fully submerged in the liquid that contains the active pharmaceutical ingredient during mixing, the product itself acts as lubricant for the sliding bearing. As there is an increasing trend towards disposable single-use system across pharmaceutical manufacturing steps, also bags mixed by rotating stirrers or rocking are now supplied, offering an alternative to stainless steel vessels, by which the effort of cleaning and cleaning validation can be avoided.[17]

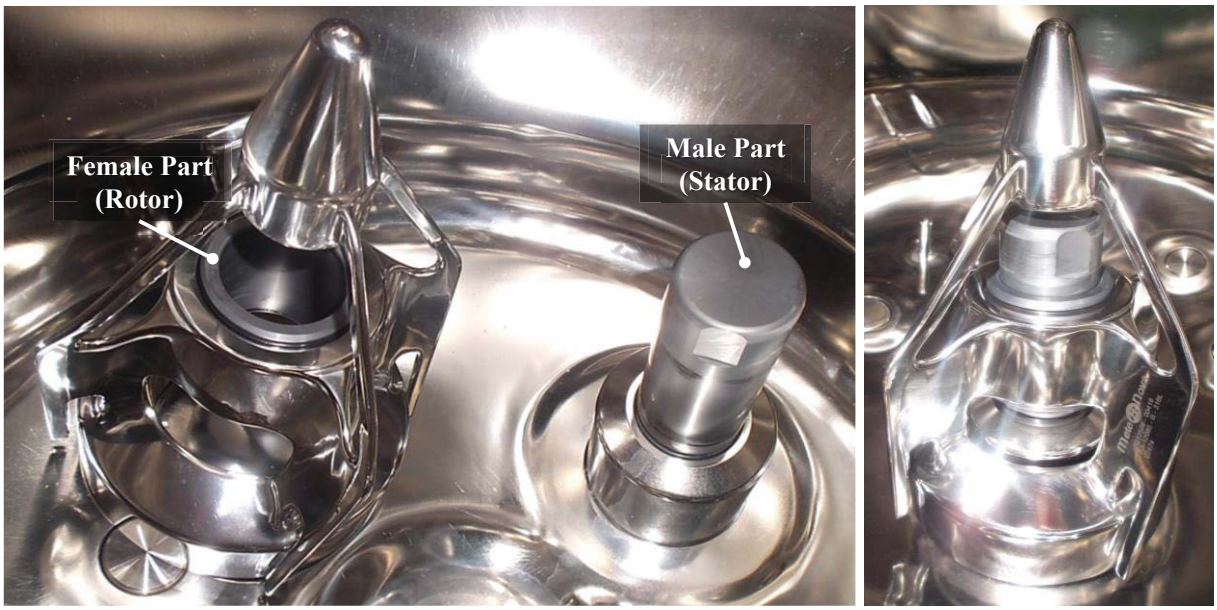

Figure 2: *Mixing vessel with a magnetic bottom type stirrer. Left: The stirring head is lifted off the stator for better visualization of the sliding bearing. Right: Assembled stirrer.*

In order to ensure product sterility, the formulated drug substance has to go through sterile filtration once the compounding is finished. In order to mitigate the risk of incomplete sterilization in the case of a filter failure, redundant filtration (two filters in series) is recommended and industry standard. Sterile filters usually consist of a polyvinylidene fluoride (PVDF) or polyether sulfone (PES) membrane with a pore size of 0.22 µm.[18] In contrast to filters for small volumes (e.g. syringe filters), which use a membrane in form of a disc, large scale filters in form of cartridges or capsules achieve high filter areas by pleated membranes.[19]

Following sterile filtration, the formulated bulk drug substance is filled into its primary container under aseptic conditions, as there is no further sterilization step. Thus, also the packaging units, typically vials, prefilled syringes or cartridges, have to be sterilized in a

separated process before filling.[13] An accurate filling into the primary packaging is ensured by the use of a dosing pump in combination with a filling needle, which are connected by a tube. Rotary piston pumps, peristaltic pumps, rolling diaphragm pumps and lobe pumps are the most common dosing pumps for manufacturing of biopharmaceuticals.[20] The combination of a stainless steel rotary piston pump and a filling needle is given in Figure 3.

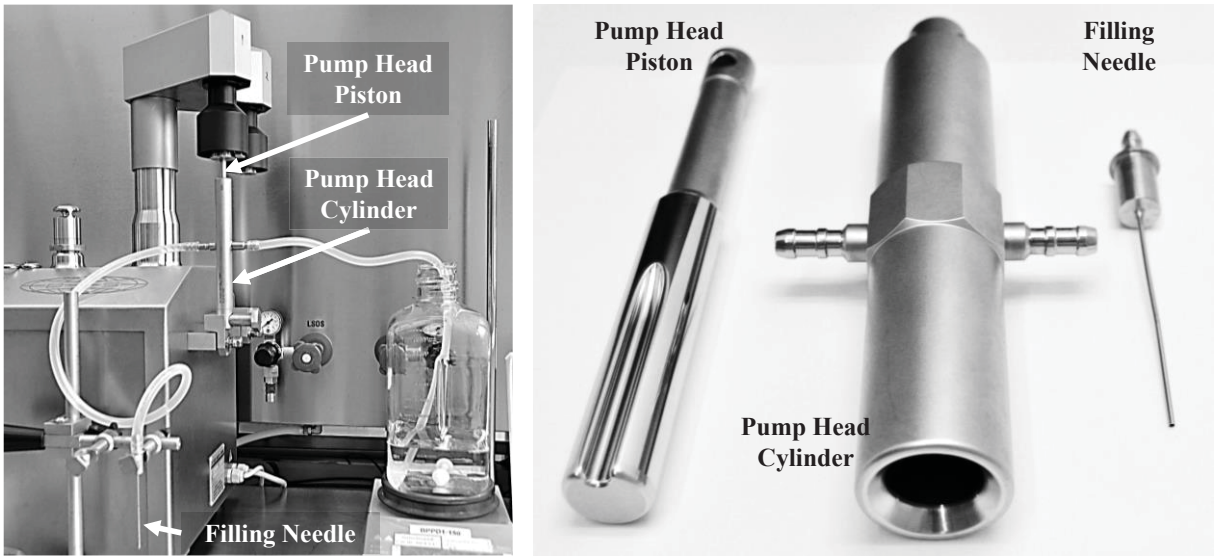

Figure 3: *Left: Assembled rotary piston pumping system consisting of a pump head, a filling needle and tubes to connect the pump head with the storage tank and the filling needle. Right: Close-up of a disassembled stainless steel rotary piston pump head and a filling needle.*

If the shelf life of a drug product is limited by its stability in a liquid form, lyophilization can be applied as an additional step. Thereby, the product is freeze-dried in its primary container. Removal of the water reduces most covalent degradation phenomena, such as isomerization or fragmentation events during storage.[13]

The final processing steps of a biopharmaceutical consist of inspection, labeling and packaging of the final dosage form, as well as subsequent storage (typically at 2-8°C), and transport to the customer.

3. Stabilities of Biopharmaceuticals

Unlike small drug molecules, biopharmaceuticals are protein based pharmaceuticals that have a high molecular weight (> 5 kDa), a large size and highly ordered structures. These macromolecules consist of a sequence of amino acids, which are the basic building blocks. Each protein has a unique three-dimensional fold that is characterized by the secondary, tertiary and quaternary structure.[13,21] However, this three-dimensional folded state is a fluctuating one, having a limited number of preferred conformations. The conformation of a protein that possesses the least energy is also the most stable one and referred to as the native state of the protein.[22] The native conformation has a strong impact on the bioactivity of the therapeutic protein and results from a balance of interactions that are involved in protein folding. The major forces that are involved in protein folding are hydrophobic interactions, electrostatic interactions, hydrogen bonding, van der Waals forces and intrinsic propensities. Among these, hydrophobic interactions have often been cited as the dominant forces, where the aversion of nonpolar residues for water is leading to a hydrophobic collapse of the protein.[23] As a result, nonpolar residues are buried in a hydrophobic core whereas polar side chains are oriented towards water.

3.1. Conformational Stability

The intra-protein and protein-solvent interactions determine the conformational stability of the folded state of the protein. The conformational stability is thermodynamically characterized by ΔG_U, which is also called the free energy of unfolding. It is a function of the temperature (T) as well as entropy (ΔS_U) and enthalpy (ΔH_U) changes of the protein and the solvent during the denaturation of the protein:

$$\Delta G_U = \Delta H_U - T\Delta S_U \quad (1)$$

A high ΔG_U indicates a stable conformation of the protein.[22,24] Interestingly, the typical conformational stability of a protein in solution is with roughly 20 – 63 kJ/mol quite small due to the presence of counteracting destabilizing forces. The unfolding process of small globular proteins can be described by a single transition step between the native (completely folded) and the completely unfolded state. Intermediate states are highly unstable, thus, they exist only in negligible amounts. During the unfolding of larger, multidomain proteins like antibodies, however, intermediate states do occur as domains can unfold locally under different

conditions.[25] Furthermore, the unfolding of proteins may be reversible or irreversible (i.e. irreversibility caused by subsequent aggregation: Native ↔ Unfolded → Aggregated)

The conformational stability or free energy of unfolding can be determined using unfolding curves. A prerequisite is that the protein shows reversible unfolding and a two-state transition (folded vs unfolded), as it can be assumed for many small globular proteins. A common method to induce unfolding of the protein is the addition of a chemical denaturant in increasing concentrations (e.g. guanidine hydrochloride – GuHCl or urea).[26] The exact mechanism of denaturant-induced unfolding of proteins is still not fully understood. Whereas hydrophobic association is not significantly affected, the strength of electrostatic interactions is significantly diminished by GuHCl. This could be induced either by solvation of charged residues or by an engagement in hydrogen bonds with the protein backbone.[27]

From the average fraction of folded (f_F) and unfolded (f_U) protein in the transition region, the equilibrium constant (K_{eq}) can be calculated for each denaturant concentration according to:[26]

$$K_{eq} = \frac{f_U}{f_F} \tag{2}$$

Subsequently, the free energy change from the folded to the unfolded state can then be derived from:[26]

$$\Delta G_U = -R * T * \ln K_{eq} \tag{3}$$

where R is the gas constant and T the absolute temperature at each set point. Finally, the conformational stability in absence of the denaturant (ΔG^0_U) can be obtained by assuming a linear dependence of ΔG_U on the denaturant concentration [D] with a slope of m:[26]

$$\Delta G_U = \Delta G^0_U - m * [D] \tag{4}$$

Another conventional method for unfolding proteins is thermal denaturation. As protein unfolding is an endergonic process, the equilibrium constant (K_{eq}) increases with temperature. At the midpoint temperature of the denaturation curve ($K_{eq} = 1$) the entropy term ($T*\Delta S_U$) equals the enthalpy term (ΔH_U), resulting in a conformational stability of 0 kJ/mol.[26] This temperature is also called the melting temperature of the protein (T_m) and can (carefully) be used for a relative comparison of the stability of proteins. However, there is no particular relationship between T_m and the conformational stability.[22] If unfolding does not follow a reversible two-

state transition, proteins can have more than one melting temperatures (local domain unfolding).[28]

3.2. Mechanical Stability

As described above, the conformational stability is a thermodynamic measure of a protein's ability to withstand changes of temperature, pH or the addition of chemical denaturants. However, sometimes proteins are subject to mechanical forces. Unfortunately, there is no correlation between the thermodynamic stability of a protein domain and the mechanical force which is required to unfold it.[29] The force at which a protein is likely to unfold is called the mechanical stability and is strongly dependent on a proteins secondary structure. Mainly alpha-helical domains typically unfold at low forces, whereas mainly beta-sheet containing domains withstand significantly higher forces. The unfolding forces of the individual domains of a protein can be determined using atomic force microscopy. The tip of the atomic force cantilever is fixed to a protein, which is immobilized on a surface. Upon retraction of the cantilever at a fixed rate, an increasing force is applied to each domain between the cantilever and the surface. If the force reaches the mechanical stability of a domain, it unfolds in a sudden rupture event, which increases the length of the protein and thereby decreases the applied force for the other domains. As the cantilever continues to increase its distance to the surface, the force is continuously increased again, until the next domain unfolds. As a result, a "saw-tooth" force extension profile is obtained, where the peak height of a tooth defines the mechanical stability of the respective domain.[29] The mechanical stability of a domain is not only influenced by its three dimensional structure, but also sensitive to environmental factors such as temperature and pH changes. Furthermore, the addition of a denaturant (GuHCl) is able to significantly lower the mechanical stability (also called "softening"), whereas the unfolding pathway and distance is not altered by the denaturant.[30]

3.3. Colloidal Stability

Besides the conformational and mechanical stability, proteins in solution can also be characterized according to their colloidal stability. The colloidal stability describes the tendency of proteins to assemble and to form higher-ordered aggregates by attractive intermolecular interactions. A common surrogate parameter for the study of overall protein-protein interactions is given by the osmotic second virial coefficient B_{22}. B_{22} (referred to as A2) directly quantifies all interaction forces between two proteins including hard-sphere, electrostatic, van der Waals and other short-range interactions.[31,32] A negative B_{22} value indicates (unfavorable) attractive

behavior as protein-protein interactions are favored, whereas a positive value reflects a repulsive behavior where protein-solvent interactions are favored.[31] The second virial coefficient can be assessed by static and dynamic light scattering.[32]

4. Instabilities of Biopharmaceuticals

Instabilities of proteins can be divided into the two general classes of chemical and physical instabilities or degradations. Chemical degradation of a protein is characterized by the involvement of any processes that break or make covalent bonds, thereby creating a new chemical entity. Physical degradations on the other hand do not alter the chemical composition of a protein, but lead to changes of the physical state of the protein, which is determined by its secondary, tertiary or quaternary structure. Although it is convenient to separate the mechanism of the initial modification of a protein into chemical and physical degradation, we have to face the fact that one can lead to the other as they may be interrelated.[33]

4.1. Chemical Instabilities

Several chemical degradation pathways of peptide and protein pharmaceuticals are known, including deamidation, aspartate isomerization, proteolysis, β elimination and racemization, disulfide exchange and scission/reduction, oxidation and condensation reactions.[34] However, in course of formulation and filling steps of biopharmaceuticals, mainly physical degradation pathways have been described to have an impact on the quality of the active pharmaceutical ingredient,[12,13,35,36] whereas chemical degradation plays a bigger role in the development of stable formulations that ensure sufficient stability over the shelf life. (An exception is the freeze-thawing step, where phase separation and cryoconcentration-related effects can happen). Thus, the chemical degradation pathways will not be discussed here in detail except for protein oxidation, which can be triggered by diverse pathways and has also been directly linked to affect the physical stability of proteins.[34]

4.1.1. Oxidation Reactions

The amino acid residues which are primarily modified via oxidative processes are methionine (Met) and cysteine (Cys), both having sulfur containing groups. In most cases methionyl residues are oxidized when exposed to the solvent at the surface of the protein. In a first step, the sulfur atom is reversibly oxidized to methionine sulfoxide. Under more extreme conditions also an irreversible second oxidation step to methionine sulfone can happen. The oxidation of the thiol group of the cysteine can result in the formation of disulfide bonds. Other sensitive

amino acid residues include histidine (His), tryptophan (Trp) and tyrosine (Tyr) which have aromatic side chains.[37]

There exist three general pathways for the oxidative degradation of proteins: metal-catalyzed oxidation, free-radical oxidation and photooxidation.[21,33]

Metal ions can be introduced into the product either as impurities of excipients like buffer salts and sugars,[38] or may be leached during the production process from stainless steel manufacturing equipment[39,40] or from the primary packaging during storage.[41] Although many proteins can bind metal ions, only some transition metals, such as Fe, Cu, Mn and Cr, can catalyze oxidative reactions.[42,43] Upon binding of a reactive metal, reactive oxygen species (ROS) can be generated which finally lead to a localized oxidative damage close to the metal-binding site.[44] As an example, human growth hormone is a protein that is known to bind the non-oxidizing zinc, which can even cause precipitation by crosslinking at higher concentrations.[45] However, also oxidation-inducing iron can bind at the same site as zinc, where Histidine residues are involved.[46]

Metal ions in combination with polysorbates may also generate free-radicals when they occur unbound in free solution, as it was shown for Fe^{3+} and PS80.[47] In general, oxidation by free-radicals is characterized by an initiation reaction and subsequent propagation until a termination event occurs. Especially ROS are an issue over the shelf life of biopharmaceuticals as the oxidation of methionine only requires mild forms of ROS like molecular or singlet oxygen.[34] Due to the fact, that solubility of oxygen is increased at lower temperatures, the oxidative reaction may even happen more rapidly during common storage conditions (2-8°C).[48] Thus, as a control strategy, oxygen content is often decreased in biopharmaceuticals by introducing nitrogen into the excipient solution or/and by a nitrogen overlay in the headspace of the product.

During the manufacturing processes, biopharmaceuticals can be exposed to light. One example is the chromatographic step, where the elution of the protein is usually monitored by UV absorption.[49] Direct damage of tryptophan, tyrosine, histidine and disulfide residues can be induced by UVA and UVB radiation by the generation of excited state species and radicals. Furthermore, in a second step the protein can be damaged by radicals and peroxides of the affected residues and via molecular reactions of photo-products.[50] Thus, testing of biopharmaceuticals for photostability is a requirement according to ICH guidelines [34].

As outlined above, the oxidation of a protein might be correlated to its physical stability.[33-35] To give an example, oxidation of methionine residues has been reported to decrease the

conformational stability of the Fc part of an IgG1 antibody, finally leading to an increased aggregation rate.[51] The aggregation behavior may be influenced by modifications of surface properties, by altered protein-protein interactions or by altered global conformations of the protein.[34]

4.2. Physical Instabilities

Changes in the physical state of the protein which do not alter the chemical composition are summarized as physical instabilities. Specifically, four processes have been identified: denaturation, surface adsorption, aggregation and precipitation/particle formation.

Eventually, all of these processes that are relevant during formulation and filling steps are related to protein aggregation:[33] Protein denaturation may be reversible, especially in diluted solutions, however, the presence of unfolding intermediates increases the probability of aggregation.[52] Particle formation simply describes the event, when the size of aggregates increases until they are too large to remain soluble.[33] Thus, particles are also referred to as insoluble aggregates.[52] Adsorption of proteins to surfaces might simply be problematic during processing as it has an impact on the concentration of the protein solution, a known issue during filtration steps.[53] However, it may also cause structural perturbation of the proteins and subsequent aggregation on the surface.[54] Precipitation on the other hand is independent of aggregation and could for example be induced by salting-out.[33] As salting-out of proteins finds no application in formulation and filling steps, it will not be further discussed here.[13]

4.3. Aggregation

The formation of soluble and insoluble aggregates was and still remains one of the most highly discussed and researched areas in academia and biopharmaceutical companies. Its inhibition is a major scientific but also regulatory challenge as the presence of aggregates in a product potentially causes immunogenicity, altered pharmacokinetics (PK), changed potency or unfavorable toxicity.[21,33,35,36,52] Whereas the tertiary structure of protein is lost upon aggregation, still significant amounts of secondary structures can be found. Interestingly, an (relative) increase in beta-sheet structures goes along with a decrease in alpha helical structures upon aggregation in proteins which show both secondary structures in the native state.[36] Different protein aggregation mechanisms or pathways are currently under discussion, which may be dependent on the protein and result in different end states:

- Unfolding intermediates are proteins which do not show the native conformation but are also not completely unfolded. As a result, these partially unfolded proteins are more flexible than in the native state and expose more hydrophobic patches. A common theory is that this initially reversible conformational change to a more aggregation prone state finally leads to the irreversible formation of aggregates.[35]
- Another pathway that does not rely on partially unfolded states is aggregation through self-association of proteins in their native conformation. The assembly of native proteins into the aggregated state is often reversible and depends on electrostatic and/or hydrophobic interactions. However, these reversible aggregates are considered to be precursors of irreversible ones. The colloidal stability, described by the osmotic second virial coefficient B_{22} (see above) is a key parameter for assessing the tendency for protein self-association.[35]
- As described in the chapter chemical instabilities, another cause of protein aggregation can be chemical degradation. Besides oxidation, the formation of aggregates upon dimerization, deamidation, hydrolysis or glycation has been described. Another mechanism that is dependent on a chemical modification of proteins is aggregation through direct chemical linkages. Especially surface-located cysteines may promote aggregation by the formation (or exchange) of intermolecular disulfide bonds.[35]

4.4. Induction Factors Causing Aggregation during Formulation, Fill and Finish Operations

Various processing steps have been identified that have an impact on product quality by the formation of aggregates during the production of biopharmaceuticals, such as fermentation/expression, unfolding/refolding, purification, freeze/thaw, shaking, shearing, pressurization, drying, etc.[35] Here we want to focus on factors occurring in formulation and fill operations that influence the physical stability of proteins and eventually cause aggregation or have an impact on product quality in general.

4.4.1. Temperature

Protein denaturation by elevated temperatures is a well-known stress to cause unfolding of a protein's structure. Due to a rapid formation of aggregates upon thermal denaturation, this process is often irreversible.[33] Elevated temperatures increase a protein's tendency to form aggregates not only by raising the percentage of unfolding intermediates in the protein population (increase in vibrational motion), but also the diffusion coefficient of proteins in

solution increases with temperature.[35] Elevated temperatures are not applied on purpose during formulation and fill operations. However, frictional heat could potentially occur for example by rotational movement of the sliding bearing of the mixing vessel or between the cylinder and the piston of a rotary piston pump.

Another temperature dependent process is the so called cold denaturation of proteins. Usually, proteins experience cold denaturation well below the freezing point of water. However, during freezing cryoconcentration-related effects can enable mobility of proteins by lowering the glass transition temperature.[33] Thus, cold denaturation might affect product quality during the freeze-thaw step prior compounding.

4.4.2. Shear

The effect of shear is probably one of the most controversially discussed factors that affect product quality during the manufacturing process of biopharmaceuticals. Stress in form of shear on proteins in solution is assumed to be caused by velocity gradient in the liquid.[20] Basically, velocity gradients occur at every processing step, where the protein solution is subject to movement. In formulation and filling steps this includes shaking during thawing, labelling, inspection and transport, transfer of the liquid in pipes or tubes, stirring during compounding, forcing the liquid through the pores of the sterile filters and dosing into the primary packaging using pumps in combination with filling needles.

The motion of fluids can show two basic characteristics. When the fluid flows in parallel layers, we speak of laminar or streamline flow. This behavior can be observed for slow fluid flows. When the liquid is in faster motion, a disruption between the layers can occur which is characterized by the formation of turbulences in form of eddies. Thus, we speak of a turbulent flow. Whether a system displays a laminar or turbulent flow regime can be estimated using the dimensionless Reynolds number (Re), which depends on the velocity, density and viscosity of the fluid and the geometry of the flow conduct.[55]

Under the conditions of laminar flow, two flow fields should be distinguished here: Couette flow (or simple shear flow) and Hagen-Poiseuille type flow (see Figure 4a and b).[56] Couette flow can be most easily explained by the development of laminar flow between a stationary and a moving plate, which are parallel to each other. Thereby, the boundary condition defines that the fluid adheres to the surface of each plate and does not slip. Once the movement of the plate starts, a velocity profile develops, which is linearly decreasing from the moving plate ($y = D$) to the stationary plate ($y = 0$).

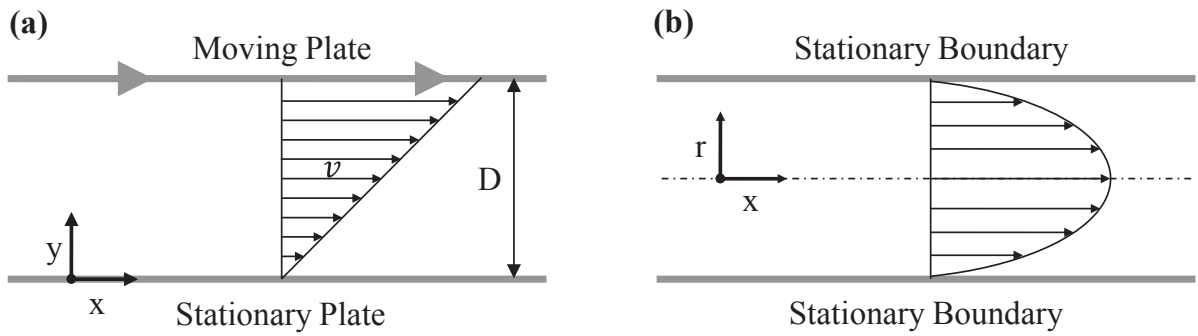

Figure 4: *(a) Under laminar flow condition a Couette flow develops between a stationary and a moving plate which are parallel to each other at a distance of D. A linear velocity profile gradient forms, resulting in a constant shear rate in the system. (b) A Hagen-Pouseuille type flow develops upon liquid flow through a circular pipe or capillary. The velocity profile is of parabolic form, the shear rate is a function of the curvature of the flow profile and the distance from the center and therefore not constant (highest at the wall, smallest in the center).*

The slope of the velocity profile (=velocity gradient) is characterized by the shear rate $\dot{\gamma}$:

$$\dot{\gamma} = \frac{dv}{dy} \tag{5}$$

where v is the velocity and y the distance from the stationary plate.

The velocity profile of laminar liquid flow through a circular pipe follows the law of Hagen-Poiseuille. Thereby, the maximal velocity occurs at the center of the pipe and the velocity profile between the two stationary boundaries is parabolic. The shear rate in case of Poiseuille flow is a function of the curvature of the flow profile and the distance from the center. The highest shear rates occur at the wall of the tube,[57] which can be expressed as:[58]

$$\dot{\gamma}_{Wall} = \frac{4 * \dot{V}}{\pi * R^3} \tag{6}$$

where $\dot{V}$ is the volumetric flow rate and R is the radius of a horizontal pipe, tube or capillary.

However, during production the flow regime is not limited to laminar conditions. Especially during compounding, turbulent conditions are favored as they ensure fast homogenization inside the stirring vessel. Many correlations between the (average and maximum) shear rate and the stirrer speed inside a stirring vessel have been published, a good overview is given by Perez et al.[59]

Possible Effects of Shear on Proteins in Solution

Two possible effects of shear on proteins have been identified and are graphically shown in Figure 5: Alignment of proteins in the direction of shear flow and (partial) unfolding in the shear field. Under laminar flow conditions, large linear molecules like DNA or fibrous particles are known to align parallel to the flow direction by shear gradients (see Figure 5a). The orientation of the molecules along the flow can be studied by linear dichroism spectroscopy.[60]As a result of an alignment of proteins in shear flow, aggregation by self-association of native monomers could somehow be stimulated.

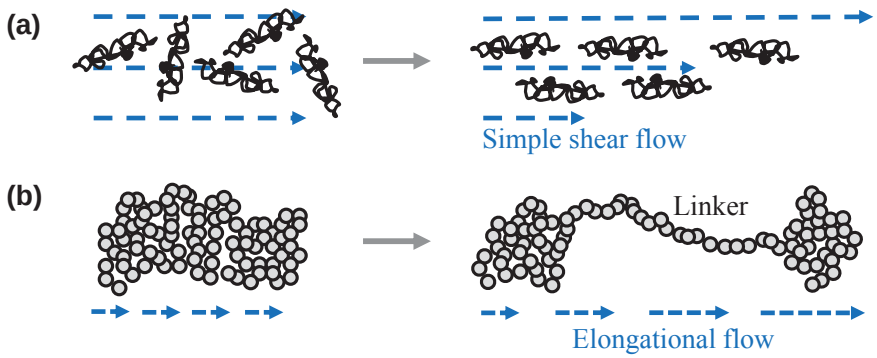

Figure 5: *Two possible effects of shear on proteins in solution: (a) Alignment of the molecules parallel to the flow direction by shear gradients. (b) Shear induced protein unfolding by stretching (adapted from Jaspe and Hagen with permission from Elsevier)[61]*

Probably the most discussed and investigated issue is the (partial) unfolding of the protein. This becomes noticeable either by a deformation of the protein, by a change in the secondary, tertiary structure or by a disruption of the quaternary structure of the protein in shear flow. All of these possibilities could potentially cause soluble or insoluble aggregates.[20,57] A simple model for shear induced denaturation was proposed by Jaspe and Hagen. The protein was considered to be a chain of spherical beads (representing the amino acids). Under the influence of an elongational flow, the chain is separated by stretching into two clusters, which are still connected by a linker (see Figure 5b). To unfold a protein, the work which is done by the fluid to separate the clusters has to equal the conformational stability (ΔG_U) of the folded state.[61] However, this is in conflict with the idea of the mechanical stability, which is independent of the conformational stability of the protein and is determined by the force that is needed to stretch a domain of a protein.[29]

Studies on the Effect of Shear on Proteins

As outlined above, the effect of shear on proteins is a strongly debated topic. Many studies have been published that present controversial results whether proteins are subject to shear induced unfolding at all or which shear rates have to be applied.

Initial work was performed by Charm et al., who used the catalytic activity of enzymes to determine the influence of shear on the structural integrity of proteins.[62] Lower catalytic activity after exposing the enzyme to stress in form of shear was assumed to derive from shear induced deformation. In their studies, catalase, rennet and carboxypeptidase were stressed using a narrow gap coaxial viscometer and a test system which pumped the solution through a capillary (catalase only). A correlation between enzyme inactivation and shear strain (= shear rate*time) was shown at shear rates between 9.15 -1155 s^{-1} and for an experimental time of 90 minutes.[63] In another study, shear was applied at rates of 10^4 s^{-1} using ultrafiltration systems. Catalase showed a similar shear-effect as in the former study, whereas rennet suffered no inactivation, which was attributed to a recovery of the enzymes structure and therefore activity upon standing (reversible unfolding).[64] Furthermore, by performing mixing studies in a cylindrical container in laminar and turbulent flow regimes, Charm et al. observed significant catalase inactivation when turbulence was given. They concluded that this might be due to the presence of air/liquid interfaces, which have been introduced by the formation of a vortex or air bubbles in the solution.[65]

Enzyme inactivation as read out was also used by other authors. In studies by Tirrell et al. urease was sheared using a coaxial cylinder viscometer. The activity of urease continuously decreased with increasing shear rate, beginning as low as 48 s^{-1}. Permanent inactivation of urease was again correlated with shear strain.[66] The effect of shear in microfiltration membranes on alcohol dehydrogenase was investigated by Bowen et al. under solution condition were alcohol dehydrogenase was destabilized. The authors draw the conclusion that the deformation of the enzyme caused an interaction with the membrane, finally resulting in decreased activity.[67] Conversely, in another study by Virkar et al. alcohol dehydrogenase showed stability in a high shear concentric viscometer up to shear rates of $2.6 * 10^4$ over 1 hour. Furthermore, the enzyme was stressed using a rotating disk reactor and pumps, all having little effect on the activity. However, in presence of air/liquid interfaces the activity was significantly decreased. Thus, the authors concluded that shear by itself is not able to unfold globular proteins in a chemically stable environment at practice-relevant shear rates.[68] Stability of alcohol dehydrogenase was also shown in a work by Thomas et al., who could not observe any deactivation of the enzyme

that was sheared in a coaxial cylinder viscometer at 30°C and a shear rate of 683 s^{-1}. Little deactivation, however, occurred at elevated temperatures and shear rates.[69] Another study which undermines the assumption of shear-induced enzyme deactivation was performed by Harrington et al. using several immobilized enzymes. Application of shear did not influence the enzymatic reaction kinetics nor the Michealis-Menten constant.[70]

An alternative method to enzyme deactivation for assessing shear-induced protein denaturation is the offline determination of the aggregate level. The presence of a higher percentage of partially unfolded proteins, which is caused by shear-induced unfolding, is very likely to increase the aggregation tendency (see section physical instabilities). Using a parallel-plate rheometer and capillary rheometer, Bee et al. exposed two mAb (IgG1) formulations to very high shear rates of 20 000 and 250 000 s^{-1} for 5 min and 30 ms, respectively. Not only was shear by itself not able to induce aggregation, but it could also not alter the aggregate population in formulations which contained preformed aggregates (heat induced). However, as in many earlier studies, they concluded that the presence of air/liquid interfaces or an interaction with solid surfaces could induce protein unfolding and aggregation.[71] A combined effect of solid/liquid interfaces with high shear was also investigated by Biddlecombe et al. In their studies, they used a high shear device, where a disc rotated in a chamber that was filled with sample solution under the exclusion of air. In the gap between the rotating disk and the wall, shear rates up to $3.4*10^4$ s^{-1} were applied to IgG4 antibodies, causing aggregation and precipitation.[72] Furthermore, the authors could identify the pH of the sample solution and the nanometer-scale surface roughness of the rotating disc as the dominant factors for the formation of insoluble aggregates under shearing. Addition of a surfactant could significantly protect the IgG from aggregation. Thus, they concluded that upon adsorption to the disc and subsequent unfolding the proteins are forming aggregates, which are finally removed from the surface by the hydrodynamic forces. A change in surface roughness could help to disrupt the laminar flow region at the surface of the disc or alter the adsorption behavior.[73] Desorption of aggregated proteins from solid surfaces was later also examined by Perevozchikova et al. In a flow cell, the adsorption of α-chymotrypsinogen and IgG1 was determined to a clean silicon oxide interface by neutron reflectivity. By applying a rinse step, they could show that a diffusive layer of native proteins was easily removed whereas unfolded proteins were resistant to desorption. However, under the conditions of strong binding, the proteins which could actually be removed by rinsing from the surface were a mixture of monomers and aggregates (α-chymotrypsinogen) or particles (IgG1).[74]

Using offline enzyme activity or aggregation level as a read out for the sensitivity of proteins against shear has a major drawback. A common idea in shear induced (partial) unfolding is a decrease in the conformational stability of the protein. Thereby, the equilibrium of unfolded/folded state is thought to be shifted towards the unfolded fraction.[61] However, if we consider unfolding to be a reversible phenomenon, the information about shear induced destabilization is lost as soon as the shear flow fades away in the sample that has been taken. Furthermore, even if the unfolding is irreversible, the fraction of partially unfolded proteins does not necessarily have to correlate with the formation of aggregates. Thus, an exact determination of a shift in the thermodynamic stability of a protein or of reversible unfolding by shear in general can only be achieved by *in situ* measurements when the protein is still subject to shearing.

Jaspe and Hagen stressed horse cytrochrome c by pressing a protein solution through a silica capillary at high speed, reaching shear rates of $2*10^5$ s^{-1}. The use of the silica capillary allowed *in situ* fluorescence measurements of cytochrome c, which sharply increases its fluorescence in the unfolded state. Furthermore, they used guanidine hydrochloride to artificially decrease the conformational stability of the protein and thereby enhance shear induced unfolding. The results showed no evidence of shear induced unfolding. However, it has to be mentioned that due to a high liquid velocity in the capillary the exposure time was with 4.2 ms (highest shear rate) quite short and the protein may not have had enough time to unfold.[61]

Longer exposure times in combination with *in situ* protein structure determination were applied in an experimental set-up by Bekard et al. The authors used a custom designed Couette cell made out of quartz glass for the creation of simple shear flow. The proteins secondary structure was determined using inline circular dichroism spectroscopy and the proteins tertiary structure was assessed by fluorescence spectroscopy. The authors observed a change in the fluorescence signal (contributable to tertiary structure changes) and a decrease in the alpha helical content of sheared bovine insulin and bovine serum albumin.[75,76] The structural changes were induced at quite low shear rates of 200 and 300 s^{-1}, respectively. Furthermore, the unfolding of the samples was irreversible and time dependent. The total exposure time was 30 minutes for bovine insulin and 60 minutes for bovine serum albumin.[75,76] No aggregation or particle formation of bovine serum albumin was observed and it was concluded that bovine serum albumin was all in monomeric form at the end of shearing.[75] The time-dependent unfolding of bovine serum albumin could however be an indication for a second unfolding mechanism which was present in the set-up used by Bekard et al. In simple shear flow, the shear rate is constant over the whole

sample. Thus, a potential unfolding by shearing would affect all proteins at the same time, resulting in a shear rate dependent but not time dependent signal change.

Exact Definition of Shear

Summarizing, the many studies on the effect of shear on proteins do not only disagree on the ability of shear to actually induce unfolding but also on its exact definition. Whereas many studies have labeled velocity gradients in liquids in combination with interfacial effects as shear, others have focused on hydrodynamic forces alone. Thus, Thomas and Geer suggested in their review to use shear as an expression of hydrodynamic forces which are created by velocity gradients in liquids and do only affect proteins in solution. This excludes any interfacial effects.[20]

4.4.3. Interfacial Effects – Adsorption at Interfaces

As discussed in the section of shear, the presence of solid/liquid or air/liquid interfaces proofed to have a strong influence on the stability of proteins. Interfaces are omnipresent in all processing steps of biopharmaceuticals and can be classified into the relevant classes of solid/liquid, air/liquid, ice/liquid and oil/liquid interfaces:

Solid/Liquid Interfaces

Adsorption of proteins to solid surfaces is a common but complex process; a good review is given by Rabe et al.[54] In general, adsorption of proteins is driven by an increase in entropy. This results from the release of salt ions, surface adsorbed water molecules as well as structural rearrangements inside a protein. Adsorption rates are influenced by the charge of the protein and the charge of the surface. The rates are highest, if the charge of the protein and the surface are opposite. However, at the isoelectric point of a protein (net charge = 0) the overall amount of adsorption seems highest as there is reduced electrostatic repulsion between adsorbed proteins, resulting in a more dense adsorption layer. The charge of the protein is determined by the pH of the solution and its isoelectric point. Other factors that determine adsorption rates are protein bulk concentration and the concentration of dissolved ions, which effects the length of the electrostatic interactions.[54]

Clearly, also surface properties play a major role in protein adsorption. A tendency of proteins has been shown to adsorb more strongly to non-polar than to polar, to high than to low surface tension and to charged then to uncharged surfaces. An exception are glycoproteins, which have hydrophobic domains buried inside a glycan shell and may adsorb extensively to hydrophilic

surfaces.[54] The size of a protein determines its diffusivity and thereby also the adsorption kinetics. Furthermore, small proteins such as lysozyme are usually referred to as rigid or hard proteins, whereas larger molecules such as IgG tend to change their structural conformation upon adsorption. The conformational state on a surface that corresponds to the free energy minimum often differs from the native state of the protein in solution, as interactions between the protein and the surface (hydrogen bonds, van der Waals interactions and coulomb forces) come into play. Thus, the proteins often show reorientations and conformational changes upon adsorption, which might affect their desorption characteristics. Another important aspect is the ability of proteins to form aggregates upon adsorption, depending on the nature of the intermolecular forces.[54]

Probably the most obvious issue of protein adsorption during the production of biopharmaceuticals is a resulting (significant) decrease in concentration of the active pharmaceutical ingredient.[35] This comes especially into play during the sterile filtration step of low concentrated products, as proteins tend to adsorb to the membranes, which have a high surface area.[53] However, also the adsorption to glass (primary packaging)[77] or plastic[78] are investigated topics.

More complicated is the presence of solid/liquid interfaces in form of nano or micro particles. Besides showing an extremely high surface/volume ratio, nano particles have been shown to cause structural changes in a specific size range. Interestingly, the surface curvature of the nano particles seems to have no direct influence on the unfolding of proteins, although often used as explanation.[79] Desorption of conformational altered proteins from the surface of nano particles does induce refolding, however not only to the native state but to an ensemble of metastable near-native conformations.[80] Exposure of a monoclonal antibody to micro particles of various materials was performed in a studies by Bee et al. Iron oxide and glass micro particles only adsorbed the monomeric protein, cellulose showed preferential adsorption of aggregates from solution. Stainless steel particles, however, caused formation of soluble aggregates in the sample solution additionally to irreversible adsorption.[71] In another study by Tyagi et al., steel particles were suggested as root cause of IgG particle formation due to pumping with stainless steel piston pumps, where the steel particles may have served as heterogeneous nuclei for protein aggregation.[81]

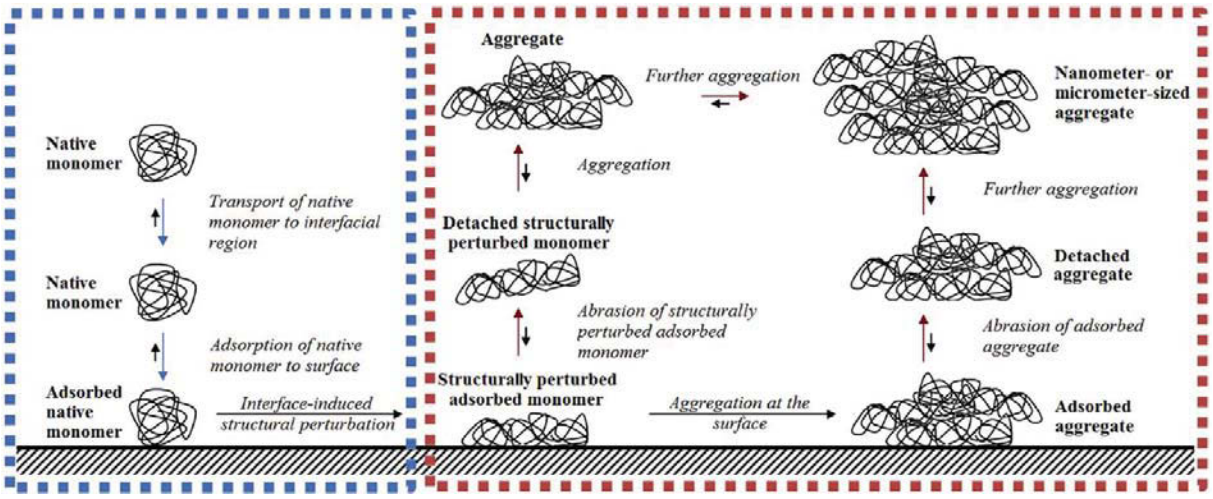

Figure 6: *Graphical representation of the proposed physical degradation mechanism in form of abrasion of adsorbed proteins by Sediq et al. Adsorption of a native monomer to a surface can induce unfolding of the protein. Subsequent abrasion brings the structurally perturbed monomer into solution where it can form aggregates with other species of its kind. Furthermore, the proteins can already form aggregates on the surface. Abrasion of the adsorbed protein layer renews the surface and enables new monomers from the solution do bind. Graph taken from Sediq et al.with permission from Elsevier.*[82]

A recently described and very interesting concept of solid/liquid interfacial-related physical protein degradation is abrasion of adsorbed proteins. The underlying mechanisms depends on an initial adsorption of proteins to a solid surface with subsequent conformational change, leading to destabilization and/or aggregation at the surface. These structurally perturbed molecules or aggregates are finally removed from the surface by contact sliding between two surfaces. Thereby, the structurally perturbed and now detached molecules can further form aggregates in solution (see Figure 6). The surfaces are renewed and subject to adsorption of a fresh protein layer. Thereby, the addition of a surfactant is able to prevent the formation of particles.[82] Such contact sliding can be found for example between a magnetic stir bar and a glass beaker but also in the sliding bearing of bottom mounted stirrers during compounding or in all kind of pumps.

Air/Liquid (Gas/Liquid) Interfaces

Air/liquid interfacial stress is considered to be the most problematic interfacial one. Air/liquid interfaces are basically present in all processing steps and in the final product during storage and transport. Due to the hydrophobic property of air relative to water, air/liquid interfaces show a hydrophobic character. This causes an alignment of proteins at this interface with an exposure of hydrophobic patches of the protein to the air and possibly initiating aggregation.[35] A good suggestion for the mechanism of protein aggregation by air/liquid interfacial stress was

published by Bee et al. During the dilation of an air/liquid interface of an antibody solution, the protein was allowed to diffuse into the fresh interface. However, upon subsequent compression of the interfacial area by a factor > 5 the proteins were crushed together, causing aggregation at the interface. The aggregates are finally released into solution once the interface is dilated again.[83] Interestingly, not only shaking leads to air/liquid interfacial stress, but also stirring seems to cause a certain turnover of the interface, resulting in aggregation of the sample.[57,84]

Oil/Liquid Interfaces

The source of oil/liquid interfaces are usually micro droplets of silicone oil, which is used as a coating of syringes or stoppers, again finally leading to aggregation of the product.[85,86] The deleterious effect of silicone oil droplets on an IgG1 antibody was shown to be strongest in the presence of a liquid flow relative to the organic surface.[87] As oil/liquid interfaces are introduced at the end of formulation and filling processes by the primary packaging of the drug, they affect the quality of the product mainly during storage and transport. During filling of the protein solution into the glass vial or syringe, however, a strong interaction between the solution and the primary packaging occurs, which is determined by the diameter and movement of the filling needle and the speed of the liquid inside the needle. Filling parameters may not only have an impact on the wetting of the surface and thereby the direct contact area to oil/liquid interfaces during filling (as well as on the creation of air/liquid interfaces), but also on the introduction of silicone oil droplets into solution by potential fluid mechanical abrasion.

Ice/Liquid Interfaces

Besides the issue of the effect of cryoconcentration on the stability of biopharmaceuticals during freeze/thawing steps, also a damage at ice/water interfaces has been reported.[88,89] This was argued by a strong correlation between the tendency of proteins to unfold upon freezing and their tendency to unfold at surfaces. Furthermore, the addition of the surfactant polysorbate 80, a surface active agent, protected the protein from freeze-induced denaturation.[88]

5. Surfactants

Surfactants are surface active agents with two distinctive regions in their molecular structure: a hydrophobic tail and a hydrophilic head group. Thus, they are also referred to as amphiphilic molecules. Surfactants can be classified based on their charge characteristics and may be non-ionic, anionic, cationic or zwitterionic. Ionic surfactants, such as sodium dodecyl sulfate, are strong protein denaturants as they can bind polar as well as nonpolar groups. Hence, ionic

surfactants are generally not used as excipients for protein stabilization, whereas non-ionic surfactants are preferred.[22] The most commonly used non-ionic surfactants in the pharmaceutical industry are polysorbate 20 and 80, which are also known as Tween® 20 and Tween® 80.[33]

In general, surfactants are added to protect proteins from damage and aggregation at interfaces. The performance of surfactants to protect the protein from aggregation has been shown at air/liquid interfaces during shaking[84,90-92] and stirring[84], at ice/liquid interfaces during freeze-thawing[88,93] and at solid/liquid interfaces.[82] Furthermore, adsorption to solid surfaces and thereby a loss in concentration can be significantly reduced by the addition of a surfactant.[53,94] In case protein adsorption is predominantly driven by electrostatic interactions like adsorption to glass, especially highly hydrophobic surfactants are powerful in reducing adsorption.[94]

Different concepts have been presented on the mechanism of protein protection by a surfactant. One hypothesis is a surface displacement of proteins by the surfactant. Thereby, a competitive adsorption between the surfactant and the protein resulted in reduced protein adsorption at the interface.[95] This mechanism was confirmed in a study by Serno et al., who showed that polysorbate 80 was capable of displacing IgG at air/liquid interfaces independent of the adsorption order.[96] Protection from aggregation could however also result from a weak binding of the surfactant to the protein. Thereby, potentially aggregation prone hydrophobic sites on the surface of the protein could be blocked. Interaction of polysorbate 20 and 80 to BSA could be shown by differential scanning calorimetry, whereas binding to lysozyme and IgG was negligible.[97] Furthermore, binding of surfactants to recombinant human growth has been reported[98,99] and there is even a protective effect by an increase in the free energy of unfolding of the protein upon binding the surfactant under discussion.[100]

Unfortunately, the use of surfactants for protection from interfacial effects gives also rise to some drawbacks. Under quiescent conditions surfactants can accelerate protein aggregation as it was shown during several stability studies.[91] This is possibly caused by a strong binding between surfactant and protein, which induces denaturation.[35] Another issue of surfactants are impurities, which are caused by auto-oxidation.[95] Auto-oxidation of polysorbates results in the formation of hydroperoxides, which can vary between lots and manufacturers and can finally lead to an oxidation of the product.[52]

6. Regulatory Background and Small-Scale Models

In order to mitigate quality related risks arising from stability problems in industrial biopharmaceutical drug product production, guidelines have been introduced by regulatory authorities and harmonized by the international council for harmonization (ICH). Basis for the pharmaceutical drug product development are the quality guidelines Q8(R2) from 2009 (Pharmaceutical Development) and Q11 from 2012 (Development and Manufacture of Drug Substances).[101,102] Although Q11 describes the development and manufacture of drug substances and does not explicitly mention drug products, its concepts can analogously be applied for drug product development.

These guidelines strongly encourage the use of Quality by Design (QbD) principles in the development and manufacturing of drug products. The QbD concept is based on a systematic characterization and a profound scientific understanding of relevant process steps. First, a risk analysis is performed in order to identify all process parameters which may have an impact on the overall process performance. Subsequently, experimental studies are designed and performed to verify the impact of the process parameters from the risk analysis. Thereby, the influence of a single process parameter on product quality should not be examined in isolation, as potential synergistic effects may arise from effects of individual production steps. Thus, the use of design of experiments is recommended for a process characterization in order to study key and critical process parameters as well as their interactions. Analysis of the results finally allows the definition of a so called design space. Within its borders a product with predictable and consistent properties meeting the defined quality requirements is obtained.[103]

As it is often impossible to perform all required studies during process development, optimization, or characterization at commercial scale, there is a need for representative small-scale or also called scale-down models. As the name itself implies, studies using small-scale models are typically performed with low volumes in the lab or pilot plant. This has not only the advantage of reducing the consumption of the drug substance and excipients in the experiment but also does not block the production site in the time frame of the study, thereby providing more temporal flexibility. Two types of small-scale models have been differentiated by Moscariello, which can be used for such studies (see Figure 7). In a miniaturized full-scale model a whole unit operation is mimicked in a reduced-size version to assess the effect of input materials and process parameters on the performance of the process and the quality of the product. In a partial or worst-case small-scale model a specific physical or biochemical

environment within a process step is simulated (e.g. high shear rates). Thereby the (presumably) worst conditions for maintaining product quality are applied by either the use of a miniaturization of the large scale unit operation or an apparatus which is capable of stressing the product under specific (un)desired conditions.[104] Worst-case small-scale models are useful in the optimization processes during formulation development and in the characterization of the sensitivity of a product.

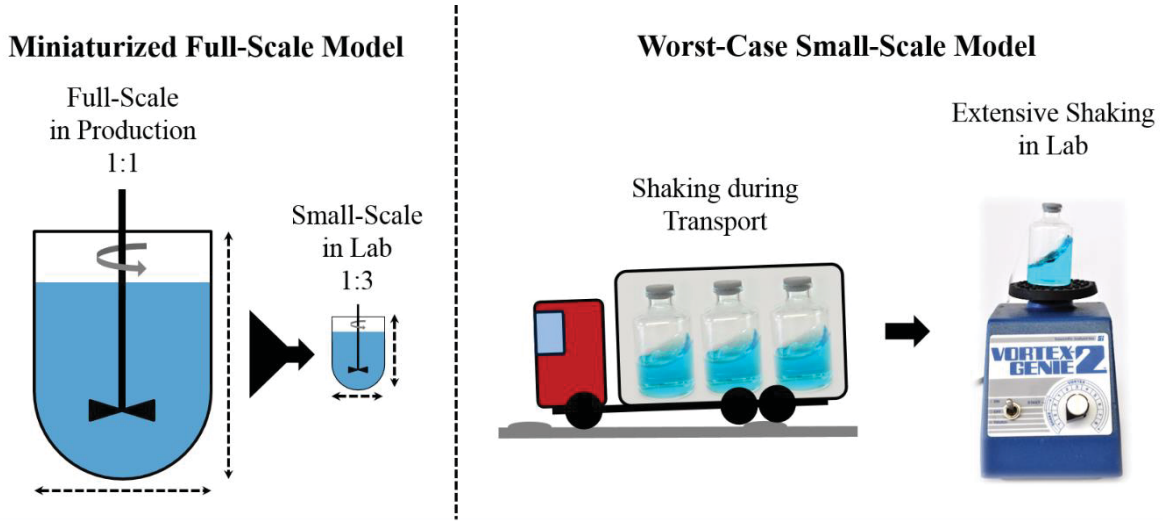

Figure 7: *Graphical representation of the two types of small-scale models: Miniaturized full-sale model (left) and worst-case small-scale model (right).*

OBJECTIVES

The aim of this doctoral thesis was a detailed investigation of formulation, fill and finish operations regarding impact on product quality. The knowledge of all potential stress factors during the various processing steps including their actual influence on product quality is of major importance for formulation development. Once a relevant stress parameter has been identified, worst-case small-scale models can be developed and used for screening for the most stable formulation. Furthermore, stress that occurs during formulation, fill and finish operations at production scale can be simulated in a miniaturized full-scale model. Thereby, the most relevant stress parameter should be kept constant in order to achieve a representative product quality at small-scale experiments so that the obtained data are predictive for large-scale operations.

Therefore, this doctoral thesis had following main objectives:

- Identification and evaluation of potential stress parameters at formulation fill and finish operations and their impact on product quality.
- Development of a worst-case small-scale model for a stress parameter with a high impact on product quality for use in formulation development.
- Design of a representative miniaturized full-scale model of the compounding vessels from the investigated production site.

DISCUSSION

1. Identification of Relevant Stress Parameters for Small-Scale Models

The aim of the first part of the work was to identify relevant stress parameters that cannot be prevented during the formulation, fill and finish manufacturing steps of biopharmaceuticals. Potential stress parameters that can be controlled, such as temperature during storage or transport, exposure to UV-light, etc., were not considered here. As the investigated production site was specialized on prefilled syringes, the lyophilization step was not investigated in course of this work.

1.1. Thawing of Drug Substance

Thawing of the drug substance is the first evaluated step in the formulation, fill-and finish unit operation. Potential stress parameters in this unit operation are variable buffer salt and protein concentrations due to cryoconcentration, which can cause deviation from the desired pH value.[14] Furthermore, protein damage at ice/liquid interfaces could affect the quality of the product.[88] In general, the drug substance is stored after manufacturing in a frozen state and aliquoted inside of sterile plastic bottles with a maximum volume of 2 L. Thus, also the effect of leachables from the container has to be considered.[13]

1.2. Formulation Step or Compounding

After the drug substance is completely thawed it is transferred into a so called compounding vessel. This is performed by carefully pouring the opened drug substance bottle inside of a so-called anti-foam inlet, which allows the liquid to slowly run down the wall of the vessel in order to prevent the introduction of air bubbles into the solution and thereby foaming. Clearly, protein denaturation at air/liquid interfaces is the most relevant stress parameter here. Alternatively, the drug substance can be transferred into the compounding vessel by the use of a peristaltic pump. Relevant stress factors arising from pumping are discussed below in the section Filling.

After the addition of the drug substance and the solution that contains the required excipients for the final drug product, the mixture is homogenized by stirring. The investigated production site was using stainless steel vessels of different sizes, which were equipped with magnetic bottom type stirrers, as can be seen in Figure 2. Based on literature research, shear and particle formation inside the sliding bearing were identified as potential stress parameters for the unit operation of mixing, which are discussed below.

1.2.1. Shear

Shear in terms of velocity gradients in liquids occurs in the whole bulk solution of the vessel. The average shear rate inside a vessel under turbulent flow conditions can be calculated according to:[59]

$$\gamma_{average} = \left(\frac{4 * N_P * \rho * {d_i}^5}{H * d_T * \pi * \mu} \right)^{1/2} * N^{3/2} \quad (7)$$

where N_P is the power number of the stirrer, ρ is the density of the liquid, d_i is the characteristic diameter of the impeller, H the height of the liquid, d_T the diameter of the tank at the smallest clearance to the impeller, μ is the dynamic viscosity of the liquid and N is the rotational speed of the stirrer. Typical shear rates from a compounding vessel from the investigated production site are in the range of roughly 200 s^{-1} (100 rpm) to 1000 s^{-1} (300 rpm), assuming a power number of 6.7 (manufacturer information) and water as liquid.

The highest shear rates can be found at the stirrer tip and within the gap of the sliding bearing of the magnetic bottom type stirrers. The shear rate at the stirrer tip can be expressed as:[105]

$$\gamma_{tip} = 3.3 * N^{1.5} * d_i * \left(\frac{\rho}{\mu} \right)^{0.5} \quad (8)$$

Using the same parameters as in the calculation of the average shear rate, a maximum shear rate at the tip of the impeller of roughly 1100 s^{-1} (100 rpm) and 5700 s^{-1} (300 rpm) is obtained. Theoretical calculations of the shear rate inside the sliding bearing are possible when the bearing is considered to be an ideal system which behaves like a Couette cell. A Couette cell consists of a static inner cylinder with a rotating outer cylinder, having a defined and constant gap width. Inside this gap, a couette flow develops upon rotation of the outer cylinder, creating a velocity profile in the liquid. However, as in reality the stirrer is subject to axial forces, the gap width will vary upon mixing the liquid. Thus, the gap width can reach very small values which results in extraordinary high theoretical shear rates and which makes theoretical shear rate calculations highly inaccurate and therefore inapplicable.

Nevertheless, the theoretical average shear rates in the stirred tank as well as the maximum shear rates at the stirrer tip are in a range where protein denaturation due to exposure to shear has been described (see Introduction section 4.4.2). Although there was also a controversial study which reported stability of proteins against shear up to 10^5 s^{-1} for 4.2 ms,[61] a long exposure

to shear during stirring (up to 5 min) could cause a cumulative stress to the protein as it was described by Bekard et al.[75] Thus, there was the need of a worst-case small-scale model which was able to assess the influence of shear on therapeutic relevant proteins up to shear rates of at least $6 \cdot 10^3$ s^{-1} at exposure times above 5 min.

1.2.2. Particle Formation inside of Sliding Bearings

Physical degradation of proteins in terms of particle formation had been observed during stirring for vessels with a magnetic bottom type stirrers. However, the exact mechanism was still unclear as the studies were designed to simply evaluate the best mixing system. Nevertheless, the authors proposed shear or shear in combination with cavitation as possible root cause of protein degradation within the sliding bearing of magnetic bottom type stirrers.[106,107] As the female and male part of the sliding bearing are most likely to touch each other upon stirring, also abrasion of adsorbed proteins and heat denaturation due to frictional heat had to be considered as root cause of protein degradation besides high shear inside the bearing. Furthermore, wear of friction could create nano or micro particles which have the potential to induce protein aggregation.[71]

1.3. Filtration Step

Pressure driven (N_2) sterile filtration is the subsequent step after compounding in production. Main issues during filtration that have an impact on product quality are filter integrity, adsorption of the API to the filter membrane, adsorption of excipients to the filter membrane as well as leachables from the filter material.[53] A factor which may not directly affect product quality but has an influence on the filtration time and thereby on economics is filter blocking. Besides filter integrity, all factors are depending on the ratio of filter membrane area to product volume as well as on the contact time and therefore on the applied overpressure at the unsterile side of the system.

1.4. Filling

Two sorts of dosing pumps are used at the investigated production site: peristaltic pump and rotary piston pump. Both pumps are connected to a filling needle via silicone or PTFE tubes. Within the tubes, product quality can be affected by adsorption and/or leachables.

As the liquid is in movement in narrow gaps inside the pump and the filling needle, also shear has to be considered as potential stress parameter. Whereas the calculation of a theoretical shear rate in the gap between cylinder and piston of the rotary piston pump is not applicable due to a

most likely varying gap width, the shear rate inside the filling needle can be calculated according to Equation (6). Calculations assuming a radius of 1 mm of the filling needle and a volumetric flow rate of 5 mL s^{-1} give a theoretical shear rate of roughly 6400 s^{-1}.

Furthermore, friction within the tube occurs in the peristaltic pump. Friction is also most likely to happen between the cylinder and the piston of the rotary piston pump as no ideal geometrical shape of the parts (see Figure 3) and no ideal behavior of the stroke can be assumed. Thus, physical protein degradation by abrasion of adsorbed proteins and an introduction of nano/micro particles by wear of friction and subsequent interaction with proteins have to be considered. If the piston head is made out of stainless steel, an introduction of metal ions has to be additionally taken into account as they could promote protein oxidation.

Once the product passes the filling needle, it enters the syringe. Thereby, the movement of the liquid is depending on the dosing curve during filling (determines the speed of the liquid) and the position and movement of the filling needle. Ideally, splashing and foaming are prevented by the use of optimized filling parameters. Nevertheless, the liquid is in contact with air/liquid interfaces and a fluid mechanical abrasion could lead to an unwanted introduction of silicone oil droplets into the product.

1.5. Inspection, Labeling, Packaging, Storage and Transport to Customer

After filling and stoppering, each syringe has to be inspected, labeled and packed for storage until it is being delivered to the patient. During these unit operations primarily interfacial effects have an impact on product quality. Every movement of the syringe brings the risk of a movement of the liquid, causing air/liquid interfacial dilations and compressions and change of the contact area to silicone oil at the wall of the syringe.

2. Evaluation of Identified Stress Parameters

2.1. Cryoconcentration-Related Effects and Ice/Liquid Interfaces

Thawing of the drug substance is performed at production and at lab scale by incubating the frozen bottle at 2-8°C in a static position. The drug substance is supplied to the production site in bottles of the same material (leachables) and size as the ones used in the lab. Thus, the only difference in thawing between small and large scale is the number of bottles which are incubated simultaneously at 2-8°C. Thereby, an exact distance between the bottles is defined. The physical proximity of the bottles is very likely to affect the thawing behavior and thereby potential cryoconcentration-related effects and the exposure to ice/liquid interfaces, as it could create a locally decreased temperature in case of insufficient convection. Often, experiments at small-scale do not require more than one bottle of drug substance, which could thaw faster if incubated alone rather than in proximity of other frozen DS bottles. A very simple approach to simulate and evaluate the exact thawing time in this case is to place bottles of the same size with frozen placebo buffer next to the drug substance.

A worst-case small-scale model for the above mentioned stress parameters can simply be obtained by exposing a drug substance bottle to multiple freeze-thawing cycles. As the thawing of the drug substance in production-scale can identically be simulated at small-scale, also the stress parameters are identical. Therefore, there was no need to develop a miniaturized full-scale model for this unit operation.

2.2. Air/Liquid Interfaces

Protein aggregation and/or particle formation at air/liquid interfaces was identified as a potential risk in almost every processing step. Thus, it is essential to have a worst-case small-scale model for this stress parameter that can be used in the optimization of the formulation of the product. A very good model of stressing proteins at air/liquid interfaces has been introduced by Bee et al., which used a half-filled rotating container to create dilation/compression cycles of the air/liquid interface.[83] Another simple model is to place the sample solution inside a closed container (can be the finally selected primary packaging such as a vial or a syringe) and shake it for a defined time period (see Figure 7). Thus, no new worst-case small-scale model had to be developed for the effect of air/liquid interfaces on product quality.

Nevertheless, in the design of a miniaturized full scale model it is important to simulate this stress parameter as accurately as possible. This is especially relevant at following three processing steps during formulation, fill and finish operations, which are discussed below.

1) At large scale the drug substance is transferred into the compounding vessel via a special inlet tube, which guides the liquid to the vessel wall where it can slowly slide down to the bottom. This prevents the formation of air bubbles and foaming. Thus, simply pouring the drug substance bottle inside the mixing system at small scale is not representative for the production scale.
2) During mixing in the compounding step, the bulk flow of the liquid creates a vortex. The formation of the vortex starts at the surface of the liquid; its final depth is depending on the type of the impeller, the impeller speed and the vessel design (e.g. baffles can prevent the vortex formation by stopping some of the angular velocity of the liquid). The impeller type of the investigated compounding vessels can be best described by a flat-blade turbine. Even though the blades are slightly pitched, rotational movement of the impeller in the speed range which is applicable for compounding creates more radial than axial flow. Above a critical speed limit, the vortex depth reaches down to the bottom-mounted stirrer which causes an introduction of air bubbles into the product and foaming. The flow characteristics inside the stirred tank are not only affecting the vortex formation but also the turnover of the air/liquid interface, which may be linked to aggregation.[84] Thus, in a miniaturized full-scale model it is important to simulate the liquid flow as good as possible during mixing by choosing a representative stirrer and vessel design as well as representative operating parameters.
3) Filling of the product inside of the syringe is performed at large scale using automated pumping systems in combination with filling needles. The size of the pumping heads does not differ from lab-scale pumps, a higher throughput is achieved by running multiple pumps in parallel. Thus, if the filling system in lab-scale consists of the same pump type, connection tube and filling needle and if the same filling curve is applied, filling in small scale is representative of large scale.

Summarizing, a representative simulation of air/liquid interfacial effects in the compounding step (including transfer of the drug substance) should be considered in a miniaturized full-scale model. Thus, the model should be capable of simulating the low foam inlet tube and have similar bulk flow and vortex formation characteristics. The filling step can be simulated using commercially available lab-scale pumps as described above.

2.3. Shear

Besides stress related to air/liquid interfaces, shear is the most commonly occurring theoretical stress parameter in formulation, fill and finish unit operations. However, due to very controversial reports on the effect of shear on the stability of proteins, there was the need of a worst-case small-scale model which was able to assess the actual influence of shear on therapeutic relevant proteins. This evaluation was one of the key aspects in this work, as the design of miniaturized full-scale models should be representative of the occurring stress parameters. Unfortunately, the chemical and physical stresses exerted by the individual process steps do not affect the protein molecules in a direct and straightforward way, which makes a linear downscaling often impossible (compare Equation (7) and (8)). Thus, process parameters at small-scale should be selected in a way that the stress with the highest impact on product quality is kept constant compared to large-scale, whereas less important stress factors might be too low or high.

Theoretical calculations of the occurring shear rates were in the range of $1.1 - 6.4 \cdot 10^3\ s^{-1}$ at maximum exposure times of 5 min (during compounding). Thus, it was a requirement to cover that range during the evaluation of the impact of shear on proteins in free solution. The basic concept behind shear induced physical protein degradation is a decrease in the thermodynamic stability of the protein which is caused by a stretching of the molecule by velocity gradients in free solution.[61] The decrease in thermodynamic stability shifts the equilibrium of unfolded to folded proteins towards partially unfolded, which can finally lead to protein aggregation or particle formation. However, if the (partial) unfolding is reversible due to rapid folding/unfolding kinetics of the investigated protein, subsequent offline analyses cannot asses the real impact of shear on proteins. Furthermore, a possible alignment of protein molecules in the shear field could somehow affect aggregation tendency. Thus, another requirement of the test system was the ability to assess the conformational changes of a protein *in situ* and during the application of shear, which enables the visualization of a potential decrease in the thermodynamic stability of the investigated protein, as well as the ability to detect a possible alignment.

A very sensitive method to determine a proteins secondary and tertiary structure is Circular Dichroism (CD) spectroscopy. In studies performed by Bekard et al. CD spectroscopy in combination with a Couette cell (for the creation of simple shear flow) was already used to show significant protein unfolding over time at low shear rates.[75,76] Thus, in course of this thesis a quartz Couette cell from Applied Photophysics was obtained that can be combined with a

Chirascan plus CD spectrometer. The Couette cell was originally developed for Linear Dichroism measurements, however, it can also be used for the determination of the Circular Dichroism of a protein. A schematic of the used Couette cell is shown in Figure 8. Due to possible end effects and slight imperfection in the geometry of the cell, the supplier of the Couette cell limited the laminar flow range to Reynolds numbers <250. Thus, experiments at a defined shear rate (theoretical calculations require laminar flow conditions) were limited to a maximum of roughly $4*10^3$ s^{-1}. However, the maximal rotational speed of the Couette cell allowed measurements up to a nominal shear rate of roughly 10^4 s^{-1} (calculation under the assumption of laminar flow, Re = 638).

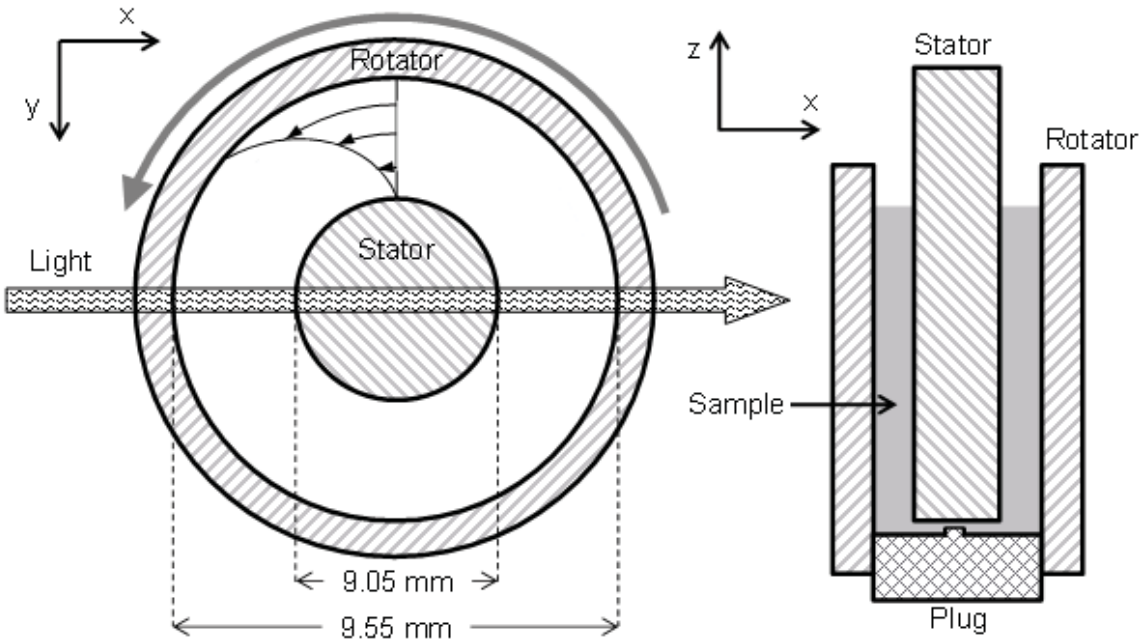

Figure 8: *Schematic of the used Couette cell taken from publication I. The cell consists of an inner static and an outer rotating cylinder made out of quartz glass. This enables transmissibility of a light beam that travels along the gradient direction of the rotating liquid in the annular gap. Along the z-axis a constant velocity profile of the liquid is assumed.*

Investigations on the effect of shear on IgG1 and recombinant human growth hormone (rhGH) using the above described system are summarized in publication I. These proteins were selected as they are representative of typical therapeutic proteins and strongly differ in size and secondary structure composition. Whereas rhGH is a relatively small (22 kDa) and mainly alpha helical protein, IgG1 is noticeable bigger (150 kDa) and its immunoglobulin fold mainly consists of beta-sheets.[108,109]

Initially, an alignment of the proteins was checked under laminar flow conditions in the Couette cell by Linear Dichroism (LD) measurements. This investigation was not only essential in order to exclude any possible aggregation-influencing effect but also for the interpretation of the CD spectra as an alignment of the molecules results in LD artefacts in the CD spectra. No alignment of IgG1 and rhGH molecules was detected by Linear or Circular dichroism.

The effect of shear on the secondary structure of rhGH and IgG1 was investigated at a shear rate of 3840 s^{-1} and an exposure time of 30 minutes. Thereby, it was shown that under the exclusion of interfacial effects the structure of the proteins was not altered by shear. This finding was confirmed using offline fluorescence measurements, where the spectrum of a stressed sample was compared to an unstressed reference. The study was repeated at the highest operational speed of the Couette cell, corresponding to a nominal shear rate of 10400 s^{-1}. Under these conditions, turbulent flow conditions were most likely to occur. Nevertheless, no unfolding of IgG1 and rhGH due to shear was observed. Interfacial effects were eliminated by the addition of a surfactant in low concentrations. Polysorbate 80 was added to IgG1 and poloxamer 188 to rhGH. As binding of the surfactant to the proteins could increase the free energy of unfolding[100] and thereby possibly stability against shear, melting curves of protein solutions with and without surfactant were compared against each other. Thereby, no significant differences in the melting temperatures were observed.

Still, it was shown in another experiment that the addition of a surfactant was essential in the experimental set up. Shearing of surfactant-free solutions of rhGH caused a time dependent and irreversible unfolding, causing a characteristic change of the far-UV spectrum which was very comparable to the results reported by Bekard et al.[75] However, the extent of unfolding over time changed over replicates of an experiment with identical shear rates. Thus, the presence of another stress parameter was predicted which was unrelated to the shear rate and could be eliminated by the use of a surfactant. Finally, it could be shown that the presence of air/liquid interfaces in form of small air bubbles, which were introduced by loading the sample solution inside the Couette cell, caused unfolding of rhGH during rotational movement.

Stability of IgG1 and rhGH against shear was shown under laminar flow conditions up to 3840 s^{-1} and under turbulent conditions up to a nominal of 10^4 s^{-1}. However, as high shear rates could locally occur in formulation fill and finish steps, it was considered necessary to investigate the effect of more extreme conditions. As the hydrodynamic forces in form of velocity gradients in free solution were limited by the maximal rotational speed of the Couette cell accessory, another approach was selected. Instead of increasing the shear rate, the conformational and mechanical

stability of the protein was artificially weakened by the addition of guanidine hydrochloride (GuHCl).[30] A potential shear-induced unfolding of the weakened protein should already happen at significant lower shear rates, simulating the effect of higher shear rates. Furthermore, the determination of the shear-induced decrease in conformational stability of the protein would allow the calculation of the critical shear rate that causes unfolding of the native protein (in absence of GuHCl). CD spectra of IgG1 and rhGH were recorded at GuHCl concentrations where a noticeable transition from the folded to unfolded state occurred (see Figure 9 for far-UV and near-UV CD spectra of rhGH). However, also the artificially weakened protein structures of IgG1 and rhGH were not affected by shear rates of 3840 s^{-1} (laminar flow) and 10400 s^{-1} (turbulent flow).

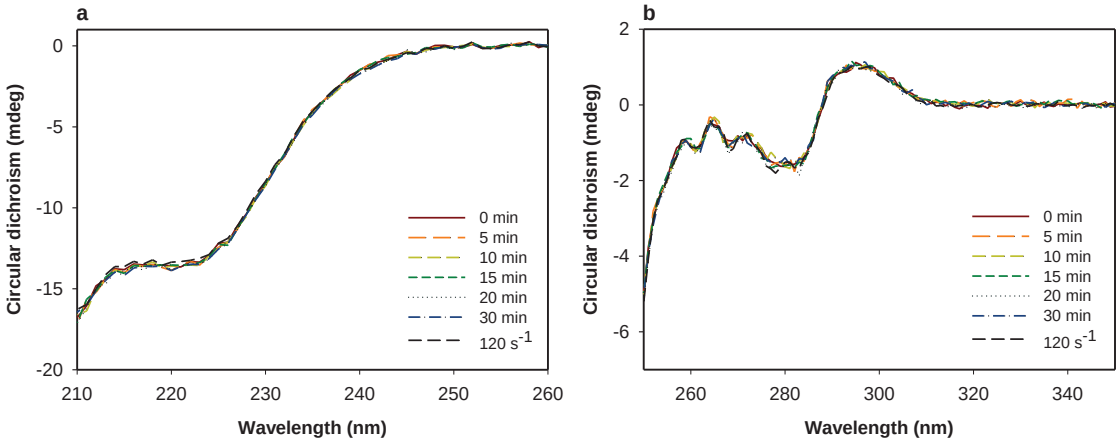

Figure 9: *Far-UV (a) and near-UV (b) CD spectra of a rhGH sample that was sheared at a constant shear rate of 3840 s^{-1} over 30 minutes and that was destabilized by 4 M GuHCl (a) or 2 M GuHCl (b). No time-dependent change in the CD signal was observed compared to a "fresh" reference sample (long dashed black line) that was recorded at the lowest possible shear rate of 120 s^{-1}. Figure taken from publication I.*

Summarizing, stability of rhGH and IgG1 against shear in free solution up to at least 10^4 s^{-1} was shown. This shear rate is covering the range of shear rates, which are occurring in the filling needle and in the compounding vessel during formulation, fill and finish operations. Furthermore, as stability was given independently of size or secondary structure composition of the investigated proteins, it is very likely that proteins in general are not affected by shear in free solution. As a consequence, it was decided not to consider shear as a relevant stress parameter and therefore not to correctly adjust the shear rate miniaturized full-scale models.

2.4. Solid/Liquid Interfaces

2.4.1. Loss in Content by Surface Adsorption

Protein and/or surfactant adsorption to the membrane is a major concern during the filtration step, as it can significantly reduce the content of the API or the surfactant in the first fraction of the filtrate. The filtration step is critical as usually high membrane areas are selected in order to avoid filter blocking. Besides the ratio of membrane area to filtrated volume, volumetric flow rate and solution temperature are the critical process parameters that define loss by adsorption. Sterile filters having consistent materials but membranes of different sizes are commercially available, which facilitates up and down-scaling. Thus, a miniaturized full-scale model ideally takes a smaller filter of the same product that is being used in large scale in order to have the same volume/membrane ratio at both scales. A worst-scale small-scale model can be obtained by changing the volume/membrane ratio. For loss in content by surface adsorption a smaller ratio corresponds to worst-case, whereas filter blocking will be more pronounced at a large volume/membrane ratio. Important is to perform the small-scale experiments at the same temperature as in production-scale. Furthermore, the pressure which drives the filtration has to be adjusted to correctly simulate the contact time of the product with the membrane. Moreover, the filter treatment should be as close as possible to the one in production (e.g. sterilization step), as this can impact the burden of leachables.

2.4.2. Friction-Related Protein Degradation

Friction between solid surfaces, which are also in contact with product solution can be found in the silicon carbide (SiC) sliding bearing of bottom-mounted magnetic-type stirrers of the compounding vessels and in dosing pumps. Even though particle formation had been previously linked to sliding bearings, the exact degradation mechanism was still unknown.[106,107] An explanation for physical degradation of proteins by pumping that could also be valid for sliding bearings was given by Tyagi et al. The authors reported particle formation by heterogeneous nucleation on stainless steel nanoparticles, which were introduced into the sample solution by wear of friction.[81] Other possible friction-related parameters that could potentially cause protein degradation and therefore had to be considered were frictional heat, abrasion of adsorbed proteins and extraordinary high shear rates which couldn't be investigated in publication I.

In order to identify the underlying mechanism of physical protein degradation inside the sliding bearing, a study, summarized in publication II, was performed by using custom designed small-scale bearings. A schematic of the used experimental set-up is given in Figure 10. The small-

scale bearing consisted of an outer static (stator) and inner rotating (rotator) part. The stator was hold in place by a stainless steel mount which allowed a certain freedom in movement to follow oscillations of the rotator. The rotator was fixed on a stainless steel stirring shaft; however, a stirring head without blades was used in order to minimize liquid flow related physical protein degradation at air/liquid interfaces. IgG1 was used as model protein as it was already characterized according to its stability against shear in publication I.

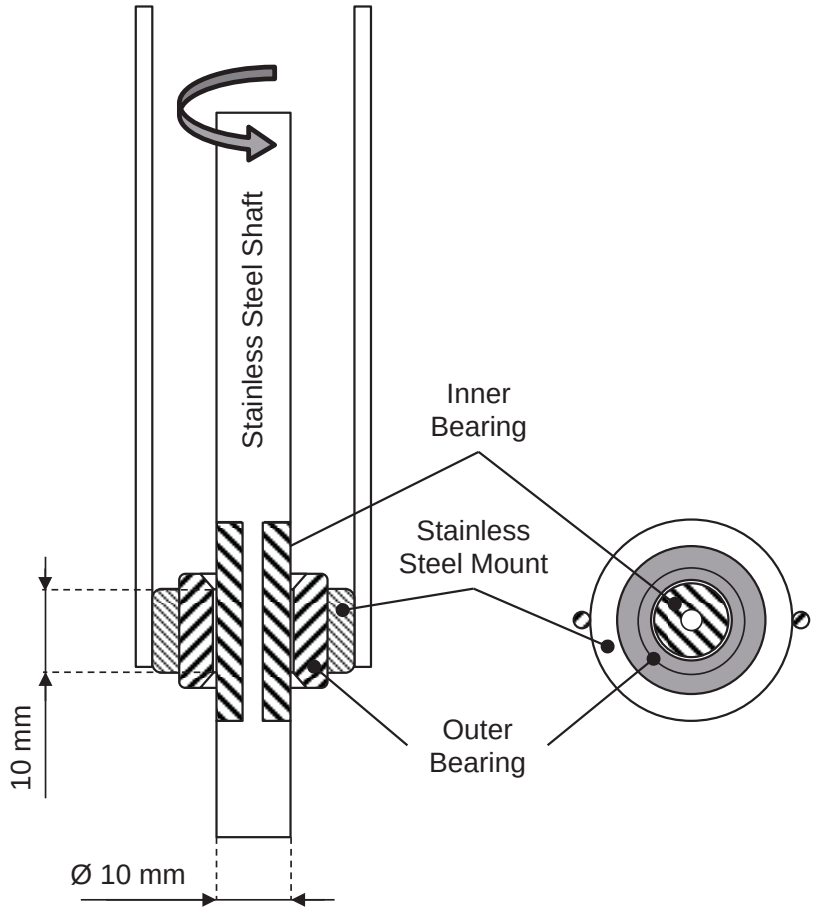

Figure 10: *Schematic (not to scale) of the custom designed small-scale sliding bearing which was for the identification of the physical protein degradation mechanism. Figure taken from publication II.*

At the beginning of the study it was shown, that the rotational movement of a SiC sliding bearing leads to pronounced physical IgG1 degradation, quantified by an increase in turbidity (particle formation) and by monomer loss. First of all, protein degradation by frictional heat creation within the SiC sliding bearing as well as heterogeneous nucleation on SiC particles that can be introduced by wear of friction were excluded as potential root cause. Subsequently, an experiment was performed to check for protein degradation by shear and abrasion of adsorbed proteins. Whereas the effect of high shear in the gap should be independent of the

material of the bearing, abrasion of adsorbed proteins depends on an initial adsorption step to solid surfaces that is determined by surface properties. By comparing protein degradation inside of a SiC and PTFE bearing in the presence of a surfactant against degradation without the protection of a surfactant, a strong dependence on the adsorption behavior to the surface of the bearing could be shown. As a consequence, abrasion of adsorbed proteins was identified as prevailing degradation mechanism, whereas shear in free solution was again excluded. Consequently, protein degradation by abrasion of adsorbed proteins within the sliding bearing was further characterized. A dependence on rotational speed, time and protein concentration in the bulk solution was shown. Furthermore, as protein degradation was a saturable process at higher protein concentrations, the monomer loss over time could be fitted by Michealis-Menten-type kinetics.

After identification of the degradation mechanism inside the sliding bearing, it was desirable to develop a worst-case small-scale model for abrasion of adsorbed proteins. As the degradation mechanism showed a high dependence on surface properties and excipients of the buffer, an important requirement for the model was the ability to screen proteins in various formulations for a wide scope of materials. Thus, a test system was introduced, where spheres of a specific material are placed inside a closed container, which is filled under the exclusion of air with sample solution (see Figure 11). Upon rotational movement of the container, the spheres create friction among each other which causes abrasion of adsorbed protein. The experimental set up of the test system had been described before, however it was not linked to a specific degradation mechanism other than “sensitivity against surfaces”.[110]

The test system was evaluated using rhGH and IgG1 as proteins and PTFE, stainless steel, glass and SiC as materials for the spheres (see publication II). Thereby, a better stability of rhGH against friction related particle formation compared to IgG1 could be shown, as well as a strong dependence of both proteins on adsorption behavior. The use of PTFE spheres in combination with a surfactant-containing sample solution minimized protein degradation for both proteins. Besides the ability of the test system to characterize stability against abrasion of adsorbed proteins, it was shown that also friction-related effects, such as the introduction of nano/micro particles or metal ions can be investigated. Thereby, it was discovered that friction between stainless steel spheres lead to an introduction of Fe^{3+} ions into the sample solution which most likely caused significant IgG1 degradation by oxidation. Finally, degradation products from the test system were compared with degradation products from various stress conditions by attenuated total reflection Fourier transform infrared (ATR-FTIR) spectroscopy. Highly similar

spectra were obtained for all friction-related degradation products, indicating a similar degradation pathway.

Figure 11: *Worst-case small-scale for abrasion of adsorbed proteins consisting of a glass vial, spheres of a specific size and material and a cover glass that is closing the system and fixed by parafilm ®. Figure taken from publication II.*

Summarizing, abrasion of adsorbed proteins was identified in publication II as a major root cause of protein degradation in processing steps where friction occurs between two solid surfaces that are in contact with the product. As a consequence, protein degradation inside a sliding bearing has to be considered in the design of a miniaturized full-scale model of a compounding vessel. With the test system in publication II, a worst-case small-scale system was introduced which can be easily used for formulation development.

2.5. Leachables

Compounds can leach into the product solution as a result of a direct contact and influence the stability during storage.[111] As the introduction of Fe^{3+} ions by friction of stainless steel led to subsequent protein oxidation (see abrasion of adsorbed proteins and publication II), it is a necessity to select all materials in miniaturized full-scale models according to large-scale.

3. Design of a Miniaturized Full-Scale Compounding Vessel

3.1. Requirements

After the evaluation of the criticality of the stress parameters on protein stability, the next step was to design a miniaturized full-scale vessel of the compounding vessels from the investigated production site. Based on the evaluation of the individual stress parameters (see above) and specific needs from the lab, the vessel had to fulfill following requirements:

- Size: 1000 – 1500 mL
- Materials: Same materials as in large-scale:

  Vessel: Stainless Steel 1.4404 (AISI 316L); Stirrer head 1.4435 (AISI 316L), Sliding bearing: SiC and EPDM gaskets

- Stirrer: Large-scale vessels are equipped with magnetic bottom type stirrer (off center) where friction-related protein particle formation can happen inside the sliding bearing. This stress parameter needs to be present in the miniaturized full-scale vessels. The stirrer design should be similar to full-scale in order to obtain a representative flow pattern (mainly radial flow).
- Inlet tube for drug substance: The drug substance is added to the compounding vessel in large scale via an inlet tube that guides the liquid to the vessel wall (low foam inlet). Thereby, potential air/liquid interfacial effects could occur that should be simulated in the miniaturized full-scale vessel.
- Possibility to create a nitrogen overlay above atmospheric pressure for pressure driven filtration
- Possibility for introduction of nitrogen into the solution in case the vessel is used for the preparation of excipient solutions
- Support for pH probes from benchtop pH meters.

3.2. Design of Miniaturized Full-Scale Vessel

The design of the vessel-body was predominantly determined by the requirement of an operating volume of about 1000 mL and geometric similarities to the production-scale vessels to obtain similar bulk-flow characteristics.[112] The resulting inner diameter of the miniaturized full-scale vessel of 115 mm demanded an impeller diameter of roughly 40 mm to obtain the production-scale ratio of impeller/vessel diameter of 0.35. This small diameter prevented the use of commercially available magnetic bottom type stirrers. For this reason, a top-entered stirrer had to be used. In order to assure a closed stirring system, the top-entered stirrer and the engine were connected using a magnetic coupling. However, in the absence of the sliding bearing of a magnetic bottom type stirrers no protein degradation by abrasion of adsorbed proteins happens during compounding. Therefore, the sliding bearing was simulated at the top entered stirrer shaft similar to the used experimental set-up of publication II (Figure 10). Thereby, the inner (rotating) part of the SiC bearing is fixed on the shaft of the stirrer. EPDM gaskets were used for sealing the gaps. The outer (static) part of the simulated SiC bearing is embedded in a stainless steel ring which is kept in position by a stainless steel fork. Thereby, the vertical position of the outer bearing is defined but the mount provides a certain freedom in movement to follow oscillations of the rotating part (see Figure 13). Identical angles of the impeller blades and an off-centered position as in production further contribute to a similar bulk flow and vortex formation characteristics.

A low foam inlet was designed to guide the liquid to the wall of the vessel as it happens in production-scale (see Figure 14 left). The support for bench-top pH meter probes has a gasket at the inside to ensure a closed system (see Figure 14 right).

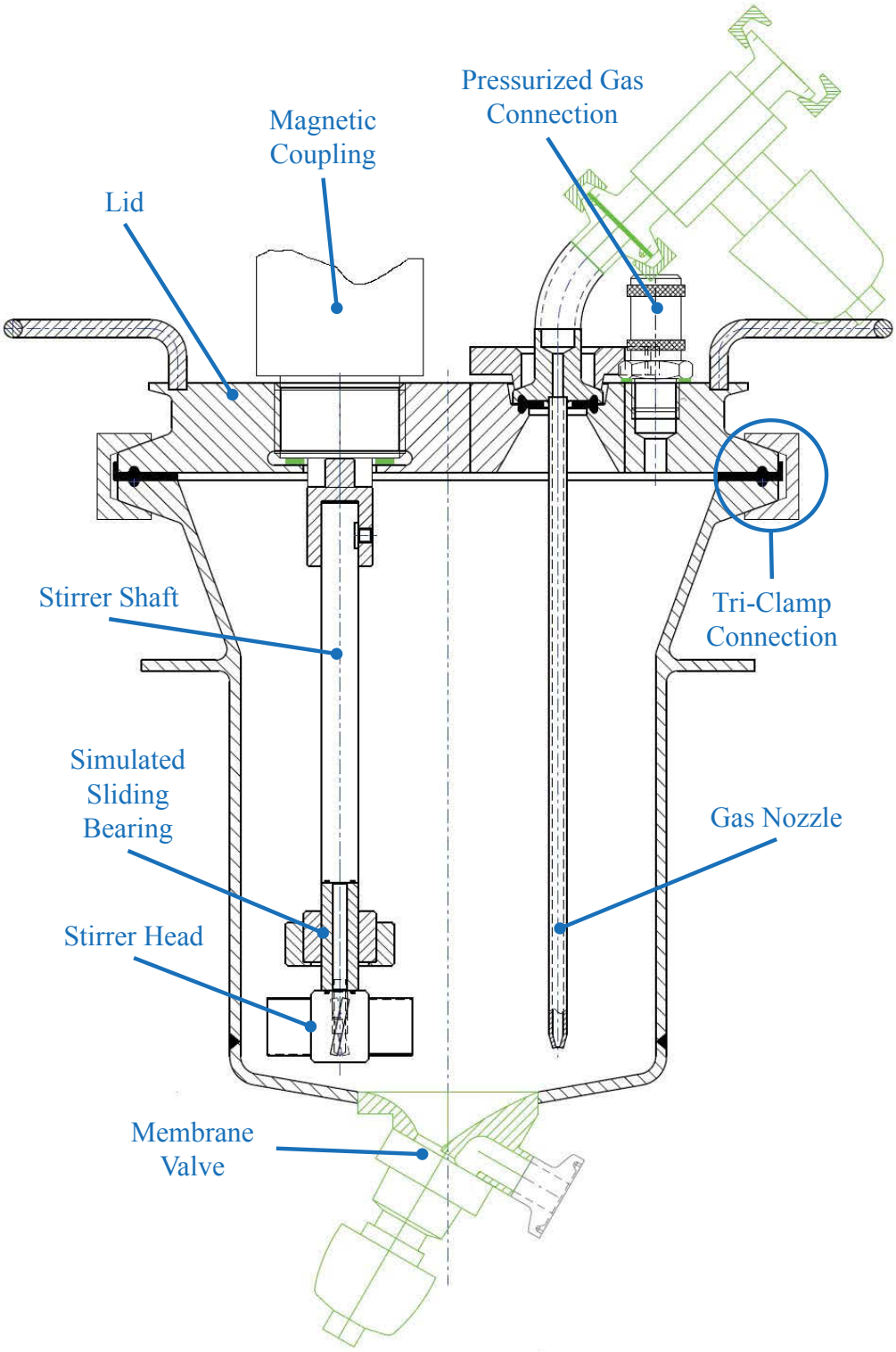

Figure 12: *Overview of the designed miniaturized full-scale vessel. The shown set-up consists of the vessel itself with a membrane valve at the bottom, the lid of the vessel which is fixed by a tri-clamp system, the top-entered stirrer which is mounted to a magnetic coupling, a connection for pressurized gas and the simulated sliding bearing. The pH probe adapter and the low foam inlet are not shown in this sectional view; however, they can be mounted using the same connection type as the gas nozzle at different positions at the lid.*

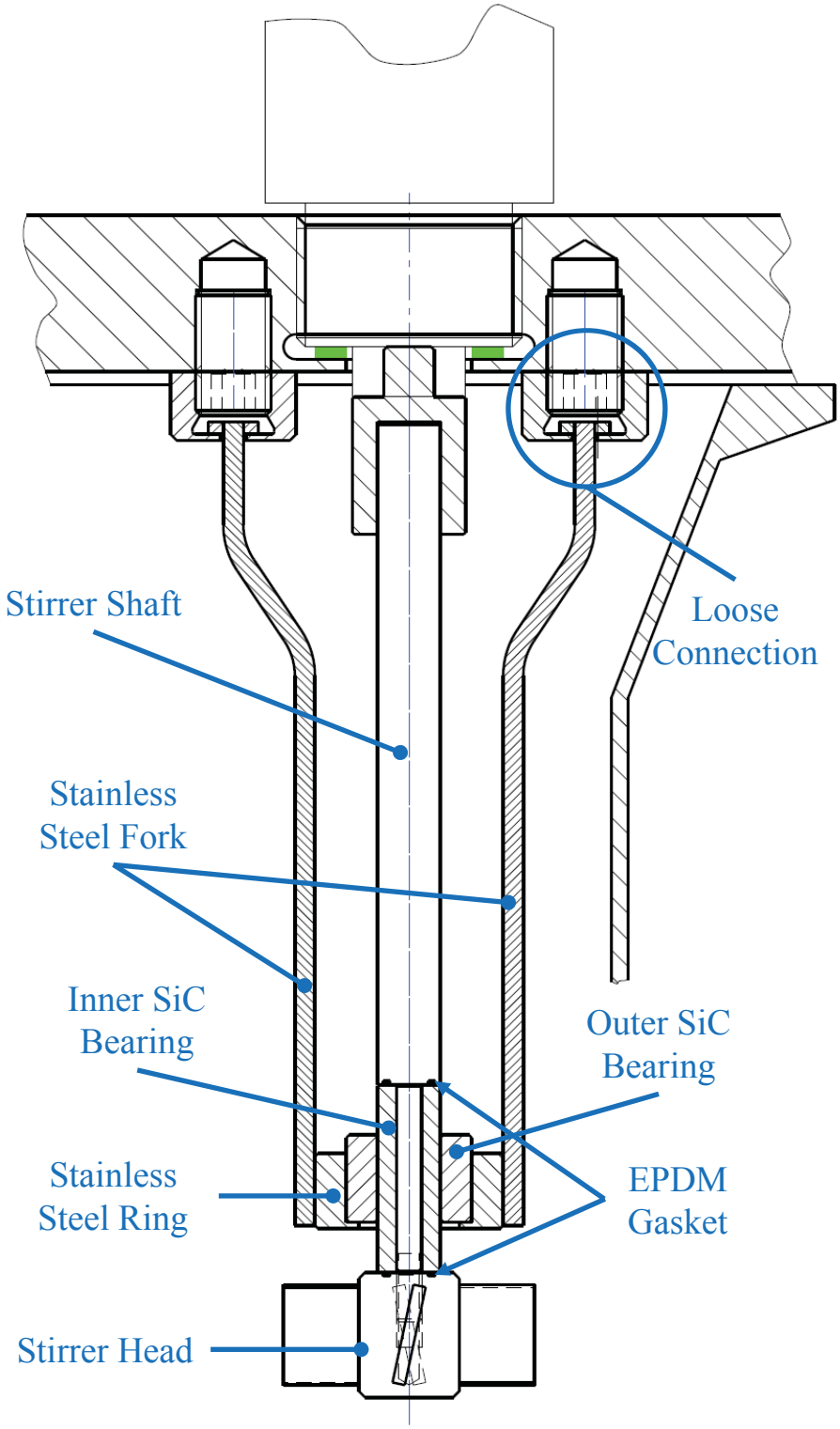

Figure 13: *Detailed view of the simulated SiC sliding bearing. The inner part of the bearing (rotor) is fixed to the stirrer shaft by the stirrer head and the gaps are sealed with EPDM gaskets. The outer part of the bearing (stator) is embedded inside a stainless steel ring which is kept in position by a stainless steel fork. The loose connection of the stainless steel fork to the lid provides a certain freedom in movement.*

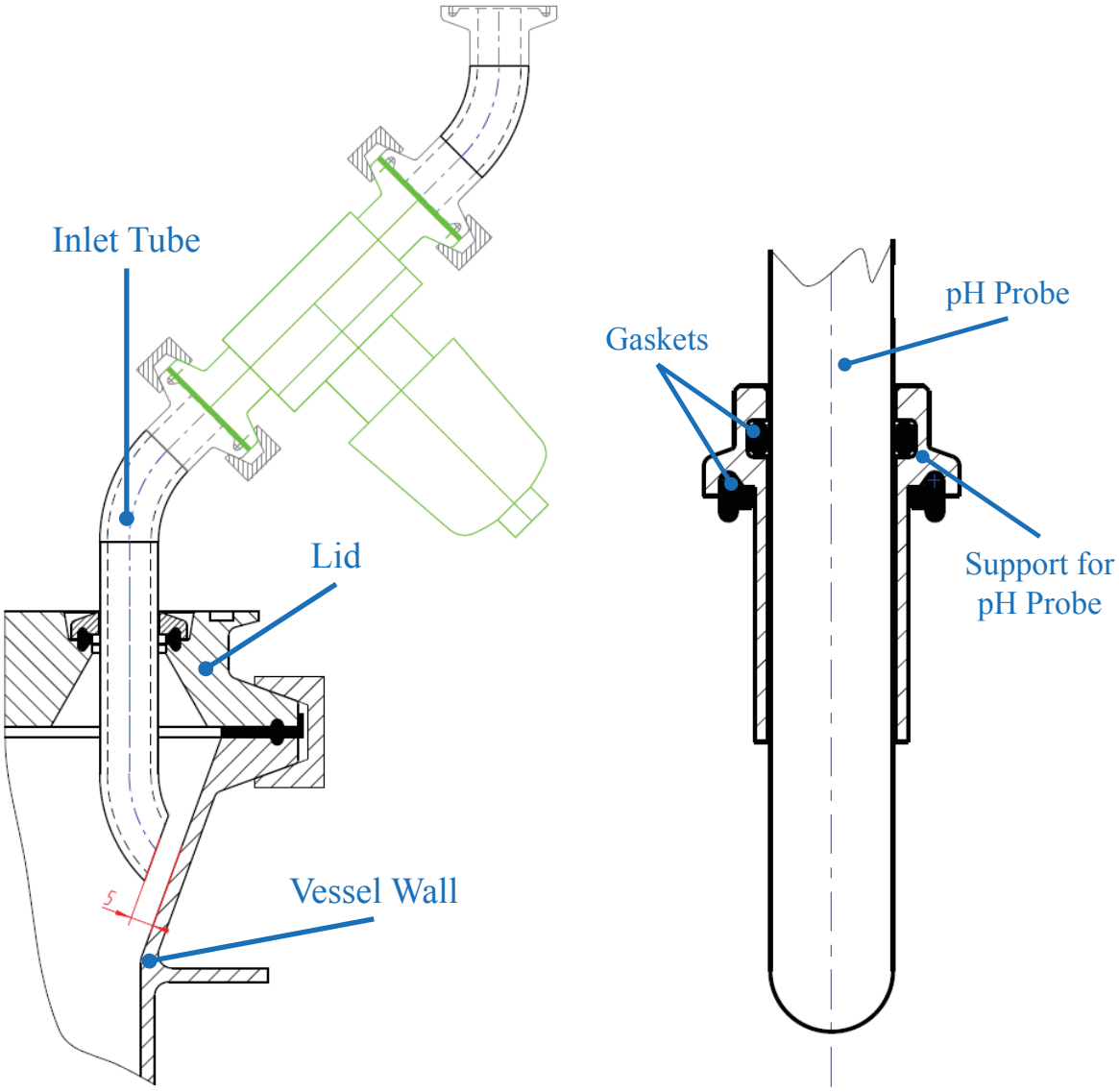

Figure 14: *Left: Detailed view of the low-foam inlet tube which can be mounted to the lid in a distance of 5 mm to the wall of the vessel. Right: Detailed view of the support for a pH probe.*

CONCLUSION

Summarizing, it can be said that the objectives of this work were met:

- After the identification of the theoretical stress parameters that can occur during formulation, fill and finish operations, an evaluation of the impact of shear on proteins in free solution was performed in publication I. This was important as shear is caused by velocity gradients in liquids which basically occur at every processing step. For the evaluation, a worst-case model was established, which allowed to determine the secondary and tertiary protein structure *in situ* during shearing. No effect of shear on recombinant human growth hormone and an IgG1 antibody in free solution was observed up to shear rates of at least 10^4 s^{-1}. Thus, it is very likely that shear does not have to be considered as relevant stress factor in the design of miniaturized full-scale models.

  Friction-related protein particle formation was investigated in publication II by means of physical protein degradation inside of sliding bearings. Thereby, extraordinary high shear rates, cavitation, heat induced denaturation and heterogeneous nucleation on nano/micro particles could be excluded as root cause for particle formation. However, abrasion of adsorbed proteins was identified as predominant degradation mechanism. Investigations using ATR-FTIR supported the concept that this mechanism is present at all processing steps, where friction occurs between two solid surfaces that are in contact to the product.
- A simple worst-case small-scale model for physical protein degradation by abrasion of adsorbed proteins is additionally presented in publication II. The model consists of a closed container which contains spheres of a certain size and material as well as the sample solution. Upon rotation of the container, the spheres begin to move and create friction between each other. As the spheres and the sample solution can be simply exchanged, the model has a wide scope of materials and formulations that can be tested against each other. Thus, this model is ideal for formulation development purposes.
- Based on the identification and evaluation of the various potential stress parameters, a miniaturized full-scale vessel was designed and produced. The vessel was equipped with a simulated SiC sliding bearing and a low-foam inlet tube. These elements are necessary to representatively simulate the stress on protein solutions during production-scale compounding operations.

REFERENCES

1. Pavlou AK, Belsey MJ 2005. The therapeutic antibodies market to 2008. European Journal of Pharmaceutics and Biopharmaceutics 59(3):389-396.
2. Johnson IS 1983. Human insulin from recombinant DNA technology. Science 219(4585):632-637.
3. Takeda A, Cooper K, Bird A, Baxter L, Frampton G, Gospodarevskaya E, Welch K, Bryant J 2010. Recombinant human growth hormone for the treatment of growth disorders in children: a systematic review and economic evaluation. Health technology assessment (Winchester, England) 14(42):1-209.
4. Elvin JG, Couston RG, van der Walle CF 2013. Therapeutic antibodies: market considerations, disease targets and bioprocessing. International journal of pharmaceutics 440(1):83-98.
5. Walsh G 2000. Biopharmaceutical benchmarks. Nature biotechnology 18(8):831-833.
6. Sanchez-Garcia L, Martín L, Mangues R, Ferrer-Miralles N, Vázquez E, Villaverde A 2016. Recombinant pharmaceuticals from microbial cells: a 2015 update. Microbial cell factories 15(1):1.
7. Pickering L 2011. Opportunities for Monoclonal Antibodies: Where Companies are Spending Their Antibody Dollars. Decision Resources, Burlington.
8. Walsh G 2014. Biopharmaceutical benchmarks 2014. Nature biotechnology 32(10):992-1000.
9. Sekhon BS, Saluja V 2011. Biosimilars: an overview. Biosimilars 1(1):1-11.
10. Burki TK 2015. First biosimilar drug approved in the USA. The Lancet Oncology 16(4):e161.
11. Shukla AA, Hubbard B, Tressel T, Guhan S, Low D 2007. Downstream processing of monoclonal antibodies—application of platform approaches. Journal of Chromatography B 848(1):28-39.
12. Rathore N, Rajan RS, Freund E 2010. Impact of Manufacturing Processes on Drug Product Stability and Quality. Formulation and Process Development Strategies for Manufacturing Biopharmaceuticals:917-940.
13. Rathore N, Rajan RS 2008. Current perspectives on stability of protein drug products during formulation, fill and finish operations. Biotechnology progress 24(3):504-514.
14. Kolhe P, Holding E, Lary A, Chico S, Singh SK 2010. Large-Scale Freezing of Biologics: Understanding Protein and Solute Concentration Changes in a Cryovessel— Part I. BioPharm International 23(6).
15. Chisti Y 1992. Assure bioreactor sterility. Chemical engineering progress 88:80-80.
16. Somiya S. 2013. Handbook of advanced ceramics: materials, applications, processing, and properties. ed.: Academic Press.
17. Shukla AA, Gottschalk U 2013. Single-use disposable technologies for biopharmaceutical manufacturing. Trends in biotechnology 31(3):147-154.
18. Mahler HC, Printz M, Kopf R, Schuller R, Müller R 2008. Behaviour of polysorbate 20 during dialysis, concentration and filtration using membrane separation techniques. Journal of pharmaceutical sciences 97(2):764-774.
19. Kumar A, Martin J, Kuriyel R 2015. Scale-up of Sterilizing-grade Membrane Filters from Discs to Pleated Cartridges: Effects of Operating Parameters and Solution Properties. PDA Journal of Pharmaceutical Science and Technology 69(1):74-87.
20. Thomas C, Geer D 2011. Effects of shear on proteins in solution. Biotechnology letters 33(3):443-456.
21. Mahler H-C, Borchard G, Luessen HL. 2010. Protein pharmaceuticals: formulation, analytics and delivery. ed.: ECV-Editio Cantor-Verlag.

22. Wang W 1999. Instability, stabilization, and formulation of liquid protein pharmaceuticals. International journal of pharmaceutics 185(2):129-188.
23. Dill KA 1990. Dominant forces in protein folding. Biochemistry 29(31):7133-7155.
24. Price NC, Dwek RA. 2009. Principles and problems in physical chemistry for biochemists. Third Edition ed.: Oxford University Press.
25. Menzen T, Friess W 2013. High-throughput melting-temperature analysis of a monoclonal antibody by differential scanning fluorimetry in the presence of surfactants. Journal of pharmaceutical sciences 102(2):415-428.
26. Pace CN, Scholtz JM 1997. Measuring the conformational stability of a protein. Protein structure: A practical approach 2:299-321.
27. O'Brien EP, Dima RI, Brooks B, Thirumalai D 2007. Interactions between hydrophobic and ionic solutes in aqueous guanidinium chloride and urea solutions: lessons for protein denaturation mechanism. Journal of the American Chemical Society 129(23):7346-7353.
28. Niesen FH, Berglund H, Vedadi M 2007. The use of differential scanning fluorimetry to detect ligand interactions that promote protein stability. Nature protocols 2(9):2212-2221.
29. Brockwell D 2007. Probing the mechanical stability of proteins using the atomic force microscope. Biochemical Society Transactions 35(6):1564-1568.
30. Cao Y, Li H 2008. How do chemical denaturants affect the mechanical folding and unfolding of proteins? Journal of molecular biology 375(1):316-324.
31. Chi EY, Krishnan S, Randolph TW, Carpenter JF 2003. Physical stability of proteins in aqueous solution: mechanism and driving forces in nonnative protein aggregation. Pharmaceutical research 20(9):1325-1336.
32. Lehermayr C, Mahler HC, Mäder K, Fischer S 2011. Assessment of net charge and protein–protein interactions of different monoclonal antibodies. Journal of pharmaceutical sciences 100(7):2551-2562.
33. Manning MC, Chou DK, Murphy BM, Payne RW, Katayama DS 2010. Stability of protein pharmaceuticals: an update. Pharmaceutical research 27(4):544-575.
34. Topp EM, Zhang L, Zhao H, Payne RW, Evans GJ, Manning MC. 2010. Chemical instability in peptide and protein pharmaceuticals. ed.: John Wiley & Sons, Inc., Hoboken, NJ, USA.
35. Wang W, Nema S, Teagarden D 2010. Protein aggregation—pathways and influencing factors. International journal of pharmaceutics 390(2):89-99.
36. Wang W 2005. Protein aggregation and its inhibition in biopharmaceutics. International journal of pharmaceutics 289(1):1-30.
37. Cleland JL, Powell MF, Shire SJ 1992. The development of stable protein formulations: a close look at protein aggregation, deamidation, and oxidation. Critical reviews in therapeutic drug carrier systems 10(4):307-377.
38. Meyer JD, Ho B, Manning MC. 2002. Effects of conformation on the chemical stability of pharmaceutically relevant polypeptides. Rational design of stable protein formulations, ed.: Springer. p 85-107.
39. Nguyen TH 1995. Oxidation Degradation of Protein Pharmaceuticals. ChemInform 26(4).
40. Chen B, Bautista R, Yu K, Zapata GA, Mulkerrin MG, Chamow SM 2003. Influence of histidine on the stability and physical properties of a fully human antibody in aqueous and solid forms. Pharmaceutical research 20(12):1952-1960.
41. Liu W, Swift R, Torraca G, Nashed-Samuel Y, Wen Z-Q, Jiang Y, Vance A, Mire-Sluis A, Freund E, Davis J 2010. Root cause analysis of tungsten-induced protein aggregation in pre-filled syringes. PDA Journal of Pharmaceutical Science and Technology 64(1):11-19.
42. Hovorka SW, Schöneich C 2001. Oxidative degradation of pharmaceuticals: Theory, mechanisms and inhibition. Journal of pharmaceutical sciences 90(3):253-269.

43. Schöneich C 2000. Mechanisms of metal-catalyzed oxidation of histidine to 2-oxo-histidine in peptides and proteins. Journal of pharmaceutical and biomedical analysis 21(6):1093-1097.
44. Buettner GR, Jurkiewicz BA 1996. Catalytic metals, ascorbate and free radicals: combinations to avoid. Radiation research 145(5):532-541.
45. Yang TH, Cleland JL, Lam X, Meyer JD, Jones LS, Randolph TW, Manning MC, Carpenter JF 2000. Effect of zinc binding and precipitation on structures of recombinant human growth hormone and nerve growth factor. Journal of pharmaceutical sciences 89(11):1480-1485.
46. Zhao F, Ghezzo-Schöneich E, Aced GI, Hong J, Milby T, Schöneich C 1997. Metal-catalyzed oxidation of histidine in human growth hormone mechanism, isotope effects, and inhibition by a mild denaturing alcohol. Journal of Biological Chemistry 272(14):9019-9029.
47. Harmon PA, Kosuda K, Nelson E, Mowery M, Reed RA 2006. A novel peroxy radical based oxidative stressing system for ranking the oxidizability of drug substances. Journal of pharmaceutical sciences 95(9):2014-2028.
48. Fransson J, FIorin-Robertsson E, Axelsson K, Nyhlén C 1996. Oxidation of human insulin-like growth factor I in formulation studies: kinetics of methionine oxidation in aqueous solution and in solid state. Pharmaceutical research 13(8):1252-1257.
49. Kerwin BA, Remmele RL 2007. Protect from light: photodegradation and protein biologics. Journal of pharmaceutical sciences 96(6):1468-1479.
50. Pattison DI, Rahmanto AS, Davies MJ 2012. Photo-oxidation of proteins. Photochemical & Photobiological Sciences 11(1):38-53.
51. Liu D, Ren D, Huang H, Dankberg J, Rosenfeld R, Cocco MJ, Li L, Brems DN, Remmele Jr RL 2008. Structure and stability changes of human IgG1 Fc as a consequence of methionine oxidation. Biochemistry 47(18):5088-5100.
52. Mahler HC, Friess W, Grauschopf U, Kiese S 2009. Protein aggregation: pathways, induction factors and analysis. Journal of pharmaceutical sciences 98(9):2909-2934.
53. Mahler HC, Huber F, Kishore RS, Reindl J, Rückert P, Müller R 2010. Adsorption behavior of a surfactant and a monoclonal antibody to sterilizing-grade filters. Journal of pharmaceutical sciences 99(6):2620-2627.
54. Rabe M, Verdes D, Seeger S 2011. Understanding protein adsorption phenomena at solid surfaces. Advances in colloid and interface science 162(1):87-106.
55. Doran PM. 1995. Bioprocess engineering principles. ed.: Academic press.
56. Bird RB, Stewart WE, Lightfoot EN 2002. Transport phenomena. Second Edition. John Wiley & Sons, Inc, New York.
57. Bekard IB, Asimakis P, Bertolini J, Dunstan DE 2011. The effects of shear flow on protein structure and function. Biopolymers 95(11):733-745.
58. Mezger TG. 2006. The rheology handbook: for users of rotational and oscillatory rheometers. ed.: Vincentz Network GmbH & Co KG.
59. Pérez JS, Porcel ER, López JC, Sevilla JF, Chisti Y 2006. Shear rate in stirred tank and bubble column bioreactors. Chemical Engineering Journal 124(1):1-5.
60. Norden B, Kubista M, Kurucsev T 1992. Linear dichroism spectroscopy of nucleic acids. Quarterly reviews of biophysics 25(01):51-170.
61. Jaspe J, Hagen SJ 2006. Do protein molecules unfold in a simple shear flow? Biophysical journal 91(9):3415-3424.
62. Charm SE, Wong BL 1981. Shear effects on enzymes. Enzyme and Microbial Technology 3(2):111-118.
63. Charm S, Wong B 1970. Enzyme inactivation with shearing. Biotechnology and bioengineering 12(6):1103-1109.

64. Charm S, Lai C 1971. Comparison of ultrafiltration systems for concentration of biologicals. Biotechnology and bioengineering 13(2):185-202.
65. Charm SE, Wong BL 1978. Shear inactivation in mixing biological material. Biotechnology and Bioengineering 20(3):451-453.
66. Tirrell M, Middleman S 1975. Shear modification of enzyme kinetics. Biotechnology and Bioengineering 17(2):299-303.
67. Bowen WR, Gan Q 1992. Properties of microfiltration membranes: The effects of adsorption and shear on the recovery of an enzyme. Biotechnology and bioengineering 40(4):491-497.
68. Virkar P, Narendranathan T, Hoare M, Dunnill P 1981. Studies of the effect of shear on globular proteins: Extension to high shear fields and to pumps. Biotechnology and Bioengineering 23(2):425-429.
69. Thomas C, Nienow A, Dunnill P 1979. Action of shear on enzymes: studies with alcohol dehydrogenase. Biotechnology and bioengineering 21(12):2263-2278.
70. Harrington T, Gainer J, Kirwan D 1991. Effects of fluid shear on immobilized enzyme kinetics. Enzyme and microbial technology 13(8):610-616.
71. Bee JS, Chiu D, Sawicki S, Stevenson JL, Chatterjee K, Freund E, Carpenter JF, Randolph TW 2009. Monoclonal antibody interactions with micro-and nanoparticles: Adsorption, aggregation, and accelerated stress studies. Journal of pharmaceutical sciences 98(9):3218-3238.
72. Biddlecombe JG, Craig AV, Zhang H, Uddin S, Mulot S, Fish BC, Bracewell DG 2007. Determining Antibody Stability: Creation of Solid-Liquid Interfacial Effects within a High Shear Environment. Biotechnology progress 23(5):1218-1222.
73. Biddlecombe JG, Smith G, Uddin S, Mulot S, Spencer D, Gee C, Fish BC, Bracewell DG 2009. Factors influencing antibody stability at solid–liquid interfaces in a high shear environment. Biotechnology progress 25(5):1499-1507.
74. Perevozchikova T, Nanda H, Nesta DP, Roberts CJ 2015. Protein Adsorption, Desorption, and Aggregation Mediated by Solid–Liquid Interfaces. Journal of pharmaceutical sciences 104(6):1946-1959.
75. Bekard IB, Asimakis P, Teoh CL, Ryan T, Howlett GJ, Bertolini J, Dunstan DE 2012. Bovine serum albumin unfolds in Couette flow. Soft Matter 8(2):385-389.
76. Bekard IB, Dunstan DE 2009. Shear-induced deformation of bovine insulin in Couette flow. The Journal of Physical Chemistry B 113(25):8453-8457.
77. Höger K, Becherer T, Qiang W, Haag R, Frieß W, Küchler S 2013. Polyglycerol coatings of glass vials for protein resistance. European Journal of Pharmaceutics and Biopharmaceutics 85(3):756-764.
78. Doran PM 2006. Loss of secreted antibody from transgenic plant tissue cultures due to surface adsorption. Journal of biotechnology 122(1):39-54.
79. Satzer P, Svec F, Sekot G, Jungbauer A 2015. Protein adsorption onto nanoparticles induces conformational changes: Particle size dependency, kinetics, and mechanisms. Engineering in Life Sciences.
80. Lundqvist M, Sethson I, Jonsson B-H 2005. Transient interaction with nanoparticles “freezes” a protein in an ensemble of metastable near-native conformations. Biochemistry 44(30):10093-10099.
81. Tyagi AK, Randolph TW, Dong A, Maloney KM, Hitscherich C, Carpenter JF 2009. IgG particle formation during filling pump operation: A case study of heterogeneous nucleation on stainless steel nanoparticles. Journal of pharmaceutical sciences 98(1):94-104.
82. Sediq AS, van Duijvenvoorde R, Jiskoot W, Nejadnik MR 2016. No Touching! Abrasion of Adsorbed Protein Is the Root Cause of Subvisible Particle Formation During Stirring. Journal of Pharmaceutical Sciences.

83. Bee JS, Schwartz DK, Trabelsi S, Freund E, Stevenson JL, Carpenter JF, Randolph TW 2012. Production of particles of therapeutic proteins at the air–water interface during compression/dilation cycles. Soft Matter 8(40):10329-10335.
84. Kiese S, Papppenberger A, Friess W, Mahler HC 2008. Shaken, not stirred: mechanical stress testing of an IgG1 antibody. Journal of pharmaceutical sciences 97(10):4347-4366.
85. Britt KA, Schwartz DK, Wurth C, Mahler HC, Carpenter JF, Randolph TW 2012. Excipient effects on humanized monoclonal antibody interactions with silicone oil emulsions. Journal of pharmaceutical sciences 101(12):4419-4432.
86. Jones LS, Kaufmann A, Middaugh CR 2005. Silicone oil induced aggregation of proteins. Journal of pharmaceutical sciences 94(4):918-927.
87. Basu P, Krishnan S, Thirumangalathu R, Randolph TW, Carpenter JF 2013. IgG1 aggregation and particle formation induced by silicone-water interfaces on siliconized borosilicate glass beads: A model for siliconized primary containers. Journal of pharmaceutical sciences 102(3):852-865.
88. Chang BS, Kendrick BS, Carpenter JF 1996. Surface-induced denaturation of proteins during freezing and its inhibition by surfactants. Journal of pharmaceutical sciences 85(12):1325-1330.
89. Strambini GB, Gabellieri E 1996. Proteins in frozen solutions: evidence of ice-induced partial unfolding. Biophysical journal 70(2):971.
90. Dasnoy S, Dezutter N, Lemoine D, Le Bras V, Préat V 2011. High-throughput screening of excipients intended to prevent antigen aggregation at air-liquid interface. Pharmaceutical research 28(7):1591-1605.
91. Wang W, Wang YJ, Wang D 2008. Dual effects of Tween 80 on protein stability. International journal of pharmaceutics 347(1):31-38.
92. Treuheit MJ, Kosky AA, Brems DN 2002. Inverse relationship of protein concentration and aggregation. Pharmaceutical research 19(4):511-516.
93. Krielgaard L, Jones LS, Randolph TW, Frokjaer S, Flink JM, Manning MC, Carpenter JF 1998. Effect of Tween 20 on freeze-thawing-and agitation-induced aggregation of recombinant human factor XIII. Journal of pharmaceutical sciences 87(12):1593-1603.
94. Duncan MR, Lee JM, Warchol MP 1995. Influence of surfactants upon protein/peptide adsorption to glass and polypropylene. International journal of pharmaceutics 120(2):179-188.
95. Kerwin BA 2008. Polysorbates 20 and 80 used in the formulation of protein biotherapeutics: structure and degradation pathways. Journal of pharmaceutical sciences 97(8):2924-2935.
96. Serno T, Härtl E, Besheer A, Miller R, Winter G 2013. The role of polysorbate 80 and HPβCD at the air-water interface of IgG solutions. Pharmaceutical research 30(1):117-130.
97. Hoffmann C, Blume A, Miller I, Garidel P 2009. Insights into protein–polysorbate interactions analysed by means of isothermal titration and differential scanning calorimetry. European Biophysics Journal 38(5):557-568.
98. Bam NB, Cleland JL, Yang J, Manning MC, Carpenter JF, Kelley RF, Randolph TW 1998. Tween protects recombinant human growth hormone against agitation-induced damage via hydrophobic interactions. Journal of pharmaceutical sciences 87(12):1554-1559.
99. Bam NB, Randolph TW, Cleland JL 1995. Stability of protein formulations: investigation of surfactant effects by a novel EPR spectroscopic technique. Pharmaceutical research 12(1):2-11.
100. Chou DK, Krishnamurthy R, Randolph TW, Carpenter JF, Manning MC 2005. Effects of Tween 20® and Tween 80® on the stability of Albutropin during agitation. Journal of Pharmaceutical Sciences 94(6):1368-1381.
101. Guideline IHT 2012. Development and Manufacture of Drug Substances(Chemical Entities and Biotechnological/Biological Entities) Q11. Step 4 Version.

102. Guideline IHT 2009. Pharmaceutical Development Q8(R2) Step 4 Version.
103. Rathore AS, Winkle H 2009. Quality by design for biopharmaceuticals. Nature biotechnology 27(1):26-34.
104. Moscariello J 2016. Scale-Down Model: An indispensable tool to biopharmaceutical process development. Pharma's Almanac (Q2):48-50.
105. Robertson B, Ulbrecht J 1987. Measurement of shear rate on an agitator in a fermentation broth. AMERICAN INSTITUTE OF CHEMICAL ENGINEERS, NEW YORK, NY(USA) 1987.
106. Ishikawa T, Kobayashi N, Osawa C, Sawa E, Wakamatsu K 2010. Prevention of stirring-induced microparticle formation in monoclonal antibody solutions. Biological and Pharmaceutical Bulletin 33(6):1043-1046.
107. Gikanga B, Chen Y, Stauch OB, Maa Y-F 2015. Mixing Monoclonal Antibody Formulations Using Bottom-Mounted Mixers: Impact of Mechanism and Design on Drug Product Quality. PDA Journal of Pharmaceutical Science and Technology 69(2):284-296.
108. Chantalat L, Jones N, Korber F, Navaza J, Pavlovsky A 1995. The crystalstructure of wild-type growth hormone at 2.5 Aresolution. Protein Pept Lett 2:333-340.
109. Bork P, Holm L, Sander C 1994. The immunoglobulin fold: structural classification, sequence patterns and common core. Journal of molecular biology 242(4):309-320.
110. Denkinger SN. 2010. Modelle zur Simulation des Abfüllprozesses biologisch-pharmazeutischer Arzneimittel (Doctoral dissertation). ed.: Universitäts-und Landesbibliothek Bonn.
111. Bee JS, Randolph TW, Carpenter JF, Bishop SM, Dimitrova MN 2011. Effects of surfaces and leachables on the stability of biopharmaceuticals. Journal of pharmaceutical sciences 100(10):4158-4170.
112. McConville FX, Kessler SB 2010. Scale-Up of Mixing Processes: A Primer. Chemical Engineering in the Pharmaceutical Industry: R&D to Manufacturing:249-267.

LIST OF FIGURES

PUBLICATIONS

I. Brückl L, Schröder T, Scheler S, Hahn R, Sonderegger C

The Effect of Shear on the Structural Conformation of rhGH and IgG1 in Free Solution.

2016, Journal of Pharmaceutical Sciences 105(6):1810-1818
http://dx.doi.org/10.1016/j.xphs.2016.03.020

II. Brückl L, Hahn R, Sergi M, Scheler S

A systematic evaluation of mechanisms, material effects, and protein-dependent differences on friction-related protein particle formation in formulation and filling steps.

2016, International Journal of Pharmaceutics 511(2):931-945
http://dx.doi.org/10.1016/j.ijpharm.2016.08.006

Graphical Abstract:

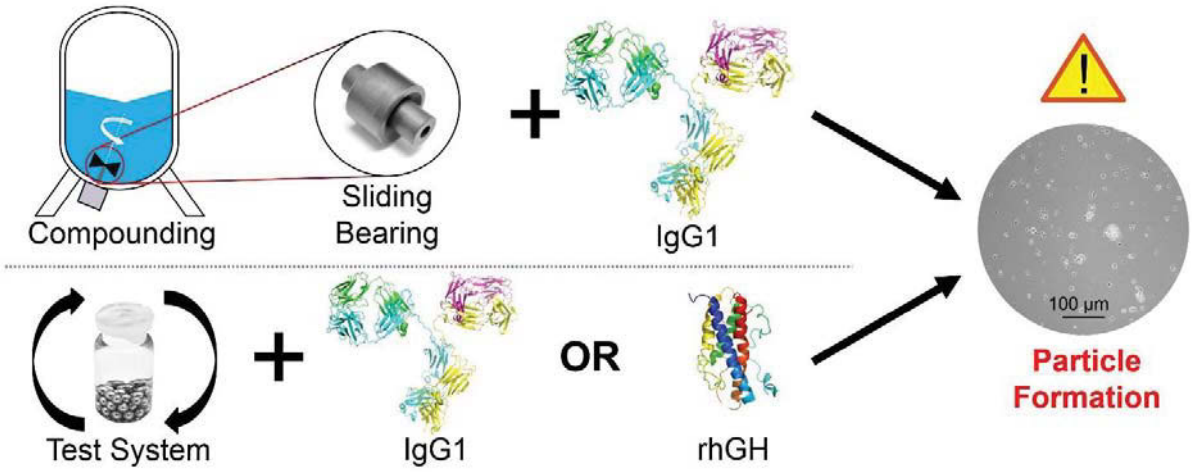

Journal of Pharmaceutical Sciences 105 (2016) 1810–1818

Contents lists available at ScienceDirect

Journal of Pharmaceutical Sciences

journal homepage: www.jpharmsci.org

Pharmaceutical Biotechnology

The Effect of Shear on the Structural Conformation of rhGH and IgG1 in Free Solution

Lukas Brückl [1, 2, *], Thomas Schröder [1], Stefan Scheler [1], Rainer Hahn [2], Corinna Sonderegger [1]

[1] Department of Pharmaceutical Development, Sandoz GmbH, 6336 Langkampfen, Austria
[2] Department of Biotechnology, University of Natural Resources and Applied Life Sciences Vienna, 1190 Vienna, Austria

ARTICLE INFO

Article history:
Received 2 November 2015
Revised 10 March 2016
Accepted 15 March 2016
Available online 28 April 2016

Keywords:
protein aggregation
physical stability
circular dichroism
IgG antibody
surfactants

ABSTRACT

The effect of hydrodynamic forces on proteins in free solution, also referred to as shear stress in multiple drug substance and drug product processing steps, was investigated by means of *in situ* and inline biophysical measurements. The use of a quartz Couette cell in combination with a circular dichroism spectrometer allowed simultaneously the creation of simple shear flow and direct measurements of the proteins' secondary and tertiary structure. Recombinant human growth hormone and an IgG1 mAb were chosen as model proteins. Under the exclusion of interfacial effects by the addition of a surfactant, no unfolding was observed due to shearing for 30 min up to the highest possible shear rate under laminar flow (3840 s^{-1}). In another experiment, guanidine hydrochloride was added to a surfactant-protected and sheared sample to lower the thermodynamic and mechanical stability of the proteins. However, even under these destabilizing conditions, the proteins showed no change in their secondary and tertiary structure. We conclude that shear stress in terms of velocity gradients is unlikely to unfold the investigated proteins in free solution up to shear rates of at least 10^4 s^{-1}.

Introduction

Since the approval of the first biopharmaceutical in 1982, the market has been growing enormously.[1,2] However, the era of protein-based drugs has brought some new challenges for the pharmaceutical industry. Protein stability over the various processing steps during manufacturing and over the claimed shelf life is a major concern. Besides changes of the primary peptide structure, including deamidation, isomerization, hydrolysis, and oxidation, which are characterized by the formation or cleavage of covalent bonds, protein-based drugs may also suffer from instabilities related to the physical state of chemically unaltered proteins.[3] As a consequence, proteins tend to denature or aggregate, thereby increasing the potential for immunogenicity, changed biological activity, or other adverse effects of the drug.[4]

One of the factors being frequently reported to have an influence on the physical stability of the proteins is shear stress. Looking at the downstream process sequence in the production of biopharmaceuticals, shear can occur in purification, formulation, and fill and finishing steps.[5,6] Many conflicting articles have been published investigating the effect of shear on proteins in solution. A critical review is given by Thomas and Geer.[7] Here we want to provide a deeper insight into the physical mechanism by which shear can harm or otherwise influence protein molecules.

No consensus has been found so far on the effect of shear flow on proteins and the magnitude that is required to trigger unfolding of their structure. Different shear rates are described for a variety of proteins that are required for changes of the secondary and higher structure levels. Beginning at shear rates $<10^2$ s^{-1},[8] fibril formation of amyloid-β,[9] loss of activity of urease[10] and catalase,[11] and dissociation of the tertiary structure configuration of BSA[12] are reported. Conversely, Thomas and Dunnill[13] exposed urease in a capillary at shear rates up to 10^6 s^{-1} but did not find any evidence of deactivation. In a more recent study by Bee et al.,[14] IgG1 was sheared in a parallel plate and a capillary rheometer, reaching shear rates up to 2.5×10^5 s^1. However, even at these high rates, the authors could not observe deleterious effects.

Another key aspect for understanding is the exact definition of shear stress. Biddlecombe et al.[15,16] considered shear stress as a

This article contains supplementary material available from the authors by request or via the Internet at http://dx.doi.org/10.1016/j.xphs.2016.03.020.

* *Correspondence to:* Lukas Brückl (Telephone: +43 5338 2008403; Fax: +43 5338 2005672).
E-mail address: lukas.brueckl@sandoz.com (L. Brückl).

http://dx.doi.org/10.1016/j.xphs.2016.03.020
0022-3549/

combination of hydrodynamic forces and interfacial effects. Using a rotating disk, they created a high shear environment at solid–liquid interfaces and observed protein aggregation over rotational time. Desorption of unfolded proteins from solid–liquid interfaces by hydrodynamic forces was proposed as underlying mechanism for particle creation in a later study by Perevozchikova et al.[17] However, so far, most articles focus on velocity gradients in free solution that excludes—at least theoretically in the evaluation and interpretation of the data—any interfacial effects.

The basic idea behind stress on proteins in terms of velocity gradients is a decrease in the free energy of unfolding (ΔG_U) in free solution itself. By lowering the thermodynamic stability of the protein, velocity gradients could cause a potential shift in the equilibrium toward partially unfolded protein.[18] Many studies performed offline analytics and correlated enzyme inactivation or aggregation and particle creation over time with partial unfolding due to shearing.[8] However, a shift in thermodynamic equilibrium of a protein that shows rapid folding/unfolding kinetics and refolding can only be visualized by *in situ* measurements when the overall fold of the proteins is determined inline during shearing.[18]

A few *in situ* studies have been conducted that investigated a potential partial unfolding of proteins under shear. Jaspe and Hagen[18] studied horse cytochrome c (12 kDa) in a silica capillary. The fluorescence of the protein, which would increase sharply on unfolding, was determined while forcing the sample through the capillary. No evidence of destabilization could be found by the authors at shear rates up to 10^6 s^{-1}. However, they predicted that the required shear rate for unfolding decreases with the molecular weight of the protein. Controversial observations were made by Bekard et al. who used a Couette cell for the creation of simple shear flow. Secondary and tertiary structures of BSA (66 kDa) and bovine insulin (6 kDa) were visualized by far-UV circular dichroism (CD) and fluorescence spectroscopy, respectively.[12,19] The *in situ* measurements revealed a time-dependent and irreversible change in secondary and tertiary structure of the proteins already at low shear rates. Interfacial effects, such as desorption from solid–liquid interfaces, were not part of the discussion.

(Partial) Unfolding of proteins simply by velocity gradients in free solution as it is described by Bekard et al. would have a major impact on the product quality in biopharmaceutical manufacturing steps. Therefore, we conducted a study on our own using a similar setup to Bekard et al. consisting of a Couette cell in combination with a CD spectrometer that allowed *in situ* and real-time structure determinations in the far- and near-UV range. The study was designed to focus primarily on the effect of velocity gradients on proteins in free solution without the influence of interfacial effects. The minimization of interfacial effects was a key parameter in the experimental setup. It enables to draw a conclusion on whether protein denaturation by hydrodynamic forces can only occur at interfaces or also in free solution. Recombinant human growth hormone (rhGH) and an IgG1 mAb were selected as therapeutic model proteins that are members of pharmaceutically highly relevant groups of proteins. These proteins strongly differ in the native protein fold and molecular size, thereby covering a broad range of properties, structural parameters, and molecular masses (22-145 kDa). Besides further investigation of the effect of hydrodynamic forces in terms of velocity gradients on the native protein fold, we additionally studied artificially weakened molecular structures. Lowering the mechanical[20] and thermodynamic stability of proteins by addition of the denaturant guanidine hydrochloride (GuHCl) allowed simulating the effect of very high hydrodynamic forces on the structural stability of the proteins.

Materials and Methods

Materials

rhGH and an IgG1 mAb were provided by Sandoz GmbH (Kundl, Austria) in form of frozen stock solutions of 10.1 and 20.8 mg mL^{-1} (rhGH) and 29.7 mg mL^{-1} (IgG1) in concentration. Sodium phosphate was obtained from Merck (Darmstadt, Germany), citric acid from Sigma-Aldrich (St. Louis, MO), Poloxamer 188 from BASF (Ludwigshafen, Germany), and Polysorbate 80 from J.T. Baker (Center Valley, PA). The isoelectric point of rhGH and IgG1 is pH 5.0-5.1 and pH 9.5-9.9, respectively. RhGH has a molecular weight of about 22 kDa and IgG1 of about 145 kDa.

Methods

Preparation of Samples

The stock solution of rhGH was formulated in 10 mM phosphate (pH 7.0). Dilutions were performed using formulation buffer with and without Poloxamer 188. The antibody was buffered in 25 mM citrate (pH 6.5). Samples were diluted adding formulation buffer with and without Polysorbate 80.

Determination of Melting Temperature

The melting temperatures of the proteins in surfactant-containing and surfactant-free solutions were determined from wavelength transitions in the far-UV and near-UV range and by intrinsic fluorescence spectroscopy. For preparation of surfactant-containing samples 0.03 mg mL^{-1}, Poloxamer 188 was added to the rhGH solution and 0.047 mg mL^{-1} PS80 was added to the IgG1 solution. CD transitions were measured with a Chirascan plus spectrometer (Applied Photophysics, Leatherhead, UK) while ramping the temperature at a rate of 1°C min^{-1} from 70°C to 95°C (far-UV) or 60°C to 90°C (near-UV). Transitions of rhGH were determined in triplicate at a fixed wavelength of 209 and 296 nm and a bandwidth of 1 nm, by averaging the signal over a period of 4 s. The measurements were carried out in 1-mm quartz cuvettes at protein concentrations of 0.8 mg mL^{-1} (far-UV) and 9.9 mg mL^{-1} (near-UV). The melting temperature of the IgG1 was determined by far-UV CD and by intrinsic fluorescence spectroscopy, the latter with an LS55 fluorescence spectrometer (PerkinElmer, Waltham, MA). IgG1 transitions in the far-UV at a protein concentration of 0.5 mg mL^{-1} were determined in triplicate at a fixed wavelength of 222 nm and a bandwidth of 1 nm using a 0.5-mm cuvette and averaging the signal over 4 s. Fluorescence was excited at a wavelength of 295 nm with a slit of 5 nm, and emission was recorded from 320 to 370 nm with a slit of 4 nm at medium gain and a protein concentration of 0.1 mg mL^{-1}.

Determination of GuHCl-Dependent Unfolding Transitions

Far-UV and near-UV spectra of solutions at the indicated GuHCl concentrations in 0.5-mm quartz cuvettes were recorded at 20°C using the Chirascan CD spectrometer. CD data were collected from 205-260 and 250-350 nm every 0.5 nm with a response time of 0.5 s and a bandwidth of 1 nm. Far-UV data of GuHCl-free samples were recorded from 180 to 260 nm. All spectra were baseline normalized, and the spectra were corrected to 0 mdeg at 260 nm.

Unfolding was performed at room temperature in formulation buffer containing the indicated concentrations of GuHCl. A 7.9 M GuHCl stock solution (Sigma-Aldrich) was used for preparation of the denaturation buffers. For determination of far-UV, rhGH was diluted to 0.152 mg mL^{-1} and the IgG1 to 1 mg mL^{-1}. Near-UV denaturation curves were recorded at a concentration of 2.5 mg mL^{-1} (rhGH) and 10 mg mL^{-1} (IgG1); 0.03 mg mL^{-1} Poloxamer 188 was added to the rhGH solutions and 0.047 mg mL^{-1} PS80 was

added to the IgG1 solutions. Samples were incubated for at least 30 min before measurement.

Furthermore, the thermodynamic stability of rhGH (a small protein for which reversible folding and refolding can be assumed in contrast to IgG1) was roughly estimated using the obtained denaturation curves in the far-UV. For evaluation of the standard free energy of unfolding (ΔG_U^0), the far-UV spectrum of rhGH was averaged between 219 and 222 nm. Each denaturation state was analyzed with a 2-state unfolding model. ΔG_U was assumed to be linearly dependent on the GuHCl concentration (GuHCl):

$$\Delta G_U = \Delta G_U^0 - m[\mathrm{GuHCl}] \quad (1)$$

with ΔG_U and m being the free energy of unfolding at a certain denaturant concentration and the slope, respectively.

For confirmation of the assumed 2-state unfolding model, refolding of rhGH on decreasing GuHCl concentrations was shown. Therefore, rhGH was initially incubated for 30 min at a concentration of 1.44 mg mL^{-1} and a GuHCl concentration of 6 M. Subsequently, refolding was induced by dilution of the incubated solution with formulation buffer to indicated GuHCl concentrations and a final protein concentration of 0.152 mg mL^{-1}.

Couette Cell CD Measurements

Inline determination of protein structure under sheared conditions was performed in a quartz Couette cell obtained from Applied Photophysics. The Couette cell consists of a static inner and a rotating outer cylinder (Fig. 1). The outer cylinder has an inner radius R of 4.775 mm. The sample is filled into the annular gap between these cylinders, which has a width of 0.25 mm. During the measurement, light passes through the gap twice resulting in a total path length of 0.5 mm. Thereby, the incident light travels along the gradient direction of the rotating liquid, which is indicated by the arrows in the annular gap in Figure 1. A constant velocity profile can be found along the z-axis. Rotational speed of the moving outer cylinder was controlled by the software SmartMotor from Applied Photophysics. CD spectra were recorded using a bandwidth of 1.8 nm. This was necessary, as the incident light beam width for the Couette cell is only 1 mm (to deal with the curvature of the cell). The same wavelength range was selected in the far- and near-UV as for the determination of the GuHCl-dependent unfolding. Due to slight imperfections in the rotors optic, it is important to sample over a half or whole number of revolutions; 1-s sampling time was, therefore, applied for each data point. The setup of the Couette cell decreases the risk of photodegradation as the sample is rotating and, therefore, only passing the light beam

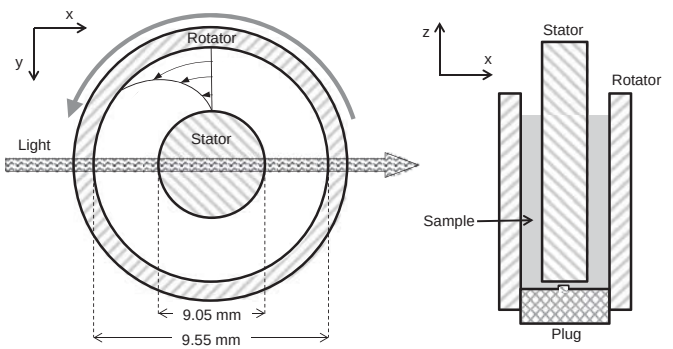

Figure 1. Schematic (not to scale) of the Couette cell accessory. The incident light beam travels along the gradient direction of the rotating liquid, which is indicated by the arrows in the annular gap. A constant velocity profile can be found along the z-axis of the cell.

for 1/30 of the time. The temperature of the sample was monitored and controlled by circulation of thermostated water in a cooling jacket within a range of 20°C-23°C. Investigations on the shear dependent unfolding of proteins were performed under defined shear rates. For the exact determination of the shear rate, laminar flow is required. On rotation of the outer cylinder, a Couette flow develops inside the gap. The boundary conditions define that the fluid does not slip at the 2 cylindrical surfaces. Using these boundary conditions, one can derive the velocity distribution and finally the shear rate $\dot{\gamma}$ according to[21]:

$$\dot{\gamma} = 2\Omega_0 \left(\frac{R}{r}\right)^2 \left(\frac{\kappa^2}{1-\kappa^2}\right) \quad (2)$$

where Ω_0 is the angular velocity, R is the radius of the outer cylinder, κ is the ratio of the radius of the inner cylinder to the radius of the outer cylinder, and r is the distance to the axis of rotation.

The software SmartMotor uses an approximation for calculating the shear rate, which represents a compromise between the shear rate at the inner and the outer cylinder.

$$\dot{\gamma} = \frac{\Omega_0}{(1-\kappa)} \quad (3)$$

The prevailing flow regime inside the Couette cell can be determined by the Reynolds number Re, which is given for the outer cylinder by[22]:

$$Re = \frac{\Omega_0 R^2 (1-\kappa)\rho}{\mu} \quad (4)$$

where ρ is the density and μ is the dynamic viscosity of the fluid. A theoretical critical Reynolds number of 2500, indicating a transition from the laminar to the turbulent flow regime, was determined for the experimental setup. However, due to small imperfections and possible end effects in the Couette cell, the supplier advised not to exceed a Reynolds number of 250. Therefore, measurements in the laminar flow regime were limited to a shear rate of 3840 s^{-1} that corresponds to a Reynolds number of 240. Instabilities in the Taylor–Couette flow which lead to so-called Taylor vortices have been described for Couette cells with a rotating inner cylinder. The used Couette cell accessory is designed to avoid these instabilities using a static inner and a rotating outer cylinder. No Taylor vortices have been described for this setup so far.[23]

Spectra of sheared samples were predominantly recorded at a shear rate of 3840 s^{-1}. To increase the stress, also a nominal of 10,200 s^{-1} (under the assumption of laminar flow) were applied in a few cases. Rotational speed for 10,200 s^{-1} gives a Reynolds number of 638, which is >250. Under this condition, turbulent flow cannot be excluded.

Spectra were determined at sample concentrations of 0.152 mg mL^{-2} (rhGH) and 1 mg mL^{-1} (IgG1) in the far-UV and at 10 mg mL^{-1} (both proteins) in the near-UV. To minimize interfacial effects 0.03 mg mL^{-1}, Poloxamer 188 was added to the rhGH samples and 0.047 mg mL^{-1} Polysorbate 80 to the IgG1. For investigations of interfacial effects on rhGH, measurements were performed without addition of a surfactant.

Couette Cell Linear Dichroism Measurements

Linear dichroism (LD) measurements were performed using the same hardware and software parts as for CD measurements. Possible alignment of rhGH and the IgG1 antibody in shear flow would result in a strong LD signal and interfere with CD measurements. Therefore, the LD signal was checked at the highest possible shear rate in the laminar regime (3840 s^{-1}). LD signal of

rhGH was recorded at 0.3 mg mL^{-1} from 180 to 260 nm using a bandwidth of 1 nm and a sampling time of 1 second per scanned wavelength. LD signal of IgG1 was recorded at 1.2 mg mL^{-1} from 180 to 260 nm using a bandwidth of 1 nm and a sampling time of 1 second per scanned wavelength. No surfactant was added to the samples.

Offline Fluorescence Measurements

Offline Fluorescence measurements of sheared samples were performed at the end of the shearing period using an LS55 fluorescence spectrometer (PerkinElmer). Fluorescence was excited at a wavelength of 295 nm with a slit of 5 nm, and emission was recorded from 310 to 380 nm with a slit of 5 nm at medium gain. Samples of rhGH and IgG1 were diluted with placebo buffer to a concentration of 0.04 and 0.05 mg mL^{-1}, respectively. Fluorescence spectra were buffer corrected, and the spectra of unstressed and sheared samples were compared by calculating the spectral center of mass (ν_g), which is given by[24]:

$$\nu_g = \frac{\sum \nu_i F_i}{\sum F_i} \quad (5)$$

where F_i is the emission at the wave number ν_i.

Size Exclusion HPLC

Shear-induced aggregation was tested for both proteins over 30 min of rotation inside the Couette cell at a shear rate of 3840 s^{-1}. Samples were stressed at concentration of 10 mg mL^{-1}. No surfactant was added as it could prevent protein aggregation. Aggregate level was determined by size exclusion HPLC (SE-HPLC) using an Agilent 1290 (Agilent Technologies, Santa Clara, CA) chromatography system with a TSKgel G3000SW_{XL} column (7.8 mm ID × 30 cm, 5 μm particle size) and an inline 2-μm filter. The system was controlled using the Dionex software package Chromeleon 6.8. 150 mM K-phosphate (pH 6.5) served as mobile phase at a flow rate of 0.4 mL min^{-1}. Before analysis, samples were filtered (0.2 μm). The column was loaded with 50 μg of protein, and UV absorbance was recorded at 210 and 280 nm.

Results and Discussion

Alignment of Proteins in the Direction of Shear

Alignment of rhGH and IgG1 in simple shear flow was investigated by LD measurements at a shear rate of 3840 s^{-1}. An alignment would cause a strong increase in the LD signal and interferes with CD measurements. As both proteins showed no LD signal and, thereby, no flow-induced anisotropy, alterations in the CD signals can be unambiguously interpreted as conformational changes rather than orientational effects. The LD signal was not checked for shear rates >3840 s^{-1}. However, a possible alignment of proteins can easily be recognized by an increase in the CD signal to the relatively same extent over the whole spectrum.

Exposure of rhGH and IgG1 to High Shear Rates in Presence of a Surfactant

The impact of shearing on rhGH in the presence of a surfactant was assessed with the Couette cell at a shear rate of 3840 s^{-1} for a total time of 30 min. An additional spectrum was taken at 120 s^{-1} at the beginning of the experiment and served as reference spectrum for an unstressed sample. The surfactant was added to protect the protein from air/liquid interfaces, which are very well known to cause protein denaturation and aggregation due to their hydrophobic character.[25,26] Furthermore, by a displacement of proteins at interfaces, potential deleterious combinations of any interfacial effects with hydrodynamic forces can be minimized by the surfactant. Experiments with added surfactant resulted in stable CD signals over shearing rate and shearing time in the far- and near-UV (data not shown). Furthermore, the experiment was repeated for far-UV at a nominal shear rate of 10,200 s^{-1}. A calculated Reynolds number of 638 for this rotational speed indicates that the assumed laminar flow regime was left. To protect the protein from potentially increasing air and liquid interfacial effects, the surfactant concentration was increased to 1 mg mL^{-1} poloxamer 188. Again, a stable CD signal was observed over 30 min of shearing and confirmed by offline fluorescence measurements, which showed an identical spectral center of mass (343.6 nm) for the reference and the sheared sample (see Supplementary Fig. S1 for respective fluorescence spectra).

Characterized by a molecular weight of 22 kDa, rhGH is a relatively small molecule, measuring roughly 6 nm in diameter.[27] Thus, it may behave differently compared with larger molecules.[18] Large linear molecules, such as DNA, are known to align in the liquid on shearing, big globular structures can deform in the direction of shear,[28,29] and the growth and morphology of protein aggregates is influenced by shear flow.[30,31] Therefore, shearing experiments at 3840 and 10,200 s^{-1} were repeated using an IgG1 mAb with a molecular weight of 145 kDa, which was also protected by a surfactant. This is noticeably bigger than rhGH and has, moreover, a completely different structure. rhGH is a mainly alpha helical protein, whereas the secondary structure of the immunoglobulin mainly consists of β sheets.[27,32] Antiparallel β sheets have a typical negative peak in the far-UV spectrum around 217 nm,[33] and the weak positive peak at 235 nm is attributable to a disulfide bond. PS80 was added as surfactant to IgG1 in a concentration of 0.047 mg mL^{-1}. Shearing of IgG1 showed the same results as for rhGH. No time- or shear rate–dependent unfolding could be observed in the far- and near-UV spectrum for 3840 s^{-1} and 10,200 s^{-1} (data not shown). Offline fluorescence measurements of the sample which was sheared for 30 min at 3840 s^{-1} showed an identical spectral center of mass as the unstressed reference sample (348.5 nm) and, thereby, confirmed the inline CD results (Supplementary Fig. S2a for respective fluorescence spectra).

Summarizing, it can be concluded that the stability of the native fold of rhGH and IgG1 in free solution is high enough to withstand shear rates up to at least 10^4 s^{-1}. This is in agreement with values reported in literature. Jaspe and Hagen[18] calculated shear rates as high as 10^7 s^{-1} necessary to cause structural changes of cytochrome c in water. In a study by Bee et al.,[14] exposure to high shear (up to 2.5×10^5 s^{-1}) could not cause aggregation of an antibody. In comparison with protein unfolding by atomic force microscopy, the investigators calculated a theoretical shear rate of 5×10^7 s^{-1} necessary to pull β-sheet motifs apart. In another study by Maa et al.[34] who also used rhGH, offline CD measurements in the near- and far-UV could not show structural changes after exposure to a shear rate of 10^5 s^{-1}. However, it has to be mentioned that on shearing, the melting temperature of rhGH was slightly decreased.

Addition of a Surfactant—Investigation of Thermodynamic Stabilization

In the shearing experiments, poloxamer 188 was added to rhGH solution and polysorbate 80 to the antibody solution at a concentration of 0.03 and 0.047 mg mL^{-1}, respectively. Both surfactants are nonionic compounds and are commonly used to decrease or prevent protein aggregation. The occupation of the interfaces and the competitive displacement of the protein molecules are assumed to be the predominant protecting effect of the surfactants. Also a direct, stabilizing interaction with the protein molecules is

under discussion. The possible involvement of the latter effect,[35] which also could prevent denaturation by shear stress, was thermodynamically investigated.

Protein melting curves of rhGH with and without poloxamer 188 were compared in the near- and far-UV. Thermal transition in far-UV CD spectra and in terms of intrinsic fluorescence was recorded for the antibody with and without polysorbate 80. Results are listed in Table 1.

The comparison of the respective melting curves and points showed no significant differences. Only the fluorescence signal of the IgG showed a slightly increased melting temperature in the presence of a surfactant. In general, a stabilization of the protein fold by an addition of surfactants could be ruled out.

Shearing of rhGH With an Artificially Weakened Conformational Stability

Typical shear rates during the processing of biopharmaceuticals are difficult to determine. Very high local shear rates can occur at (sometimes unexpected) points in the processing system, for example, in the gap between the piston and cylinder of a piston pump. Thus, it was highly desirable to find a way to investigate the behavior of proteins also under more extreme conditions. One possibility is an increase in rotational speed of the Couette cell. However, shear rates beyond 10^4 s^{-1} cannot be reached by the Couette system without leaving the laminar flow regime and, thereby, the possibility to calculate the shear rate. Instead of increasing the hydrodynamic forces to overcome the stability of the protein, another approach is to artificially weaken the stability of the sheared protein by the addition of a denaturant. Thereby, the protein becomes more susceptive to shear-induced unfolding.

GuHCl was chosen as chemical denaturant. The exact mechanism of how GuHCl lowers the free energy of unfolding (ΔG_U) is not yet completely known. Protein denaturation could result from solvation of charged residues or engagement in hydrogen bonds with the protein backbone. Furthermore, the guanidium ion can diminish the strength of interaction between ion pairs.[36] Besides decreasing the thermodynamic stability of proteins, GuHCl can also weaken the mechanical stability as it was shown by single-molecule atomic force microscopy for GB1. With increasing denaturant concentration, the unfolding force of the protein was significantly decreased.[20]

Figure 2 shows the denaturant-induced unfolding of rhGH determined in the far-UV (a) and near-UV (b). Notable transition from folded to unfolded state happens between GuHCl concentrations of 4 and 5.5 M in the far-UV region. Furthermore, the determined transition curve was congruent for unfolding and refolding. The tertiary structure fingerprint of the protein, which can be obtained by near-UV measurements, did not show a clear transition from folded to unfolded. Ellipticity at 277.5 nm was decreasing with GuHCl concentration up to 4 M, whereas the signal at 293 nm had the transition in the same concentration range as identified in the far-UV. Applying a 2-state transition model for the reversible transition recorded in the far-UV, a thermodynamic stability of 14.7 kcal mol^{-1} could be obtained, which is in good agreement with a reported value[37] of 14.5 kcal mol^{-1}. The denaturation curve of rhGH is shown in the Supplementary Figure S3.

Table 1
Comparison of Melting Temperatures of rhGH and IgG1 With and Without Surfactant

Protein (Measurement Mode)	No Surfactant (°C)	Surfactant Added (°C)
rhGH (far UV)	85.2 ± 0.5	84.9 ± 0.2
rhGH (near UV)	71.9 ± 0.4	71.8 ± 0.1
IgG1 (far UV)	73.0 ± 0.3	72.9 ± 0.2
IgG1 (fluorescence)	70.1 ± 0.1	70.8 ± 0.1

SD results from triplicate determinations.

As mentioned earlier, weakening and notable unfolding of the protein secondary structure (as seen in far-UV) happen above GuHCl concentrations of about 4 M. A weakening of the tertiary structure can be observed >2 M (see Fig. 2b). Therefore, GuHCl concentration in the range of these values should be used for enabling the investigation of shear stress at shear rates that are lower than it would be necessary to damage the native protein. For this purpose, far-UV CD spectra of rhGH at GuHCl concentrations of 4, 4.5, and 4.75 M were acquired under shearing. For tertiary structure investigations, in the near-UV 2 M and 3 M, GuHCl was added. Besides the fact, that intramolecular bonds are weakened by GuHCl, measurements in concentration ranges at which proteins are half folded ($D1/2$, $\Delta G_U = 0$) are more sensitive in the detection of decreased protein stability. Even a small change in the ΔG_U would cause a detectable shift in the ratio of natively folded/(partially) unfolded protein. $D1/2$ of rhGH occurs at a GuHCl concentration of roughly 4.7 M.

However, even under the destabilized conditions, no change in ellipticity could be observed over 30 min of shearing at 3840 s^{-1}. The experiments were stopped after 30 min as no time-dependent conformational change was observed. Figure 3 illustrates the CD signal in the far- and near- UV for a selected GuHCl concentration (4 M).

Finally, using a GuHCl concentration of 4 M, the rotational speed of the Couette cell was increased to the maximum, reaching a nominal shear rate of 10,200 s^{-1}; rhGH in combination with 4 M GuHCl served as sample solution. The Reynolds number is slightly decreased by the higher viscosity of the 4 M GuHCl solution. A 4 M GuHCl solution shows a 1.27 times increased viscosity over water at 25°C.[38] However, a shear rate of 10,200 s^{-1} exceeds with a Reynolds number of 502 the critical value of 250 which marks the transition from the laminar toward turbulent flow pattern for our setup. Nevertheless, rhGH kept its initial conformational state in the far-UV over the period of the measurement (30 min, data not shown, similar to Fig. 3). The combination of steep velocity gradients, turbulence flow and weakening of the conformational stability, and intramolecular interactions of the protein by GuHCl was not able to change the secondary and tertiary structure of rhGH in free solution. Therefore, it is very unlikely that the investigated protein gets damaged in free solution during biopharmaceutical processing steps.

Shearing of IgG1 With an Artificially Weakened Conformational Stability

GuHCl-mediated unfolding and shearing experiments under GuHCl destabilization were repeated using the IgG1 mAb. Again, PS80 was added to minimize interfacial effects.

Figure 4 shows the GuHCl-mediated unfolding of IgG1 without the application of shear stress, which was observed between 2 and 3 M GuHCl in the far-UV and near-UV. Figure 5 illustrates the CD signal in the far- and near-UV for a selected GuHCl concentration (2 M) which shows no time- and shear rate–dependent change. Summarized, this time and shear rate independence of CD spectra could be observed for GuHCl concentrations of 0, 2, 2.5, and 3 M. Furthermore, a shear rate of 10,200 s^{-1} was applied at a GuHCl concentration of 2 M, and the sheared sample was compared with an unstressed reference sample by offline fluorescence analytic giving very similar spectral centers of mass of 348.1 and 348.2 nm, respectively (Supplementary Fig. S2b for respective fluorescence spectra). Again, the inline CD results could be confirmed by the offline analytics. Despite its bigger size compared with rhGH, also the artificially weakened IgG1 showed no structural changes under the influence of steep velocity gradients in free solution. Based on these results, a damage of IgG1 by shear stress in free solution is very unlikely to happen during biopharmaceutical processing steps.

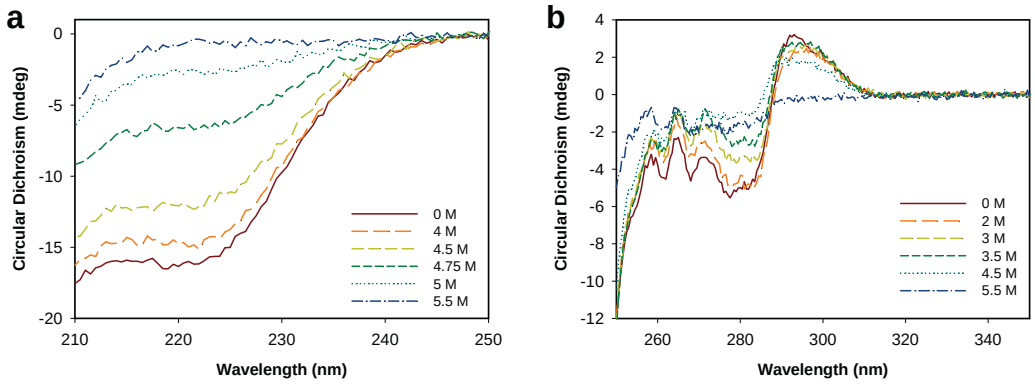

Figure 2. Denaturant-induced unfolding of rhGH monitored in a rectangular quartz cuvette in the far UV (a) and near UV (b). The shown molarities represent the GuHCl concentration in the sample.

Inline CD Measurements of rhGH Without a Surfactant

Additional experiments of rhGH were performed without the protection of a surfactant. The absence of the surfactant allows for the possibility of interfacial effects. Shearing of rhGH in phosphate buffer was performed in the Couette cell at a constant rate of 3840 s^{-1} for a total of 60 min. Air bubbles were carefully removed from the system, and it was tried to create a flat and even surface on the liquid to minimize the effect of air–liquid interfaces. Dilations and subsequent compressions of air–liquid interfaces are known to lead to particle formation[26]; therefore, it was tried to exclude fluctuations of air–liquid interfaces as good as possible. CD spectra in the far-UV were recorded after 0, 15, 30, 45, and 60 min. The spectrum recorded at time point 0 represents the CD signal of an unstressed sample and was, therefore, used as reference. CD spectra of the sheared rhGH sample showed no differences to the reference spectrum over the experimental time (data not shown). Again, an unfolding of the protein caused by velocity gradients in free solution can be excluded up to the selected shear rate. Furthermore, it can be concluded that interfacial effects were not strong enough to give a detectable shift of the CD spectrum over time.

However, when the experiment was performed in the presence of air bubbles, the CD signal showed a characteristic shift over time and particles in the visible range were detected in the sample. Figure 6 shows spectra of a sample, which was sheared for a total of 60 min in the presence of air–liquid interfaces. The shear rate was kept constant at 3840 s^{-1}. Protein concentration was determined by offline absorbance at 277 nm and showed a decrease by 10% over 60 min of shearing. Therefore, spectra in Figure 6 are concentration corrected. A characteristic and irreversible decrease in ellipticity over time, which is not concentration related, can be observed for rhGH while exposed to stress inside the rotating Couette cell. Irreversibility describes here the fact that the spectra were not only altered during rotational movement of the Couette cell but kept their altered shape during static measurements at the end of the shearing period. This behavior was not observed under the protection of a surfactant that competitively displaces proteins at interfaces and, thereby, minimizes the possibility of deleterious combinations of hydrodynamic forces with interfacial effects. The time-dependent and irreversible denaturation is very similar to results obtained for BSA by Bekard et al.[12] BSA and rhGH are both mainly alpha helical proteins.[27,39] CD spectra show 2 negative signals at 222 and 208 nm and a positive peak at 193 nm, which is a typical pattern of α-helical structure.[33] In the natively folded structure, the ellipticity at 208 nm reveals a stronger negative value than at 222 nm. On rotation of the Couette cell, the signal intensity is not decreasing to the same ratio over the whole far-UV spectrum and also the shape of the curve is changing. Hence, in the course of 60 min of shearing, the signal ratio of 222/208 nm changes from <1 to >1. Due to the alteration of the curve shape, the isosbestic point occurs at 199 nm (positive ellipticity). In contrast, a thermal unfolding (melting point at ~85°C) of rhGH (data not shown) results in a constant 222/208 nm signal ratio and an isosbestic point at 201.5 nm with a negative ellipticity. The shape of the curve in the

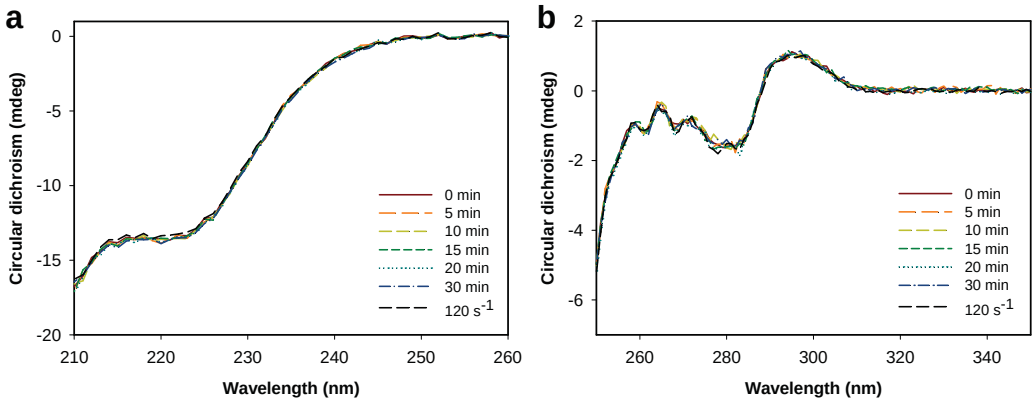

Figure 3. Time-independent CD signal of rhGH constantly sheared at 3840 s^{-1} and destabilized by addition of GuHCl. Far-UV signal (a) was recorded at 4 M GuHCl and near-UV signal (b) at 2 M GuHCl. The reference spectrum (long dashed black line) indicates a "fresh" sample at the lowest possible shear rate of 120 s^{-1} (1 rps).

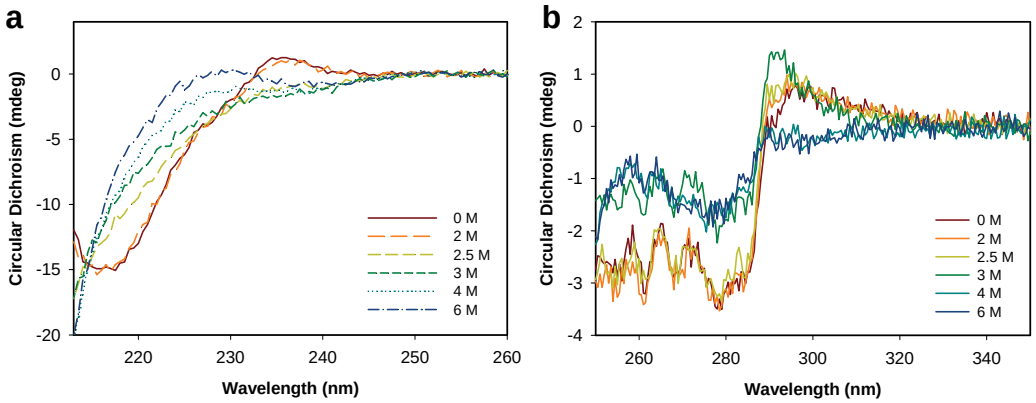

Figure 4. Denaturant-induced unfolding of IgG1 monitored in a rectangular quartz cuvette in the far UV (a) and near UV (b). The shown molarities represent the GuHCl concentration in the sample.

far UV spectrum is defined by the secondary structure composition of the protein.[33] Differences in shape indicate a different secondary structure composition and, thereby, a different unfolding product.

Whereas the characteristic shift in the CD spectrum of rhGH could give a possible explanation for the reported unfolding of BSA, the formation of particles differs from Bekards results. Bekard did not observe an increase in turbidity and aggregate content and, therefore, concluded the absence of particle formation. A time-dependent change of the protein structure could, however, indicate the presence of an different unfolding mechanism to shearing in free liquid. Velocity gradients in free solution act uniformly in the whole sample. Therefore, a potential destabilization of the native protein fold by a certain shear rate affects all molecules at the same time and should give a shear rate–dependent structural change. If only a small fraction of the proteins is irreversible unfolded as it may happen by desorption from solid–liquid interfaces,[17] the amount of unfolded protein would continuously increase over time and give a time-dependent and irreversible signal shift.

Investigation of Time-Dependent Change of rhGH

Further investigations were performed to gain more insight into the underlying mechanism of the characteristic unfolding of rhGH. The possibility of deleterious air–liquid interfaces was investigated *ex situ*. Nitrogen was carefully bubbled into an rhGH sample. Particle creation was observed in the visible range. Protein concentration was determined by offline absorbance at 277 nm and showed a decreased by 27% over 5 min of bubbling. Spectra in Figure 7 were concentration corrected and show a clear unfolding of the protein. There are small differences in the far-UV spectra of the bubbled sample compared with the time-dependent unfolding of rhGH in the shear experiment without the protection of a surfactant. The isosbestic point of the bubbled sample is located at 0 ellipticity, the signal ratio of 222/208 nm stays rather constant and <1, whereas the unfolding in the Couette cell showed an increase in the 222/208 nm ratio and a positive ellipticity at the isosbestic point. Again, this is attributable to differences in the secondary structure composition of the unfolding products.

It is known from literature that the relative magnitude of the 222 and 208 nm peaks depend on the hydrophobicity of the environment. The hydrophobicity can be increased by dimerization or folding of proteins that try to protect their hydrophobic surfaces from the solvent, resulting in ratios ≥1. Furthermore, the ratio can be influenced by insertion into membranes and H-bonding.[40]

Considering these facts, a combination of interfacial and hydrodynamic forces or any other effect caused by the rotation of the Couette cell might be responsible for the observed small differences in the CD spectrum of the rhGH samples that irreversibly unfolded inside the Couette cell. Besides the air–liquid interface, an additional hydrophobic surface can be found in the Couette cell accessory of Applied Photophysics: a PEEK plug is used for sealing the outer rotating cylinder at the bottom. On rotation of the outer cylinder, the plug is moving along and friction can occur between the static inner cylinder and the plug. However, further research is

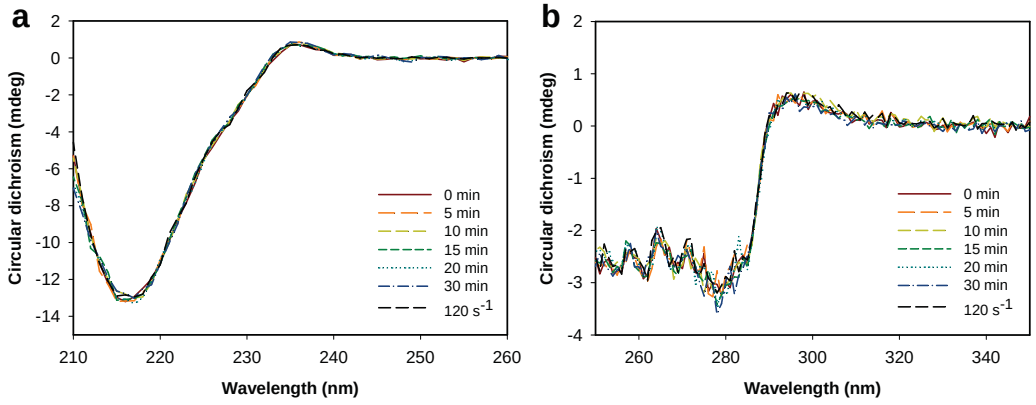

Figure 5. Time-independent CD signal of IgG1 constantly sheared at 3840 s^{-1} and destabilized by addition of GuHCl. Far-UV signal (a) and near UV signal (b) were recorded at 2 M GuHCl.

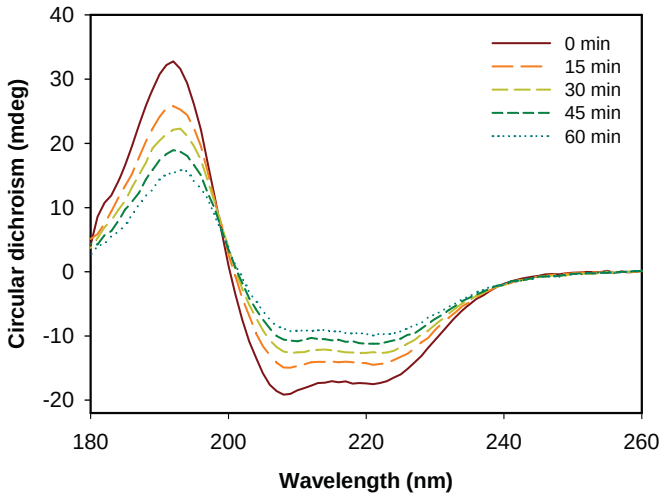

Figure 6. Time-dependent change in CD signal of rhGH (0.15 mg mL^{-1}) in phosphate buffer at pH 7.0 constantly sheared at 3840 s^{-1}. Spectra are concentration corrected.

needed to identify the relevant parameters in the unfolding process and to fully understand potential deleterious effects of possible combinations of shear stress with surface effects.

Shear-Induced Aggregation

Secondary and tertiary structure changes due to hydrodynamic stress in simple shear flow could not be shown for rhGH and the IgG1 antibody. In the absence of shear-induced (partial) unfolding, it is very unlikely that pronounced protein aggregation happens. Nevertheless, analysis of the aggregate content was performed to confirm the results of the inline CD measurements and to check for the possibility of enhanced protein aggregation by any liquid flow–related phenomena. Soluble aggregate levels were determined by SE-HPLC after shearing of protein samples without surfactant at 3840 s^{-1} for 30 min. No samples containing GuHCl and/or surfactant were analyzed as these excipients could influence or suppress the aggregation tendency. Only sheared IgG1 and rhGH samples with a stable CD signal on shearing were analyzed as already visible particles were observed in samples with an unstable signal. No sample that was analyzed by SE-HPLC showed an increased content of higher molecular weight variants (Supplementary Fig. S4 for SE-HPLC chromatograms).

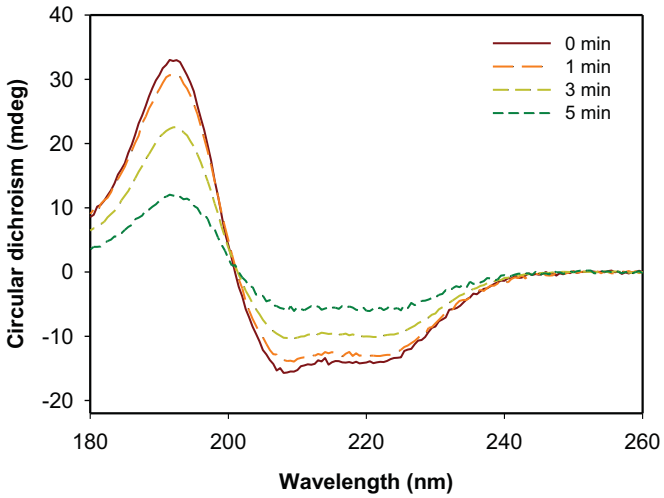

Figure 7. Denaturation of rhGH over time by the creation of air/liquid interfaces in form of nitrogen bubbles. Spectra are concentration corrected.

Conclusions

The influence of shear stress in terms of velocity gradients in free solution on rhGH and IgG1 was investigated using inline and real-time CD measurements. A surfactant was added to protect rhGH and the IgG1 antibody from interfacial interactions inside the Couette cell by a competitive displacement of protein molecules. Under the exclusion of interfacial effects, velocity gradients in free solution, as they occur, for example, during mixing inside of a vessel, were not able to unfold the secondary or tertiary structure of rhGH and IgG1 up to a shear rate of 3840 s^{-1} in laminar flow conditions. Furthermore, even an increase of the shear rate inside the Couette cell to a nominal of 10,200 s^{-1} showed no destabilization of the proteins' structural conformation. Due to end effects and small imperfections in the geometry of the Couette cell, the assumed laminar regime was left at this high shear rate.

To simulate the effect of very high shear rates on the conformational stability of proteins, the mechanical and thermodynamic stability of the proteins was artificially weakened by the addition of GuHCl. Again, interfacial effects were excluded using a surfactant. However, even under these destabilizing conditions, shear was not able to alter the protein fold of rhGH and IgG1 in free solution.

The behavior of rhGH in presence of interfaces was investigated in further experiments without any surfactant. Rotational movement of the Couette cell in the presence of air bubbles resulted in a time-dependent and irreversible unfolding of rhGH and particle creation. A combination of hydrodynamic forces with interfacial phenomena was able to irreversible unfold proteins and could explain previous reports of protein denaturation by shear-related effects.

Summarizing, we showed stability of 2 representative therapeutic proteins against velocity gradients in free solution up to a shear rate of at least 10^4 s^{-1}. Stability is most likely given at even higher shear rates as the experiments with artificially decreased mechanical stability showed. Using a small globular and mainly alpha helical protein (rhGH) and a typical IgG1 antibody containing mainly β sheets, we covered a broad range of protein characteristics. Therefore, we conclude that product quality in biopharmaceutical processing steps is mainly affected by liquid flow–related effects at interfaces, which are a potential root cause for protein unfolding, aggregation, and particle creation. However, velocity gradients in free solution by itself without the involvement of interfacial effects are very unlikely to affect the conformational stability of the investigated proteins.

Acknowledgments

The authors thank the Biophysical Characterization Group in Oberhaching (Sandoz) for providing measurement time at the CD and fluorescence spectrometer. Guidance and comments given by Alexander Bepperling and Kerstin Grassl have been a great support. Special thanks to Andreas Hoffmann for the many helpful discussions and talks and Otmar Hainzl for his advice and his help with the Couette cell accessory.

References

1. Johnson IS. Human insulin from recombinant DNA technology. *Science*. 1983;219(4585):632-637.
2. Walsh G. Biopharmaceutical benchmarks 2010. *Nat Biotechnol*. 2010;28(9):917-924.

3. Manning MC, Chou DK, Murphy BM, Payne RW, Katayama DS. Stability of protein pharmaceuticals: an update. *Pharm Res*. 2010;27(4):544-575.
4. Wang W, Nema S, Teagarden D. Protein aggregation—pathways and influencing factors. *Int J Pharm*. 2010;390(2):89-99.
5. Rathore N, Rajan RS. Current perspectives on stability of protein drug products during formulation, fill and finish operations. *Biotechnol Prog*. 2008;24(3):504-514.
6. Patro SY, Freund E, Chang BS. Protein formulation and fill-finish operations. *Biotechnol Annu Rev*. 2002;8:55-84.
7. Thomas C, Geer D. Effects of shear on proteins in solution. *Biotechnol Lett*. 2011;33(3):443-456.
8. Bekard IB, Asimakis P, Bertolini J, Dunstan DE. The effects of shear flow on protein structure and function. *Biopolymers*. 2011;95(11):733-745.
9. Dunstan DE, Hamilton-Brown P, Asimakis P, Ducker W, Bertolini J. Shear flow promotes amyloid-β fibrilization. *Protein Eng Des Selection*. 2009;22(12):741-746.
10. Tirrell M, Middleman S. Shear modification of enzyme kinetics. *Biotechnol Bioeng*. 1975;17(2):299-303.
11. Charm S, Lai C. Comparison of ultrafiltration systems for concentration of biologicals. *Biotechnol Bioeng*. 1971;13(2):185-202.
12. Bekard IB, Asimakis P, Teoh CL, et al. Bovine serum albumin unfolds in Couette flow. *Soft Matter*. 2012;8(2):385-389.
13. Thomas C, Dunnill P. Action of shear on enzymes: studies with catalase and urease. *Biotechnol Bioeng*. 1979;21(12):2279-2302.
14. Bee JS, Stevenson JL, Mehta B, et al. Response of a concentrated monoclonal antibody formulation to high shear. *Biotechnol Bioeng*. 2009;103(5):936-943.
15. Biddlecombe JG, Craig AV, Zhang H, et al. Determining antibody stability: creation of solid-liquid interfacial effects within a high shear environment. *Biotechnol Prog*. 2007;23(5):1218-1222.
16. Biddlecombe JG, Smith G, Uddin S, et al. Factors influencing antibody stability at solid–liquid interfaces in a high shear environment. *Biotechnol Prog*. 2009;25(5):1499-1507.
17. Perevozchikova T, Nanda H, Nesta DP, Roberts CJ. Protein adsorption, desorption, and aggregation mediated by solid–liquid interfaces. *J Pharm Sci*. 2015;104(6):1946-1959.
18. Jaspe J, Hagen SJ. Do protein molecules unfold in a simple shear flow? *Biophys J*. 2006;91(9):3415-3424.
19. Bekard IB, Dunstan DE. Shear-induced deformation of bovine insulin in Couette flow. *J Phys Chem B*. 2009;113(25):8453-8457.
20. Cao Y, Li H. How do chemical denaturants affect the mechanical folding and unfolding of proteins? *J Mol Biol*. 2008;375(1):316-324.
21. Bird RB, Stewart WE, Lightfoot EN. *Transport Phenomena*. 2nd ed. New York, NY: John Wiley & Sons, Inc; 2002.
22. Andereck CD, Liu S, Swinney HL. Flow regimes in a circular Couette system with independently rotating cylinders. *J Fluid Mech*. 1986;164:155-183.
23. Dou H-S, Khoo BC, Yeo KS. Instability of Taylor–Couette flow between concentric rotating cylinders. *Int J Therm Sci*. 2008;47(11):1422-1435.
24. Jameson DM, ed. *Introduction to Fluorescence*. Boca Raton, FL: Taylor & Francis; 2014.
25. Dasnoy S, Dezutter N, Lemoine D, Le Bras V, Préat V. High-throughput screening of excipients intended to prevent antigen aggregation at air-liquid interface. *Pharm Res*. 2011;28(7):1591-1605.
26. Bee JS, Schwartz DK, Trabelsi S, et al. Production of particles of therapeutic proteins at the air–water interface during compression/dilation cycles. *Soft Matter*. 2012;8(40):10329-10335.
27. Chantalat L, Jones N, Korber F, Navaza J, Pavlovsky A. The crystal structure of wild-type growth hormone at 2.5 Aresolution. *Protein Pept Lett*. 1995;2:333-340.
28. Chien S, Usami S, Dellenback RJ, Gregersen MI. Shear-dependent deformation of erythrocytes in rheology of human blood. *Am J Phys*. 1970;219(1):136-142.
29. Norden B, Kubista M, Kurucsev T. Linear dichroism spectroscopy of nucleic acids. *Q Rev Biophys*. 1992;25(01):51-170.
30. Foderà V, Pagliara S, Otto O, Keyser UF, Donald AM. Microfluidics reveals a flow-induced large-scale polymorphism of protein aggregates. *J Phys Chem Lett*. 2012;3(19):2803-2807.
31. Loksztejn A, Dzwolak W. Vortex-induced formation of insulin amyloid superstructures probed by time-lapse atomic force microscopy and circular dichroism spectroscopy. *J Mol Biol*. 2010;395(3):643-655.
32. Bork P, Holm L, Sander C. The immunoglobulin fold: structural classification, sequence patterns and common core. *J Mol Biol*. 1994;242(4):309-320.
33. Kelly SM, Jess TJ, Price NC. How to study proteins by circular dichroism. *Biochim Biophys Acta*. 2005;1751(2):119-139.
34. Maa YF, Hsu CC. Effect of high shear on proteins. *Biotechnol Bioeng*. 1996;51(4):458-465.
35. Chou DK, Krishnamurthy R, Randolph TW, Carpenter JF, Manning MC. Effects of Tween 20® and Tween 80® on the stability of albutropin during agitation. *J Pharm Sci*. 2005;94(6):1368-1381.
36. O'Brien EP, Dima RI, Brooks B, Thirumalai D. Interactions between hydrophobic and ionic solutes in aqueous guanidinium chloride and urea solutions: lessons for protein denaturation mechanism. *J Am Chem Soc*. 2007;129(23):7346-7353.
37. Brems D, Brown PL, Becker G. Equilibrium denaturation of human growth hormone and its cysteine-modified forms. *J Biol Chem*. 1990;265(10):5504-5511.
38. Kawahara K, Tanford C. Viscosity and density of aqueous solutions of urea and guanidine hydrochloride. *J Biol Chem*. 1966;241(13):3228-3232.
39. Majorek KA, Porebski PJ, Dayal A, et al. Structural and immunologic characterization of bovine, horse, and rabbit serum albumins. *Mol Immunol*. 2012;52(3):174-182.
40. Roberts GCK, Association EBS, eds. *Encyclopedia of Biophysics*. Heidelberg, Germany: Springer; 2013.

SUPPLEMENTARY MATERIAL

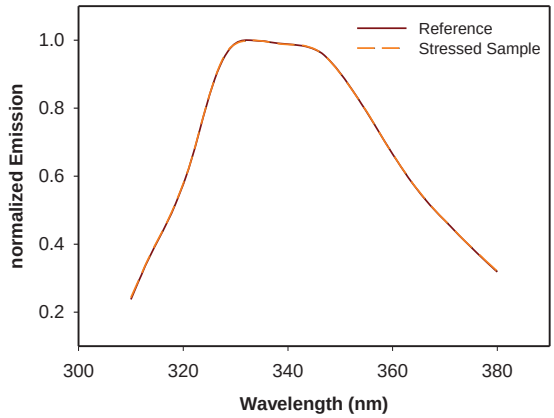

Figure S1: Intensity normalized fluorescence spectrum of a rhGH sample which was sheared at 10200 s^{-1} for 30 minutes (0 M GuHCl) compared to an unstressed reference sample.

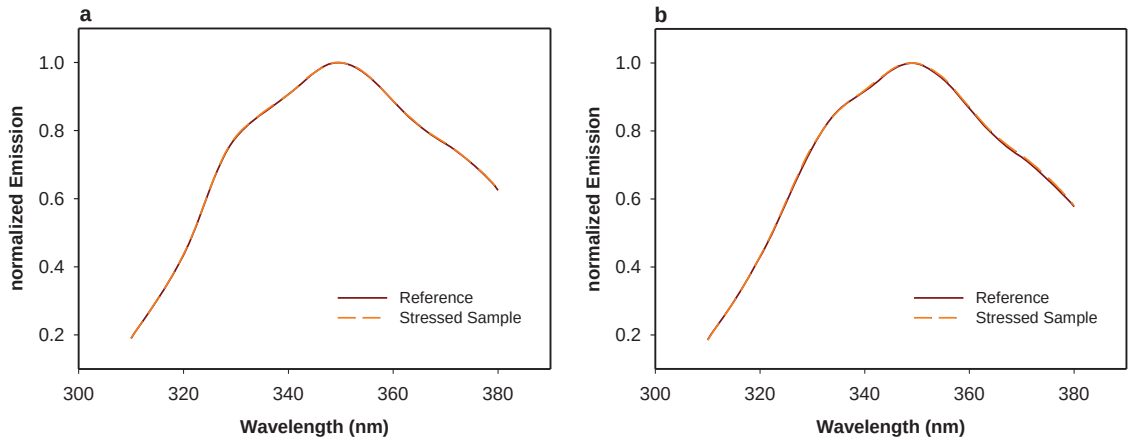

Figure S2: (a) Intensity normalized fluorescence spectrum of an IgG1 sample which was sheared at 3840 s^{-1} for 30 minutes (0 M GuHCl) compared to an unstressed reference sample. (b) Intensity normalized fluorescence spectrum of an IgG1 sample which was sheared at 10200 s^{-1} for 30 minutes (2 M GuHCl) compared to an unstressed reference sample.

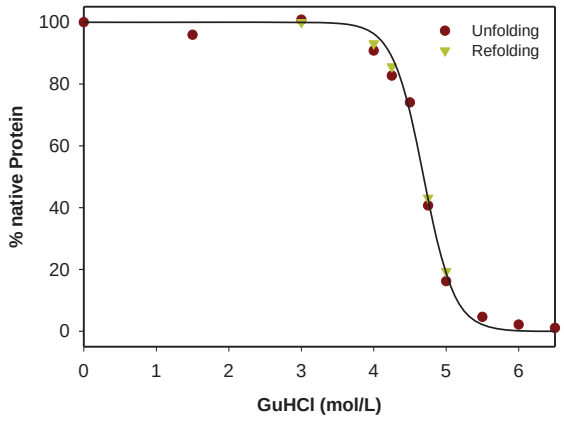

Figure S3: Guanidine hydrochloride (GuHCl) induced denaturation of recombinant human Growth Hormone (rhGH).

The free energy of unfolding (ΔG_U) can be calculated for every data point in the denaturation curve by applying following relationship:

$$K_{eq} = \frac{unfolded\ fraction}{folded\ fraction} \quad \text{(S1)}$$

$$\Delta G_U = -R * T * ln(K_{eq}) \quad \text{(S2)}$$

where R is the ideal gas constant and T is the temperature.
The standard free energy of unfolding (ΔG^0_U) of the protein in buffer without guanidine hydrochloride (GuHCl) can be estimated by extrapolation of the linear descending part of the ΔG_U curve to 0 M GuHCl.

Linear regression gives a standard free energy of unfolding (ΔG^0_U) of the protein in formulation buffer of 61.5 kJ mol^{-1} which corresponds to 14.7 kcal mol^{-1}.

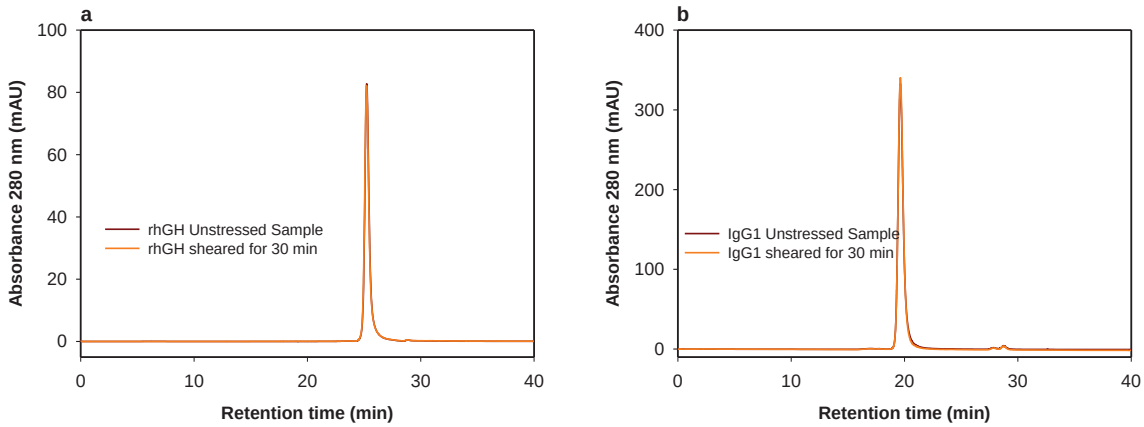

Figure S4: SE-HPLC chromatogram of an unstressed sample and a sample which was sheared inside of the Couette Cell for 30 minutes at 3840 s^{-1} of rhGH (a) and IgG1 (b).

International Journal of Pharmaceutics 511 (2016) 931–945

Contents lists available at ScienceDirect

International Journal of Pharmaceutics

journal homepage: www.elsevier.com/locate/ijpharm

A systematic evaluation of mechanisms, material effects, and protein-dependent differences on friction-related protein particle formation in formulation and filling steps

Lukas Brückl[a,b,*], Rainer Hahn[b], Mauro Sergi[a], Stefan Scheler[a]

[a] Department of Pharmaceutical Development, Sandoz GmbH, Langkampfen, Austria
[b] Department of Biotechnology, University of Natural Resources and Life Sciences Vienna, Vienna, Austria

ARTICLE INFO

Article history:
Received 20 June 2016
Received in revised form 2 August 2016
Accepted 3 August 2016
Available online 4 August 2016

Keywords:
Protein stability
Adsorption
IgG antibody
Surfactant
Compounding
Abrasion

ABSTRACT

Particle formation by physical degradation during the compounding step of biopharmaceuticals is a common concern and found in vessels with bottom mounted stirrers. It was potentially linked to sliding bearings, however, the exact mechanism was still unclear. In this study, custom designed small scale bearings in combination with an IgG1 antibody as model protein were used for investigations of the degradation mechanism inside a bearing. Thereby, abrasion of adsorbed proteins by contact sliding was identified as prevailing protein degradation mechanism and was quantified by an increase in turbidity and by monomer loss. As the protein degradation was highly dependent on combinations of the material of the bearing and the buffer solution, a test system was introduced which allowed to study these effects. Results from the test system using IgG1 and recombinant human growth hormone confirmed a protective effect of Polysorbate 80 by a reduction of protein adsorption, which was strongest in combination with a highly hydrophobic sliding material (PTFE). Finally, a comparison of degradation products from various stresses by ATR-FTIR revealed a high similarity between friction-related degradation products. Therefore, abrasion of adsorbed proteins is very likely the prevailing physical degradation mechanism in processing steps where contact sliding occurs.

1. Introduction

The manufacturing process of a typical protein pharmaceutical drug product includes so called formulation, fill and finish processing steps, where a purified and concentrated drug substance solution is processed into its final dosage form for the market. During the formulation step, also called compounding, the drug substance is diluted to a predetermined concentration and excipients are added to increase the stability of the molecule during processing, handling and long term storage (Rathore and Rajan, 2008). After homogenization by stirring in the compounding vessel the solution has the composition of the final drug product. Subsequent processing steps are sterile filtration, filling into the primary packaging and, if needed, lyophilization. In course of the processing steps the physical state of the protein can change. Diverse stresses have been described to affect the physical stability of proteins, including heat, freezing, light, dehydration, interfacial effects, shear, pressure and pH (Chang and Yeung, 2010). Exposure to such stress conditions can induce aggregation and particle formation which can change the biological activity of the drug and increase the potential for immunogenicity (Wang et al., 2010). Furthermore, particles created during compounding negatively influence the fouling behavior of the subsequent filtration step (Rajniak et al., 2008).

Here we want to focus on the stress that is caused by stirring in a compounding vessel with a bottom mounted magnetic type stirrer. Bottom mounted stirrers enable mixing of low volumes and are usually magnetically coupled impellers as this lowers the risk of contamination due to the absence of mechanical shaft seals that can fail (Chisti, 1992). Therefore, vessels with a bottom mounted stirrer are nowadays widely used for compounding. The impeller is kept in position by a sliding bearing, which consists of a fixed male part (stator) that is mounted to the vessel and a female part (rotor), that is embedded in the rotating mixing head (see Fig. 1). Typically, the bearing is manufactured of very hard ceramics (such as silicon carbide—SiC) which enable high wear and corrosion resistance (Somiya, 2013). The bearing is fully submerged inside the vessel.

* Corresponding author at: Biochemiestraße 10, 6336 Langkampfen, Austria.
E-mail address: lukas.brueckl@sandoz.com (L. Brückl).

http://dx.doi.org/10.1016/j.ijpharm.2016.08.006
0378-5173/

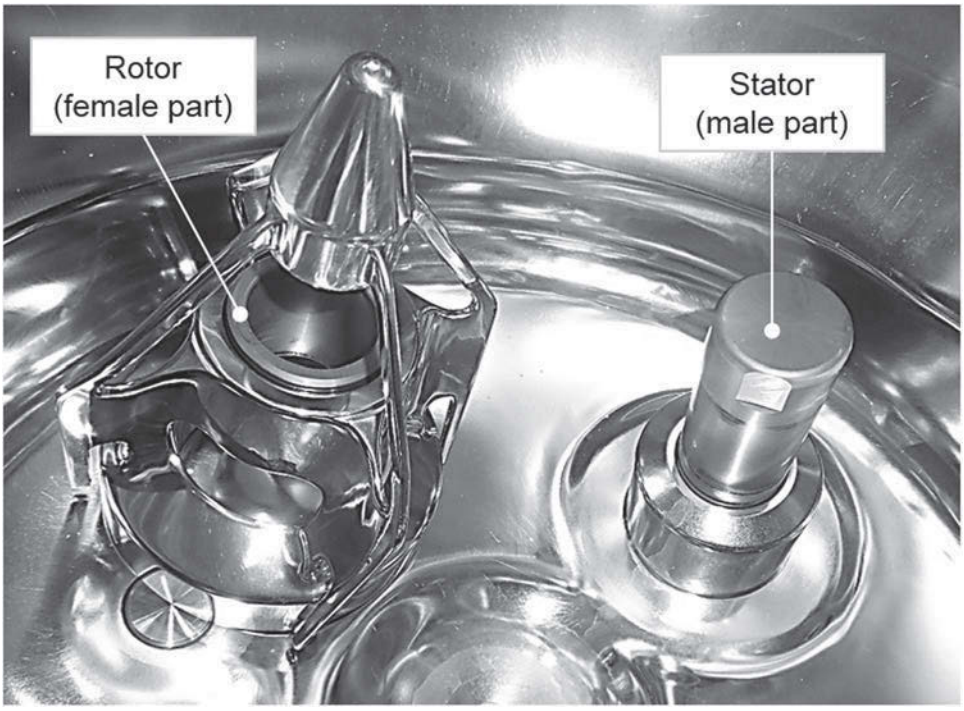

Fig. 1. A typical bottom mounted-magnetic type stirrer. The mixing head with the embedded female part of the sliding bearing has been removed from the male part of the bearing for better visualization.

Thus, the liquid containing the active pharmaceutical ingredient is serving as lubricant for the sliding bearing.

There is a growing awareness throughout the pharmaceutical community that bottom-magnetic type stirrers have an impact on drug product quality. In a study performed by Ishikawa et al. a mixing system using a top entering type stirrer was compared to a bottom-magnetic type stirrer. Stirring of a monoclonal antibody solution resulted in particle formation and therefore filter fouling in a subsequent filtration step when a bottom-magnetic type stirrer was used. No formation of particles could be observed for the top entered stirrer (Ishikawa et al., 2010). An evaluation of the impact of the design of different types of bottom mounted stirrers on monoclonal antibody solutions was performed later (Gikanga et al., 2015). The authors could show that mixers which were designed to have only a small gap between rotor and stator or even touching parts induced particle formation upon rotation. Both studies draw the conclusion that shear stress inside the gap of the sliding bearing was the most likely mechanism for the observed physical protein degradation. Cavitation alone as well as cavitation in combination with shear was additionally considered by Gikanga et al. However, it has to be mentioned that the studies were designed to evaluate the best mixing system and not to identify the exact degradation mechanism.

From the physical protein degradation mechanisms that are currently under discussion in fill and finish steps, we identified 5 mechanisms that could be responsible for protein degradation inside the sliding bearing.

1) Heat induced protein denaturation: Contact sliding of the inner and outer part of the bearing could generate heat. Heat induced protein denaturation is a well-known phenomenon (Chang and Yeung, 2010) and could be responsible for the reported protein degradation by rotational movement of the sliding bearing.
2) Nano/micro particle heterogeneous nucleation: Micro/nano particles of stainless steel have been described to cause aggregation of IgG1 over 30 min of incubation (Bee et al., 2009a). Furthermore, they are under discussion to promote IgG1 particle formation by heterogeneous nucleation during stainless steel rotary piston pump filling operations (Tyagi et al., 2009). Contact sliding of the male and female part could introduce ceramic particles into the sample solution, which could serve, similar to steel particles, as heterogeneous nuclei for particle formation.
3) Cavitation and air/liquid interfacial effects: The phenomenon of rapidly forming vapor cavities (bubbles) inside of a liquid is called cavitation. Upon collapse of the bubbles, shock waves, extreme pressure, temperature or highly turbulent flow conditions could be responsible for protein aggregation, as well as a potential formation of hydrogen radicals (Mahler et al., 2009). Furthermore, cavitation creates a temporary air/liquid interface, which is destroyed again after the bubble is burst. It could be shown that especially the dilation and subsequent compression of air/liquid interfaces causes particle formation of a monoclonal antibody (Bee et al., 2012). Finally, it has to be mentioned, that additional air/liquid interfacial effects exist during stirring (e.g. vortex formation), which are not directly related to a sliding bearing. As these effects are also found in systems having top entering type stirrers, they were not considered as potential root cause of particle formation in our magnetic-bottom stirring studies.
4) Shear stress induced unfolding: Unfortunately, the term “shear” can be interpreted in different ways. Here we want to follow the definition of Thomas and Geer, who described shear as the effect of hydrodynamic forces in terms of velocity gradients on proteins in free liquid (Thomas and Geer, 2011). Shear related effects at interfaces, on the other hand, are considered below (see abrasion of adsorbed proteins). The effect of shear on proteins in solution is an interesting and debated topic with many conflicting studies. Whereas some authors claim to have observed shear induced unfolding already at moderate shear rates below $10^3\,s^{-1}$ (Ashton et al., 2009; Bekard et al., 2011, 2012; Tirrell and Middleman, 1975), contrary papers report

shear rates higher than $10^4\,s^{-1}$ (Bee et al., 2009b; Brückl et al., 2016; Jaspe and Hagen, 2006) have no influence on protein stability. However, extremely high shear rates ($10^7\,s^{-1}$) could lead to protein unfolding (Jaspe and Hagen, 2006) and subsequently aggregation. As high shear rates could locally occur within the sliding bearing upon rotational movement, shear stress as possible root cause for protein degradation has to be investigated.

5) Abrasion of adsorbed proteins: Recently, there have been publications which proposed a new mechanism of protein aggregation or particle formation that is based on desorption or abrasion of adsorbed proteins from solid surfaces (Perevozchikova et al., 2015; Sediq et al., 2016). After adsorption to solid surfaces the native fold of a protein is often destabilized, leading to conformational changes or even aggregation (Rabe et al., 2011). Subsequent abrasion by contact sliding or by hydrodynamic forces leads to an increase in particle content of the sample solution (Perevozchikova et al., 2015; Sediq et al., 2016). Also Gikanga mentioned in his discussion, that mixing systems with contact between stator and rotor are very likely to cause particle formation (Gikanga et al., 2015). A rotating stirring head is subject to axial and radial forces upon mixing and contact between stator and rotor is very likely to happen. Therefore, unspecific protein adsorption at the sliding bearing and subsequent abrasion has to be considered as possible mechanism of protein degradation.

Our study was designed to characterize physical protein degradation inside the sliding bearing of bottom-magnetic type stirrers and to specifically unravel the underlying mechanism. Thus, we used a custom designed sliding bearing to simulate the effect of stirring in a compounding vessel. The study was performed with a monoclonal IgG1 antibody, which has already been characterized for its stability against shear in free solution in a former study (Brückl et al., 2016). Another objective of our study was to develop a simple test system that mechanistically simulates protein degradation inside the sliding bearing. For evaluation of the test system also recombinant human growth hormone (rhGH) was used as additional model protein. Physical protein degradation by aggregation and particle formation was monitored by size exclusion high performance chromatography (SE-HPLC), turbidity measurements and single particle optical sizing (SPOS). Additional characterization of the degradation products was performed by attenuated total reflection Fourier transform infrared (ATR-FTIR) spectroscopy and scanning electron microscopy in combination with energy dispersive X-ray spectroscopy (SEM-EDX).

2. Materials and methods

2.1. Materials

Frozen stock solutions of a monoclonal IgG1 antibody (145 kDa) and recombinant human growth hormone (rhGH, 22 kDa) were provided by Sandoz GmbH (Kundl, Austria). The isoelectric point of IgG1 and rhGH is pH 9.5–9.9 and pH 5.0–5.1, respectively. The concentration of the IgG1 and rhGH stock solution was 29.7 mg mL^{-1} and 7.5 mg mL^{-1}, respectively. Citric acid and sodium thiocyanate was obtained from Sigma Aldrich (Saint Louis, USA), sodium phosphate and iron(III) chloride hexahydrate from Merck (Darmstadt, Germany), Polysorbate 80 from J.T. Baker (Center Valley, USA) and Poloxamer 188 from BASF (New Jersey, USA). High precision spheres (4 mm in diameter) of following materials were purchased from Spherotech GmbH (Fulda, Germany): stainless steel (316L, 1.4404), SiC, PTFE and borosilicate glass. Mucasol®, an alkaline cleaning agent containing >30% phosphates, <5% anionic surfactants, amphoteric surfactants, complexing agents, corrosion inhibitors and auxiliary agents, was obtained from Brand GmbH + Co. KG (Wertheim/Main, Germany).

2.2. Methods

2.2.1. Preparation of samples

Stock solutions were gravimetrically diluted to the respective concentrations with buffer. The antibody was buffered by 25 mM sodium citrate (pH 6.5) and rhGH by 10 mM sodium phosphate (pH 7.0).

2.2.2. Protein degradation in a simulated sliding bearing

A SiC sliding bearing that simulates the sliding bearing of magnetic bottom stirrers in large scale vessels was used to study potential protein degradation during rotational movement. The SiC bearing consisted of an inner rotating cylinder which was fixed to a stainless steel shaft. The outer cylinder was fixed to a mount that prevented its rotational movement and defined its vertical position. However, the mount was designed to give a certain freedom in movement to the outer cylinder which needs to follow oscillations of the rotating shaft. In order to minimize liquid flow related protein degradation at air/liquid interfaces, a stirring head without blades was used. A schematic drawing is given in Fig. 2. The clearance between inner and outer sliding bearing was 0.06 mm. The contact area between the male and the female part of the sliding bearing is in total 6.28 cm^2 (3.14 cm^2 per part). Besides SiC an additional bearing made out of PTFE was used. During experiments at different rotational speeds (stated in the results section) the sliding bearing was fully submerged in 90 mL sample solution inside a 100 mL borosilicate glass beaker. This gives a volume to contact area (theoretical area where friction occurs inside the sliding bearing) ratio of 14.3 cm^3/cm^2. Visible air bubbles were carefully removed from the system using a syringe and a cannula. Furthermore, a PTFE magnetic bar stirrer was placed inside the beaker which was used to homogenize the solution before sampling. Therefore, the stirrer was turned on for 15 s prior to every sampling point. Cleaning of the bearing was performed after every experiment by rinsing with water, submerging the bearing in 2% Mucasol® solution for 15 min with rotational movement and as final step an extensive rinse with water.

2.2.3. Determination of temperature of rotating sliding bearing

An infrared picture of the rotating sliding bearing was taken during rotational movement with an E50 Infrared camera from FLIR (Wilsonville, Oregon, USA). Therefore, the sliding bearing was initially rotated at 750 rpm for 10 h. Subsequently, it was carefully lifted until the top part was not covered anymore with sample solution and the picture was taken still during rotational movement.

2.2.4. Determination of turbidity

A 2100AN Turbidimeter from Hach (Loveland, Colorado) in combination with a cell adapter for small volumes was used. The turbidity of the samples is reported in NTU units. For small sample volumes the turbidity of the solution was compared using absorbance values at 420 nm which were determined on a Lambda 35 UV/VIS spectrometer (Perkin Elmer, Massachusetts, USA).

2.2.5. Single particle optical sizing (SPOS)

The size distribution and number of particles was determined using an AccuSizer 780 SIS optical particle sizer from Particle Sizing Systems (Santa Barbara, California, USA) which was controlled by the software AccuSizer XI. The system uses light obscuration and light scattering to detect particles in the range of 0.5–500 μm. After a flush volume of 1 mL a sample volume of 4 mL was analyzed

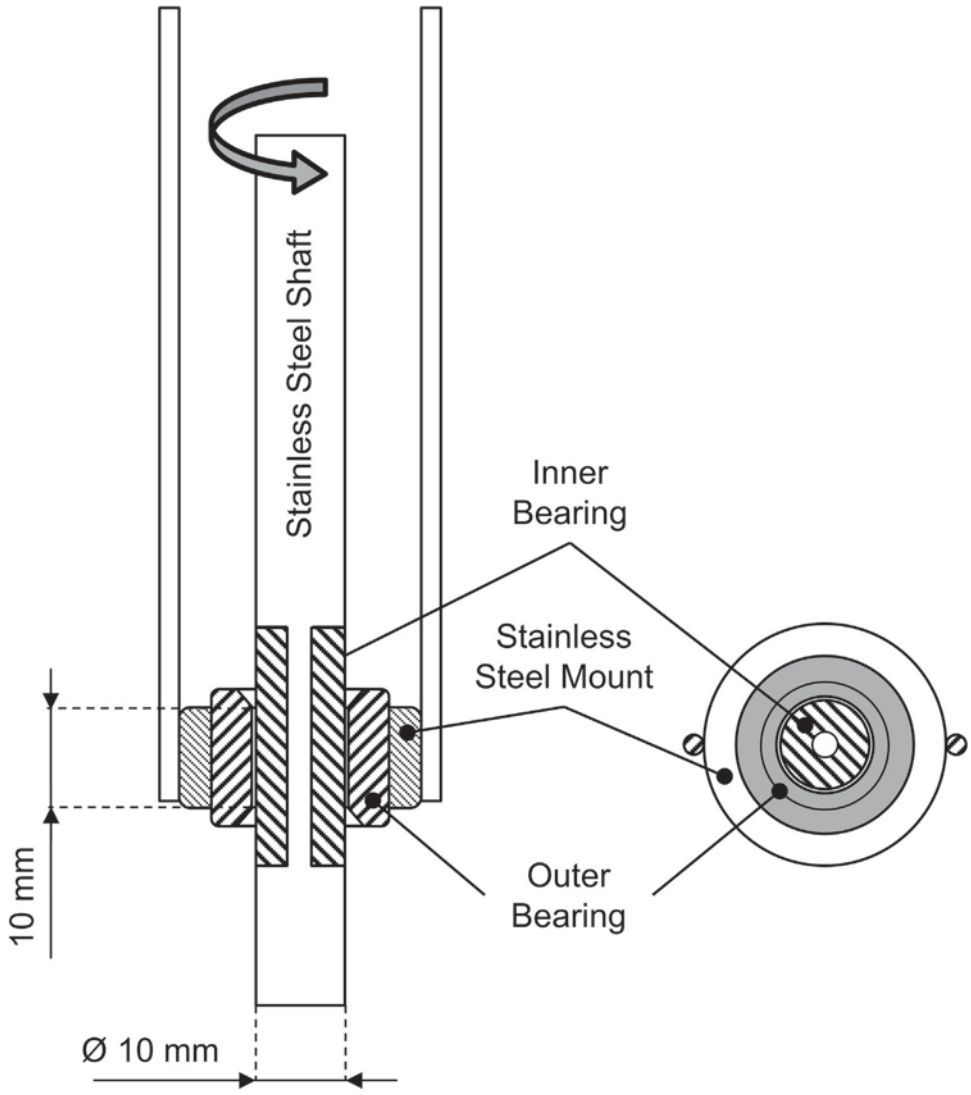

Fig. 2. Schematic of the custom designed SiC sliding bearing (not to scale) which was used to investigate potential protein degradation inside the sliding bearing of magnetic bottom stirrers in compounding vessels. The stirring head was manufactured without blades to avoid vortex creation.

from each sample using a flow rate of 20 mL min^{-1}. This was repeated 3 times to give a total analysis volume of 12 mL. Between two samples, the detector was extensively cleaned with water in order to avoid cross contamination.

2.2.6. Size exclusion high performance liquid chromatography (SE-HPLC)

Monomer content, aggregation level and lower molecular weight variants of the stressed protein solutions were determined using a 1290 Agilent (Santa Clara, USA) chromatography system with a TSKgel G3000SW_{XL} column (7.8 mm ID × 30 cm, 5 μm particle size) and an inline 2 μm stainless steel frit. The system was controlled using the Dionex software package Chromeleon 6.8. A flow rate of 0.4 mL min^{-1} was applied using a 150 mM potassium phosphate (pH 6.5) as mobile phase. Prior to analysis samples were filtered (PVDF, 0.2 μm), the first drops were discarded to avoid potential inaccuracies caused by adsorption effects. The column was loaded with roughly 7 μg of protein, UV absorbance was recorded at 210 and 280 nm using an Agilent 1290 Infinity DAD. Fluorescence was excited at 295 nm and emission was recorded at 345 nm by an Agilent 1260 FLD.

2.2.7. Determination of contact angle

The contact angle between water and the solid materials SiC, glass, PTFE or stainless steel was determined using the sessile drop technique after the surface was cleaned with ethanol and dried over acetone. A small drop of water (1–5 μL) was placed on the specific material in horizontal position. A picture of the drop was taken against an illuminated background using a Nikon SMZ-U stereomicroscope with a Nikon D5000 camera. Subsequently, the picture was analyzed using the free software ImageJ in combination with the plugin DropSnake or LB-ADSA (Stalder et al., 2006). All contact angle measurements were carried out along a flat and horizontal base line, except for the determination on the inside of the outer bearing of the sliding bearing. As there is no flat baseline, the contact angle from picture was evaluated manually using the tangent to the drop contour and the tangent to the base contour. Contact angle between water and SiC was tested at the outside of an outer bearing, the outside of an unused inner bearing, the outside of a used inner bearing where friction had taken place, the inside of an unused outer bearing and at the inside of a used outer bearing where friction had taken place. Contact angle between water and glass was determined at the surface of a cover glass

Fig. 3. Test system consisting of spheres inside a glass vial that is closed by a cover glass. The cover glass is fixed by wrapping parafilm around.

made of borosilicate glass. Contact angle between water and PTFE was determined at a flat PTFE stirring bar, at the outside of the outer PTFE bearing and at the outside of the inner PTFE bearing. Contact angle between water and stainless steel was determined at the stirrer shaft, the mount of the outer bearing and at the bottom of a stainless steel beaker. Values are reported as the average of one material with standard deviation.

2.2.8. Test system for physical protein degradation by abrasion of adsorbed proteins

50 spheres of a specific material were placed inside a 6R vial (Schott, Fiolax Clear TopLine). Subsequently, a sufficient volume of sample solution was filtered (0.2 μm, PVDF, first drops were discarded) into the vial to the very top which gave a sample volume to sphere surface area ratio of 0.34 cm^3/cm^2. Air was excluded as good as possible. The vial was then sealed using a cover glass (borosilicate glass, Ø 19 mm, VWR) which was fixed with Parafilm. Subsequently, the vial was rotated at a certain speed on an end over end rotator for a certain time. For each material a vial with spheres and sample solution was additionally incubated in a static position and served as an unstressed reference sample.

2.2.9. Determination of protein adsorption to stainless steel, SiC and glass micro-powder

IgG1 and rhGH adsorption to stainless steel, SiC and glass was determined by solution depletion. In order to achieve a measureable depletion, a micro-powder of the respective materials, which has a very high surface to weight ratio, was added to the sample solution. The particle size of the stainless steel (Goodfellow Cambridge Ltd., Huntingdon, England), SiC (Alfa Aesar, Karlsruhe, Germany) and glass (Schott, Landshut, Germany) micro-powder was 45 μm, 30 μm and 16 μm, respectively. IgG1 or rhGH concentration inside the sample solution was 0.2 mg mL^{-1}. In a 2 mL Eppendorf tube, 250 μg of stainless steel powder or 50 μg of SiC or glass powder was mixed with 500 μL sample solution. After an incubation time of 2.5 min, the micro-powder was spun down at 14500 rpm and the sample was 0.2 μm filtered (PVDF, first drops were discarded). Protein depletion was subsequently determined by SE-HPLC and compared against a control sample which was incubated without powder. Adsorption was determined in triplicate for protein formulations with and without 0.7 mg mL^{-1} PS80.

2.2.10. Detection and quantification of Fe^{3+}

300 μL of an acidic sodium thiocyanate solution (2% w/w) was added to 1 mL of sample solution. In the presence of Fe^{3+} ions a red complex forms between a Fe^{3+} and three thiocyanate ions. Quantification of the Fe^{3+} ion was performed by comparing the absorbance of the sample at 490 nm with the absorbance values of a Fe^{3+} chloride standard solution. Therefore, the Lambda 35 UV/VIS spectrometer (Perkin Elmer, Massachusetts, USA) was used.

2.2.11. Fe^{3+} spiking study

52.5 μL of a 2×10^3 mol L^{-1} Fe^{3+} chloride solution was added to 7 mL of IgG1 sample solution (0.2 mg mL^{-1}) with or without Polysorbate 80 and incubated at room temperature for 20 h in a closed 6R glass vial. Negative controls were performed by adding 52.5 μL of water to the sample solution. After incubation, analysis was performed by SE-HPLC. Samples were prepared in triplicate. The experiment was repeated using rhGH (0.2 mg mL^{-1}).

2.2.12. Protein degradation by diverse stress conditions for comparison by ATR-FTIR

The IgG1 antibody and rhGH were formulated without a surfactant at a concentration of 29.7 mg mL^{-1} and 6 mg mL^{-1}, respectively, for experiments of protein degradation by heat, sulfuric acid, rotating vials with spheres and air/liquid interface compression and dilation cycles. Protein degradation studies by the SiC sliding bearing, ceramic piston pump and stainless steel piston pump were performed at an IgG1 concentration of 10 mg mL^{-1} and a rhGH concentration of 1 mg mL^{-1}.

- Heat denaturation studies were performed in a 2 mL Eppendorf tube by heating 1.5 mL of sample solution to >80 °C for 1 h.

- Protein precipitation by sulfuric acid was performed by adding concentrated sulfuric acid to 1.5 mL sample solution in a 2 mL Eppendorf tube until protein precipitation was observed at room temperature.
- Protein degradation by contact sliding of spheres was performed as described above. The vials were rotated for 48 h at a speed of 20 rpm at room temperature.
- Air/liquid interfacial stress was applied in form of repeated compression and dilation of the interfacial area as described by Bee et al. (Bee et al., 2012). For this purpose, a 10 mL reagent tube was filled with 5 mL of sample solution, sealed with Parafilm and rotated end over end at 5 rpm for 24 h at room temperature.
- Mechanical stress in form of contact sliding of the SiC sliding bearing was performed as described above. The bearing was rotated at a speed of 500 rpm for 24 h.
- Pumping stress was applied by using a Bausch & Ströbel piston pump with pump heads made out of stainless steel and ceramic (cylinder: Al_2O_3, piston: ZrO_2). Small sized pump heads were chosen (0.15–1.1 mL) in order to increase the surface to volume ratio inside the head. Maximum stroke height and speed were selected and 60 mL of sample solution were pumped in circles for 20 h at room temperature.

2.2.13. Fourier transform infrared spectroscopy (FTIR)

A Tensor 27 FTIR spectrometer from Bruker (Massachusetts, USA) which was controlled by the software Opus 7.2 was used in combination with a temperature controlled BioATR cell II from Harrick (Pleasantville, NY, USA). Protein degradation products in form of precipitates from diverse stress experiments were spun down in a centrifuge and washed with buffer 3× prior to analysis by FTIR. Measurements were performed at 20 °C and results are reported as cumulative spectra from triplicate determinations (n = 3) of 120 scans each. Spectra have been buffer corrected and an atmospheric compensation was performed.

3. Results

The results are divided into three main chapters. In the first chapter, results of the investigation of the degradation mechanism inside the sliding bearing are presented. The influence of various process parameters on protein degradation inside the sliding bearing is covered by the second chapter. Finally, the third chapter summarizes experiments of a test system that was introduced in order to simulate abrasion of adsorbed proteins, a recently proposed physical protein degradation mechanism (Sediq et al., 2016).

3.1. Identification of the degradation mechanism inside the sliding bearing

3.1.1. Heat development by contact sliding

Heat generation of the experimental set up was studied after running the bearing for 10 h at a rotational speed of 750 rpm by the use of an infrared camera (Fig. 4). A moderate temperature of roughly 21 °C was observed at the surface of the inner and outer part of the ceramic bearing, as well as the solution.

3.1.2. Investigation of heterogeneous nucleation of IgG1 particles on SiC micro/nano particles

The generation of SiC particles by material abrasion and its impact on protein degradation during rotational movement of the sliding bearing was investigated. For this purpose, the SiC sliding bearing was submerged in 0.2 μm filtered (PVDF, first drops were discarded) buffer without IgG1 (25 mM Citrate, pH 6.5, no surfactant) and rotational movement at 300 rpm was performed for 23.5 h. Analysis by single particle optical sizing showed an increase in content from 84 particles mL^{-1} (blank) to roughly 30,000 particles mL^{-1} after rotational movement, which were mostly below 4 μm. At high particle concentrations light obscuration measurements can result in negative bias due to coincidence, i.e. presence of more than one particle in the sensing

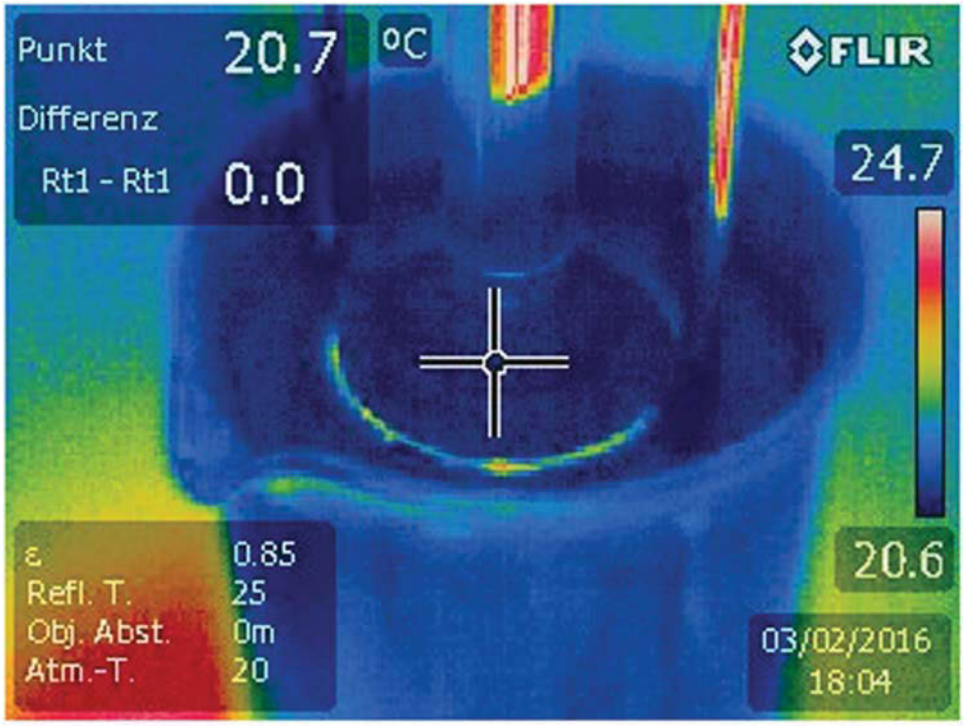

Fig. 4. Infrared picture of the SiC sliding bearing at a rotation speed of 750 rpm. The sliding bearing was lifted out of the sample solution to avoid a coverage.

zone. Therefore, the particle count of the SiC particles is most likely even higher (supported by analysis of diluted samples, data not shown). Subsequently, a high concentrated IgG1 solution was added to the pre-treated buffer to obtain a final IgG1 concentration of 0.2 mg mL^{-1}. The solution was homogenized and incubated at RT for 23.5 h, analyzed by SE-HPLC and compared against a mixture with an untreated buffer. No increase in IgG1 higher molecular weight variants (soluble aggregates) could be detected. Furthermore, the monomer content did not decrease, which was the main indication of protein degradation in the following experiments.

3.1.3. Investigation of the effect of the formulation and the material of the bearing on protein degradation

Protein degradation studies were performed using two different materials of the sliding bearing and two different IgG1 formulations (with or without 0.7 mg mL^{-1} PS80) at a concentration of 0.2 mg mL^{-1}. Besides the SiC sliding bearing, a bearing with identical dimensions but manufactured from PTFE was used. At a rotational speed of 300 rpm the monomer loss for all combinations of bearing materials and formulations was determined over 23.5 h and is shown in Fig. 5.

Pronounced IgG1 degradation was observed by the SiC bearing, the addition of a surfactant could only slightly improve the amount of retained monomer (60% versus 54%, respectively). PTFE in combination with a formulation without PS80 resulted in pronounced monomer loss of 25% after 23.5 h of stress. However, a combination of a PTFE sliding bearing with a sample solution where PS80 was added could prevent monomer loss within the detection limit. Determination of the turbidity affirmed this observation. While the turbidity of the sample from the PTFE bearing without surfactant increased by 28 NTU, no significant increase in turbidity could be observed for the sample with surfactant. The degradation rates between the PTFE and SiC sliding bearing cannot be directly compared. As PTFE is a soft material, it was slightly changing its dimensions when it was fixed to the rotating shaft. This could cause differences in the grinding pressure and behavior between stator and rotor.

3.2. Characterization of IgG1 degradation inside the SiC sliding bearing

3.2.1. Effect of rotational movement and reproducibility of IgG1 degradation inside the SiC sliding bearing

The effect of contact sliding by rotational movement of the custom SiC bearing at 300 rpm was investigated for an IgG1 solution at a concentration of 0.2 mg mL^{-1}. No surfactant was added. After a rotational time of 23.5 h, the experiment was stopped and the stressed solution was analyzed by SE-HPLC. Furthermore, the turbidity of the solution was determined. The experiment was repeated twice to a total of three runs (n = 3).

An average loss in monomer content by 37% of the initial content was observed by SE-HPLC. No increase in higher molecular weight variants (soluble aggregates) could be seen after 23.5 h. The turbidity of the solution was strongly increased from <1 to 81 NTU after 23.5 h of contact sliding. Triplicate determination showed a good reproducibility with a standard deviation of 4% in relative monomer loss and of 3 NTU in turbidity.

Analysis by single particle optical sizing after 23.5 h of rotational movement showed a particle size distribution that peaked at 15 μm, which could be confirmed by inspecting the sample under a microscope.

Like to like exchanges of the sliding bearing or even just a reassembling of the set up using identical parts affected the protein degradation rate (notice difference in monomer loss to Fig. 5, where a different set up was used—37% vs approximately 42% monomer loss). Thus, the following results were all collected using the identical SiC bearing in an unchanged set-up.

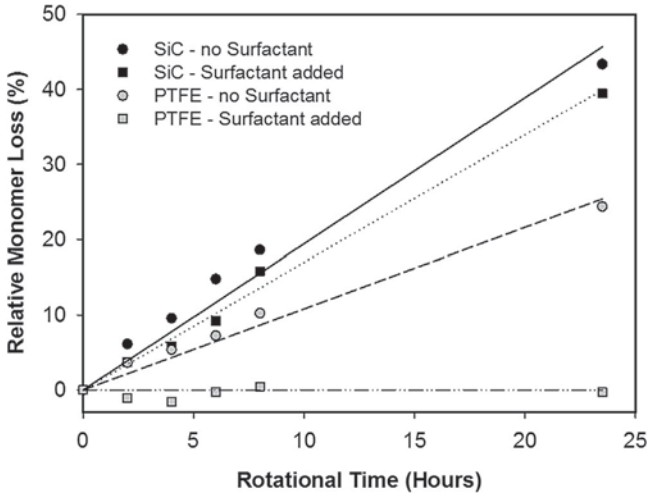

Fig. 5. Dependence of IgG1 degradation on the buffer solution (with or without surfactant) and on the material of the sliding bearing. A linear regression was assumed for the loss in monomer content. The loss is reported in percentage of the monomer area of the unstressed sample at time point 0 h (100%).

3.2.2. Dependence of IgG1 degradation on rotational time

An IgG1 solution (0.36 mg mL^{-1}) without surfactant was stressed at 500 rpm for a total of 72 h. Loss in monomer content (SE-HPLC) and turbidity values (absorbance at 420 nm) were determined at predefined time points and are shown in Fig. 6a. At the beginning, an almost linear relationship between rotational time and monomer loss can be observed which confirms the data from Fig. 5. However, after 24 h the curve flattens out. Again, analysis by SE-HPLC showed no content increase in soluble aggregates over rotational time.

3.2.3. Dependence of IgG1 degradation on IgG1 concentration in sample solution

The dependence of protein degradation on the concentration of the sample solution was investigated using antibody solution at concentrations of 0.2 mg mL^{-1}, 0.4 mg mL^{-1}, 0.8 mg mL^{-1}, 1.6 mg mL^{-1} and 3.2 mg mL^{-1}. All sample solutions were stressed using the SiC sliding bearing at a rotational speed of 300 rpm for 23.5 h. Protein degradation is given in relative monomer peak area (% compared to an unstressed reference sample) and absolute monomer loss (in mg) and is shown in Fig. 6b. The absolute monomer loss doubles with the concentration 0.2–0.4 mg mL^{-1} (comparable relative monomer loss) but flattens out at higher protein concentrations.

3.2.4. Dependence of IgG1 degradation on rotational speed

Dependence of protein degradation on rotational speed was checked for an IgG1 antibody solution at a concentration of 0.25 mg mL^{-1} between 25 rpm and 750 rpm for a constant rotational time of 23.5 h each with or without 0.7 mg mL^{-1} PS80.

Fig. 7 shows the total monomer loss of the respective sample solutions at different speeds, where each data point represents a separate experiment where the solution was stressed for 23.5 h.

The monomer loss of the sample solution without PS80 rises to a maximum at about 750 rpm and then declines again with increasing rotational speed. PS80 was able to reduce protein degradation inside the sliding bearing over the whole tested range. The monomer loss for 500 rpm is comparable to the monomer loss reported in Fig. 6a, which was determined at an initial protein concentration of 0.36 mg mL^{-1}. This strengthens the data of Fig. 6b, where the relative monomer loss is almost identical for sample solutions with initial protein concentrations of 0.2 and 0.4 mg mL^{-1}.

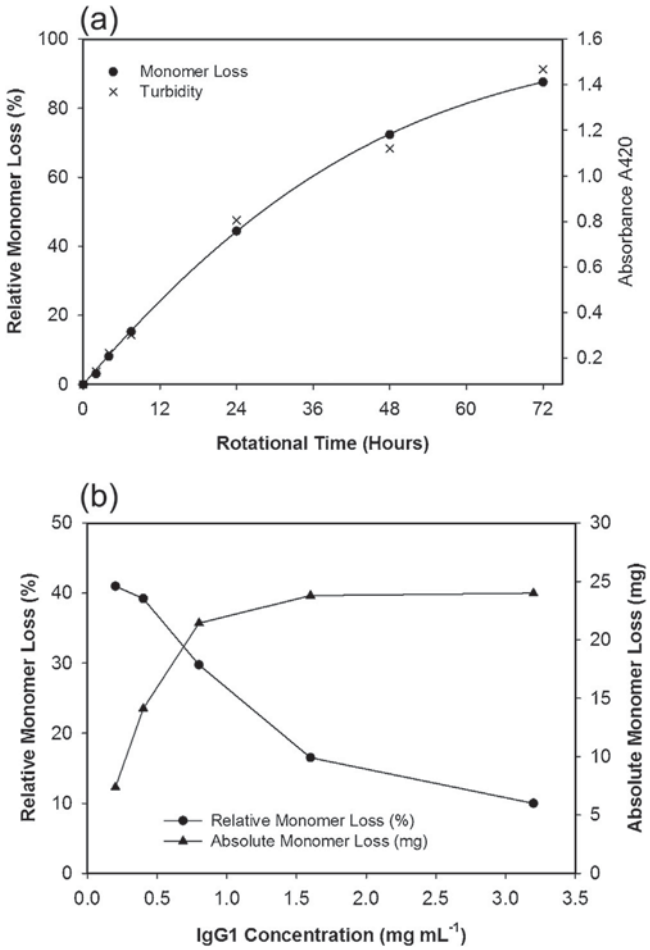

Fig. 6. (a) Increase in monomer loss and in turbidity over time of an IgG1 sample at 0.36 mg mL^{-1}. Protein degradation was caused by rotational movement of a SiC sliding bearing at 500 rpm. (b) Dependence of the protein degradation inside the bearing after 23.5 h of rotational movement at 300 rpm on the initial protein concentration.

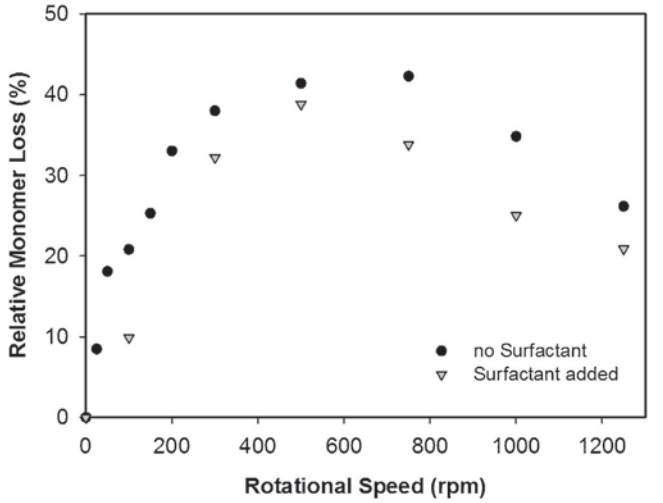

Fig. 7. Dependence of protein degradation within the sliding bearing on the rotational speed at a constant rotational time (23.5 h). Protein degradation is reported in monomer loss (% of monomer peak area at time point 0) for an IgG1 solution with or without PS80.

3.2.5. Determination of the contact angle between water and PTFE, glass, SiC and stainless steel

In order to assess the influence of surface properties, contact angle measurements were performed which are a marker for surface hydrophobicity. The average contact angle of a water drop on the surface of the respective material was 105.4 ± 4.5° (PTFE, n = 10), 56.3 ± 4.9° (glass, n = 3), 53.7 ± 7.4° (SiC, n = 10) and 50.4 ± 9.6° (stainless steel, n = 6). PTFE showed by far the highest hydrophobicity of all tested materials.

3.3. Evaluation of the test system for protein degradation by abrasion of adsorbed proteins

3.3.1. IgG1

The IgG1 antibody was formulated at a concentration of 0.2 mg mL^{-1} with and without 0.7 mg mL^{-1} Polysorbate 80. 50 spheres of four different materials were end-over-end rotated in closed vials (as shown in Fig. 3) under the exclusion of air/liquid interfaces at 5 rpm for 24 h and at 20 rpm for 6 h. This gives a total of 7200 rotations for both combinations of speed with rotational time. Furthermore, to study the effect of micro/nano-particles, which are abraded from the spheres, the samples that had been rotated at 20 rpm for 6 h were additionally incubated 18 h in a static position after rotational movement to give a total incubation time of 24 h. Samples were analyzed using SE-HPLC. Protein loss in percent of the initial protein concentration is reported as average of triplicate determination and shown in Fig. 8 (n = 3).

The test system for protein abrasion using rotating spheres showed a strong degradation of IgG1 with all materials as shown by formation of particles, increase in turbidity, and loss of monomer except for the combination of PTFE with surfactant-containing IgG1 solution. SE-HPLC analysis revealed the highest monomer loss of samples from stainless steel spheres, followed by SiC, glass and PTFE samples. The addition of a surfactant was not able to significantly decrease monomer loss in combination with stainless steel spheres. Protein degradation at SiC, glass and PTFE surfaces was reduced by the surfactant.

The experiment at higher rotational speed (20 rpm) showed an overall decreased monomer loss compared to the slow rotating experiment (5 rpm). Additional incubation for 18 h of the samples which have been rotated at 20 rpm did not lead to further monomer loss or aggregation.

SE-HPLC chromatograms of all samples showed no increased level of higher molecular weight variants compared to the reference control.

3.3.2. Further investigations of IgG1 samples—presence of Fe^{3+} and spiking studies

IgG1 placebo solution (25 mM citrate at pH 6.5, no protein) was stressed for 6 h at 20 rpm in the test system with and without the addition of 0.7 mg mL^{-1} PS80. Subsequently, 7 mL of the placebo solution were placed in a fresh glass vial and spiked with high concentrated IgG1 to obtain a final concentration of 0.2 mg mL^{-1}. The solution was then incubated at room temperature for 24 h and finally analyzed using SE-HPLC. The same steps were performed using a stressed placebo solution which was 0.1 μm filtered (PES, first drops were discarded) before IgG1 was added.

Addition of IgG1 to a placebo solution that was pretreated with glass, PTFE or SiC spheres, did not show an increased monomer loss compared to a negative control. Spiking IgG1 to a placebo solution without PS80 that was pretreated using stainless steel spheres resulted in a monomer loss of about 10% of the initial protein concentration. In the presence of PS80 a monomer loss of about 32% was observed. The 0.1 μm filtrated sample (which removes abraded steel particles) did not show a reduced monomer loss compared to the non-filtrated one.

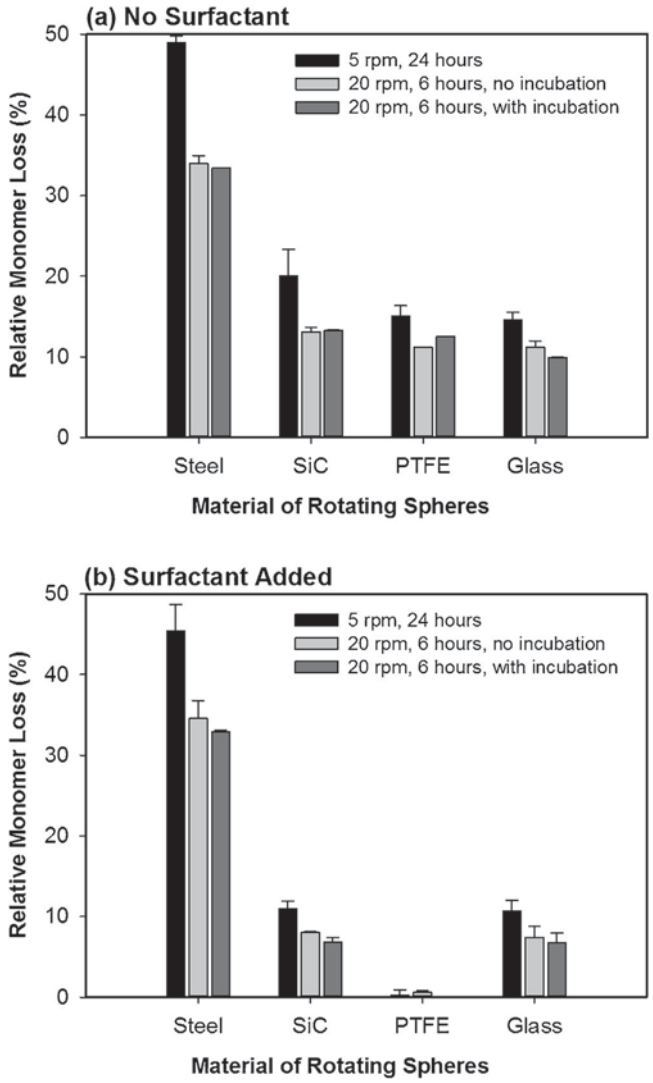

Fig. 8. IgG1 degradation by abrasion from spheres of different materials inside rotating vials given in terms of monomer loss compared to a static incubated and therefore unstressed reference sample. IgG1 was formulated without (a) and with (b) 0.7 mg mL^{-1} PS80 and used as sample solution at a concentration of 0.2 mg mL^{-1}. The solution that was rotated at 20 rpm was additionally incubated for 18 h (in legend "with incubation") to give a total incubation time of the test solution with particles of 24 h. The standard deviation results from triplicate determinations (n = 3).

Elevated levels of Fe^{3+} ions were detected in all placebo solutions which have been stressed in the test system using stainless steel spheres in a concentration of roughly 1.5×10^{-4} mol L^{-1}. To investigate the effect of Fe^{3+} ions, a Fe^{3+} solution was spiked to unstressed IgG1 samples (0.2 mg mL^{-1}) with or without PS80 to obtain a final Fe^{3+} ion concentration of 1.5×10^{-4} mol L^{-1}. Samples were prepared in triplicate (n = 3). After 20 h of incubation at room temperature IgG1 samples without surfactant showed a monomer loss of 9.9 ± 0.1% compared to a non-spiked reference control. A monomer loss of 46.7 ± 0.2% was observed for the PS80 containing and spiked IgG1 solution. An increase in HMW variants was not detected.

3.3.3. rhGH

rhGH was formulated at a concentration of 0.2 mg mL^{-1} with and without 0.7 mg mL^{-1} Polysorbate 80. 50 spheres of four different materials were end-over-end rotated in closed vials at 5 rpm for 40 h and at 25 rpm for 8 h, giving a total of 12000 rotations in both cases. Furthermore, to study the effect of micro/nano-particles, which are abraded from the spheres, the samples that had been rotated at 25 rpm for 8 h were additionally incubated 32 h in a static position after rotational movement to give a total incubation time of 40 h. Samples were analyzed using SE-HPLC. Protein loss in percent of the initial protein concentration is reported as average of triplicate determination and shown in Fig. 9 (n = 3).

The formation of particles and an increase in turbidity was observed for all samples except for all glass samples and the combination of PTFE with surfactant-containing rhGH solution. Contact sliding of stainless steel spheres caused the highest monomer loss of a rhGH solution without surfactant. Contact sliding of PTFE and SiC spheres lead to a comparable monomer loss of approx. 5% in absence of a surfactant, sliding of glass spheres showed a decrease in the monomer content by roughly 1%. The addition of a surfactant reduced the monomer loss

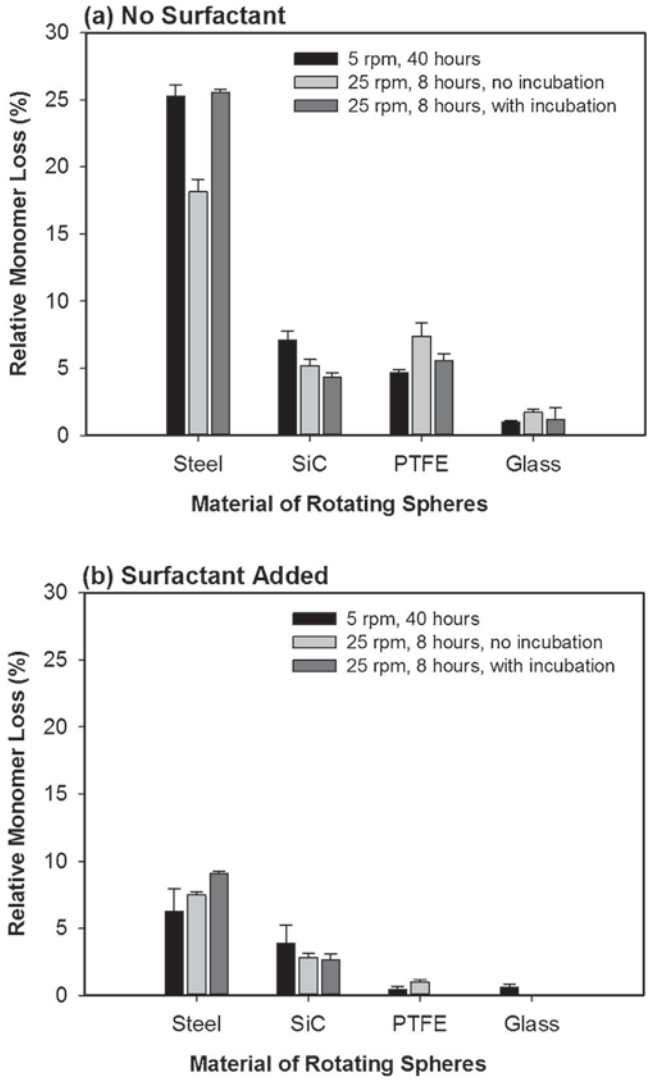

Fig. 9. Protein degradation by abrasion from spheres of different materials inside rotating vials given in terms of monomer loss compared to a static incubated and therefore unstressed reference sample. rhGH was formulated without (a) and with (b) 0.7 mg mL^{-1} PS80 and used as sample solution at 0.2 mg mL^{-1}. The solution that was rotated at 25 rpm was additionally incubated for 32 h (in legend "with incubation"), to give a total incubation time of the test solution with particles of 40 h. The standard deviation results from triplicate determinations (n = 3).

significantly for the stainless steel and PTFE samples and slightly for the SiC samples. Glass samples showed almost no monomer loss without the protection of a surfactant so no clear difference between samples with and without a surfactant could be observed.

The monomer loss of stainless steel samples still increased during additional static incubation, giving a final monomer loss which was very comparable to the slower rotated samples. No significant monomer loss could be observed for all samples containing a surfactant during additional incubation.

A significant increase in higher molecular weight variants could only be observed for stainless steel samples without surfactant. The level in higher molecular weight variants of stainless steel samples without surfactant are as follows: 11% (40 h at 5 rpm), 8% (8 h at 25 rpm) and 12% (8 h at 25 rpm + Incubation). Addition of PS80 strongly reduced the formation of soluble aggregates during rotational movement of the steel samples (2–2.5% HMW variants) and prevented further aggregation during subsequent static incubation. A static incubated reference sample showed no increase in soluble aggregates.

Spiking of Fe^{3+} ions to rhGH at a concentration of 1.5×10^{-3} mol L^{-1} (n = 3) and additional incubation for 20 h did not show the same effect as for IgG1. On average, rhGH samples without surfactant showed a monomer loss of 1.0 ± 0.3% compared to a non-spiked reference control, the presence of PS80 lead to a monomer loss of 2.0 ± 0.8%.

3.3.4. Characterization of IgG1 and rhGH particles from the test system by FTIR spectroscopy

Protein particles that formed in the test system and during rotational movement of the sliding bearing were characterized by ATR-FTIR spectroscopy and the resulting FTIR spectra were compared to protein particles from other stress conditions: heat, protein precipitation by sulfuric acid, air/liquid interface compression/dilation cycles and pumping with a stainless steel or ceramic piston pump. IgG1 and rhGH were used as sample proteins at different concentrations without the protection of a surfactant. FTIR spectra have been normalized to minimum and maximum absorbance between a wavenumber of 1800 cm^{-1} and 1400 cm^{-1}.

Fig. 10a compares the respective FTIR spectra of the antibody in the native conformation and after exposure to heat, concentrated sulfuric acid and air/liquid interface compression/dilation cycles. Fig. 10b compares interfacial stress at ceramic surfaces (test system with SiC spheres, SiC sliding bearing and ceramic piston pump) and air/liquid interfaces (compression/dilation cycles). Clear differences can be observed in the shape of the amide I (1700–1600 cm^{-1}) and amide II bands (1600–1500 cm^{-1}) and in the ratio of the intensity of the amide I and amide II band of the spectra in Fig. 10a. IgG1 spectra from Fig. 10b differ slightly in the intensity of amide I and II bands.

The FTIR spectra of the native, heat treated, sulfuric acid precipitated and air/liquid interfacial stressed rhGH samples are shown in Fig. 11a. The heat stressed sample showed an additional peak at 1617 cm^{-1}. A shoulder of the amide I peak formed in the spectra of samples that were treated with sulfuric acid and air/liquid interfacial compression/dilation cycles. Differences in the amide II band can be described in form of a broadening of the peak. FTIR spectra of samples which have been exposed to stress at ceramic surfaces or at an air/liquid interface are compared in Fig. 11b. Between the FTIR spectra of samples which were abraded from different materials differences could be found in the intensity ration of amide I to II, however, the shape of the bands were very comparable (data not shown).

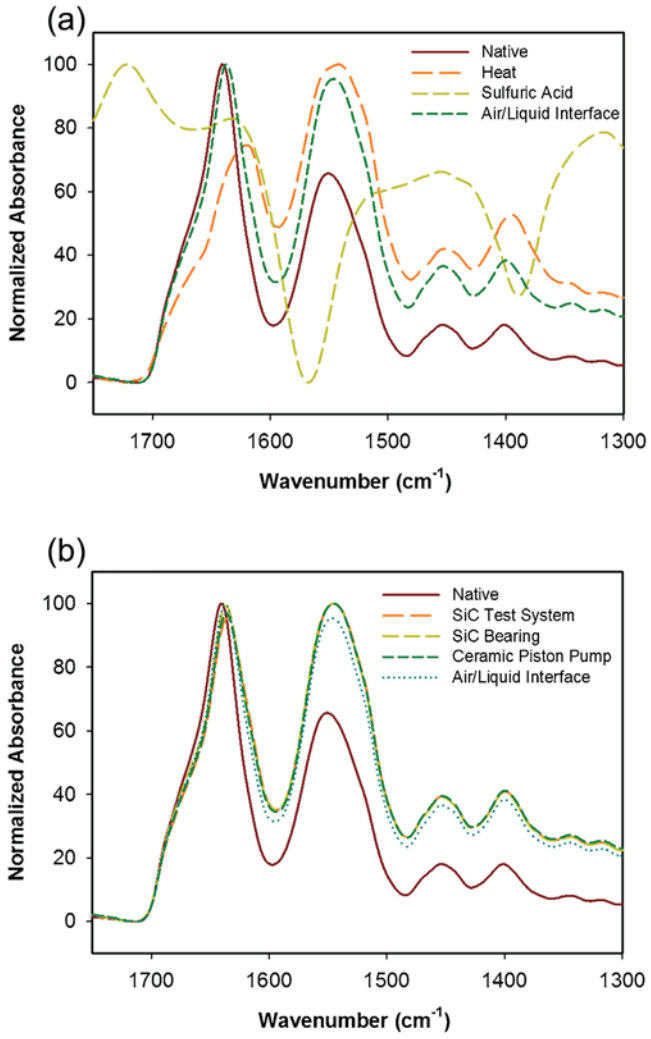

Fig. 10. Comparison of FTIR spectra of IgG1 samples which have been subjected to various stress conditions. Spectra have been normalized to maximum and minimum absorbance between a wavenumber of 1800–1400 cm^{-1}.

3.3.5. Adsorption of IgG1 and rhGH to stainless steel, SiC and glass micro powder

The ability of PS80 to reduce protein adsorption was tested using micro-powders of stainless steel, SiC and glass. It was confirmed by experimental measurements that after the applied incubation time of 2.5 min the adsorption of rhGH and IgG1 had reached equilibrium (data not shown). Table 1 shows the adsorbed amount in percent of the initial protein concentration of a 0.2 mg mL^{-1} sample solution with and without surfactant (0.7 mg mL^{-1} PS80) after 2.5 min. The standard deviation results from triplicate determinations (n = 3).

3.3.6. PS80 factor

The addition of PS80 reduced the monomer loss during rotational movement of the spheres in the test system and the adsorption to micro-powders, which was also determined in terms of monomer loss (solution depletion). For better comparison with each other, a PS80 factor was calculated by dividing the monomer loss of the sample solution without surfactant by the monomer loss of the surfactant-containing sample solution. Three independent experiments with different rotational parameters have been performed for the test system per protein and material. The PS80 factor was individually calculated for each

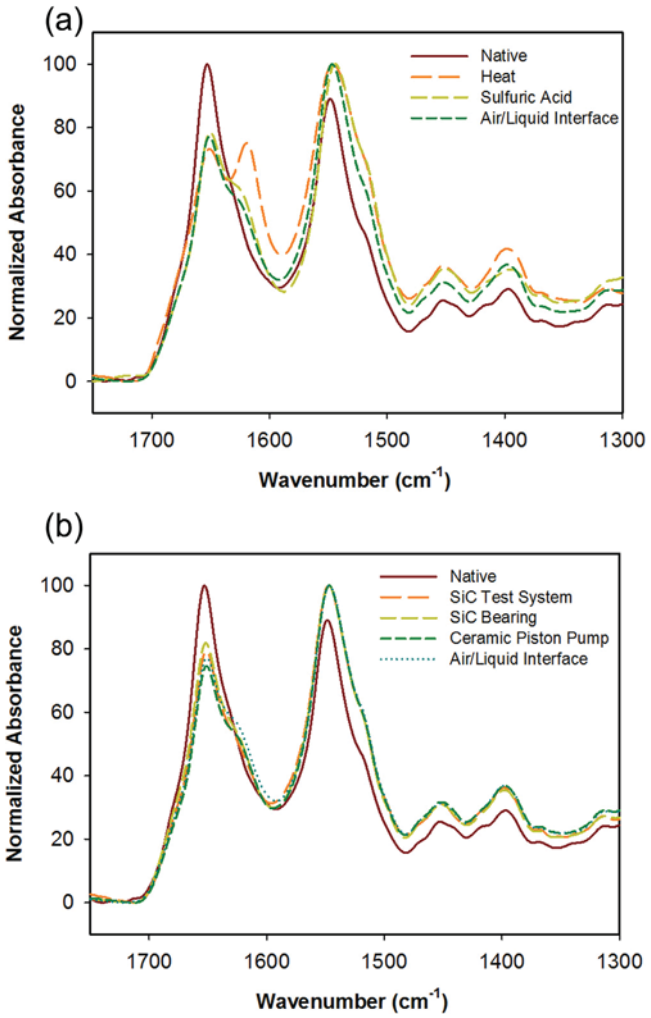

Fig. 11. Comparison of FTIR spectra of rhGH samples which have been subjected to various stress conditions. Spectra have been normalized to maximum and minimum absorbance between a wavenumber of 1800–1400 cm^{-1}.

Table 1
Amount of adsorbed protein to a micro-powder of steel, SiC or glass given in percent of a 0.2 mg mL^{-1} sample solution.

Material	Adsorbed Amount (% of initial protein concentration)			
	IgG1	IgG1 + PS80	rhGH	rhGH + PS80
Stainless Steel	48.6 ± 1.4	7.0 ± 0.2	47.3 ± 5.3	10.6 ± 0.3
SiC	55.4 ± 2.3	36.3 ± 0.9	29.2 ± 1.5	16.4 ± 0.2
Glass	75.9 ± 1.7	66.4 ± 0.9	12.9 ± 1.7	1.6 ± 0.2

experiment and is given here as average of the three independent experiments.

4. Discussion

4.1. Identification of the degradation mechanism inside the sliding bearing

4.1.1. Heat induced IgG1 degradation

Searching for the root cause of aggregate and protein particle formation during mixing in a compounding vessel with bottom mounted stirrers, heat-induced denaturation was one of the assumptions. However, the results of infrared temperature measurements during operation of the SiC bearing even at high rotational speed of 750 rpm did not support this hypothesis (Section 3.1.1., Fig. 4). From the measured temperature of only 21 °C at the bearing surface, it can be concluded that the heat transfer within the sample solution is sufficiently efficient to prevent a detrimental temperature increase. Thus, heat denaturation of the protein can be excluded.

4.1.2. Heterogeneous nucleation of IgG1 particles on SiC micro/nano particles

Heterogeneous nucleation of IgG1 particles, which are created by material abrasion of the sliding bearing, was the next degradation mechanism to be investigated. The presence of abraded SiC particles (< 4 μm in size) did not cause a decrease in monomer content or an increase in higher molecular weight variants of an unstirred IgG1 sample over an incubation time of 23.5 h (Section 3.1.2). Thus, even if there is a chance that SiC particles could induce protein aggregation or particle formation over long time storage, they can be excluded as the root cause for protein degradation in the time frame of mixing operations.

4.1.3. Shear or cavitation induced IgG1 degradation

In former studies, shear or shear in combination with cavitation was reported to be the prevailing degradation mechanism (Gikanga et al., 2015; Ishikawa et al., 2010). Hydrodynamic forces inside the bearing are caused by velocity gradients of the sample solution which are affected by the gap width and the rotational speed. As the sliding bearing is slightly oscillating, the gap width varies and reaches very small values. Thus, extraordinary high shear rates and turbulences could occur which could overcome the intramolecular stabilizing forces that shape the secondary and tertiary structure of the protein. Denaturation effects which are caused by these hydrodynamic forces in free liquid, however, are per definition independent from the surface and material properties of the bearing and can be recognized by this fact.

For this reason, stirring studies using two different materials of the sliding bearing (SiC and PTFE) and two different formulations (with and without surfactant) were performed (Fig. 5). With both materials pronounced protein degradation occurred when the bearings were operated in the absence of a surfactant. Addition of a surfactant (PS80) completely inhibited protein degradation by the PTFE bearing. However, in combination with a SiC sliding bearing the protein degradation was only slightly reduced. As the surfactant was not able to decrease protein degradation inside the SiC bearing to the same extent as inside the PTFE bearing, the stabilizing effect is unlikely to act on IgG1 in free solution but must somehow be related to the material.

Surprisingly, the protein degradation rate declined above a rotational speed of 750 rpm for the SiC bearing (see Fig. 7), though hydrodynamic forces and thereby shear stress obviously increase at higher rotational speed. In consideration of these observations, shear in terms of hydrodynamic forces in free solution can be excluded as prevailing degradation mechanism.

The same reasoning does also apply to cavitation. The formation of bubbles during cavitation is dependent on hydrodynamic flow effects which cause the pressure to fall below the vapor pressure (Brennen, 2013). A protection from cavities by the surfactant could be given by a competitive displacement at the gas/liquid interface of the cavities. Again, this protective mechanism should be independent of the material of the slide bearing. As a material dependence was observed, also cavitation can be excluded as possible degradation mechanism inside the sliding bearing.

4.1.4. IgG1 degradation by abrasion of adsorbed proteins

As discussed above, protein degradation by rotational movement of the sliding bearing was dependent on the material and therefore most likely on the surface properties. Thus, abrasion of

adsorbed proteins, a degradation mechanism that depends on the interaction of the proteins with the surface (Sediq et al., 2016), should be considered here. By reducing protein adsorption to a bearings surface, less molecules are abraded at each touching event and thereby the protein degradation rate is reduced. Protein adsorption can be influenced by the material of the surface and the addition of a surfactant, which acts by preferential adsorption and steric displacement (Kerwin, 2008). Unfortunately, the degradation rates of the PTFE and SiC sliding bearing cannot be compared to each other due to differences in gap width and oscillation behavior. However, conclusions can again be drawn from the effect of a surfactant (Fig. 5).

The better protection by the surfactant against protein degradation inside the PTFE than inside the SiC bearing (Fig. 5) can be explained by its strong interaction with the PTFE surface. As determined in contact angle measurements with water, the hydrophobicity of PTFE was considerably higher compared to SiC, glass or stainless steel surfaces. When PTFE is submerged in a solution containing PS80, the surfactant adsorbs to the hydrophobic surface with its hydrophobic tail. A film of oriented surfactant molecules at the PTFE surface results in a hydrophilic layer which is presented towards the liquid and prevents protein adsorption by strong preferential adsorption and steric displacement (Kerwin, 2008; Mollmann et al., 2005). As the interaction between the more hydrophilic SiC and PS80 is weaker, protein adsorption is very likely to be reduced to a smaller extent, which eventually leads to higher protein degradation. Thus, it can be argued, that degradation was directly influenced by the extent of protein adsorption on the surface of the bearing.

Furthermore, a like to like exchange of parts in the experimental set-up or a reassembly caused differences in the protein degradation rate. This can be explained by slight variations in the orientation of the stator to the rotor of the sliding bearing, which determines the grinding pressure. The magnitude of the pressure has been described to directly influence particle formation during contact sliding (Sediq et al., 2016).

Summarizing, the dependence of protein degradation on surface related effects strongly support abrasion of adsorbed proteins as degradation mechanism inside a sliding bearing.

4.2. Characterization of IgG1 degradation inside the SiC sliding bearing

As all protein degradation mechanisms besides abrasion of adsorbed proteins could be excluded, the results of the characterization of the sliding bearing in matters of IgG1 degradation should be discussed in relation to abrasion of adsorbed proteins.

Over the time of rotation, the bulk concentration of IgG1 is constantly decreasing due to the formation of particles (Fig. 6a). The dependence of protein degradation on the time of rotation showed a flattening of the curve over time. This can be explained by following mechanism: a lower bulk concentration results in slower protein adsorption and/or lower protein density at the surface which decreases the amount of abraded molecules per touching event, as the kinetics of unspecific protein adsorption to solid surfaces are known to be dependent on the protein bulk concentration (Rabe et al., 2011). On the other hand, experiments with increased initial IgG1 concentrations resulted in higher absolute IgG1 monomer loss, thereby confirming this explanation (see Fig. 6b). However, this effect is limited to a concentration, where surface saturation by protein adsorption is reached, which can be recognized by the flattening of the curve of absolute monomer loss. As degradation by abrasion of adsorbed proteins is dependent on the protein concentration and the rate is limited by surface saturation, the degradation can be analyzed similar to an enzymatic reaction rate and described by a Michaelis-Menten-type kinetics. Thereby, the maximal velocity (v_{max}) can be observed at a protein concentration where abrasion of saturated surfaces occurs. The affinity of adsorption between sliding bearing and protein is described by the factor K_M. Thus, the experimental data was fitted to Michaelis-Menten-type kinetics using the following function, which is of logistic form:

$$[S](t) = K_M + \ln\left(1 + \left(e^{\frac{[S_0]}{K_M}} - 1\right)e^{-\frac{v_{max}\cdot t}{K_M}}\right) \quad (1)$$

where $[S_0]$ is the initial protein concentration and [S](t) is the protein concentration at time point t. Note that the above function is not the exact solution of the Michaelis-Menten equation. The latter uses the W-Lambert function which can only be implicitly defined and as such fitting the exact solution to the data is not straight-forward. The above function provides a sufficiently accurate substitute for the exact solution and can be fitted to the data with standard methodology (Putz et al., 2006). Finally, a maximum IgG1 degradation rate (v_{max}) of 564 $\mu g\,h^{-1}$ was obtained from the fit. This maximum degradation rate is valid for the used SiC small scale bearing at a rotational speed of 500 rpm.

More difficult to discuss is the dependence of IgG1 degradation on the rotational speed of the sliding bearing (Fig. 7). The doubling in monomer loss from 25 to 50 rpms can be easily explained. By doubling the rotational speed the touching events per time double and thereby also the extent of protein degradation. However, the direct relationship between touching events and protein degradation is not valid any more at rotational speeds higher than 50 rpm. We suggest two possible explanations for the limitation in protein degradation at high rotational speeds. The first possible explanation is that protein degradation could be limited by diffusion of native monomer molecules. In the gap of the sliding bearing IgG1 monomers are constantly removed from the liquid by adsorption to the bearing and the formation of aggregates or particles upon abrasion. A concentration gradient develops that decreases the nonspecific adsorption to the ceramic surface (Kim and Yoon, 2002). The second possible explanation is a limitation in the kinetics of protein adsorption. Unspecific protein adsorption to solid surfaces can take several minutes until saturation (Rabe et al., 2011). The smaller the time period within two consecutive touching events at the same surface area becomes, the less proteins have adsorbed to the surface so the abrasion affects fewer molecules in total. As the rotational movement created a liquid flow inside the sample solution, the second explanation has to be favored.

As can be seen from Fig. 7, protein degradation inside the SiC sliding bearing of the IgG1 solution without surfactant peaked at a rotational speed of about 750 rpm and decreased significantly at higher speed. In contrast to the above discussed flattening of the curve, this behavior cannot be explained by adsorption kinetics. However, the mechanism of protein degradation by abrasion of adsorbed proteins also depends on an interface-induced structural perturbation of the protein on adsorption (Sediq et al., 2016). A native monomer can undergo conformational changes upon adsorption, which are described as relatively slow processes. Furthermore, perturbed proteins can aggregate on the surface (Rabe et al., 2011). Subsequent abrasion of such structurally perturbed or aggregated proteins finally leads to the observed particle formation, which is not the case for native molecules. Assuming that the time scale of conformational re-organization of the proteins is similar to the time frame between two consecutive abrasion events, an increase in rotational speed will result in abrasion of more native molecules. As a consequence, protein degradation is decreased as a lower percentage of abraded proteins is unfolded and able to form particles. Based on the limited information from the data, no clear statement or explanation can

be given to this observed effect. The explanation above should be seen as a suggestion for further research.

Summarizing, severe protein degradation happened by rotational movement of the simulated sliding bearing which was most likely caused by abrasion of adsorbed protein. The addition of PS80 was able to slightly reduce monomer loss. The ratio of sample volume to theoretical friction area of the sliding bearing (14.3 cm^3/cm^2) intentionally was kept very low in order to facilitate the determination of degradation. In a typical compounding vessel from production the relative amount of protein degradation will be decreased. Assuming a capacity of 100 L and a friction area of 66 cm^2 for a typical compounding vessel gives a ratio of 2020.5 cm^3/cm^2. Nevertheless, thorough knowledge of protein degradation inside a bearing is important for the correct selection of process parameters and batch sizes as well as for the future design of compounding vessels.

4.3. Evaluation of the test system for protein degradation by abrasion of adsorbed proteins

As protein degradation by abrasion was highly dependent on the material of the surfaces that are in contact and the excipients of the buffer, it was desirable to develop an experimental set up by means of which proteins in various formulations can be easily screened for friction-mediated interactions with a wider scope of different materials. A very simple but very revealing approach is to put spheres of a specific material and diameter into a rotating container under the exclusion of air. As containers glass vials were chosen which were closed using a cover glass as seen in Fig. 3. This experimental set up has already been described (Denkinger, 2010), however, the author did not connect the protein degradation to a specific mechanism other than “sensitivity against surfaces”.

4.3.1. IgG1 sample solution—monomer loss due to particle formation

Protein degradation of IgG1 samples was noticed by particle formation and monomer loss in SE-HPLC, which did not show an increase in HMW variants. When stressing the samples for a fixed number of rotations, the monomer loss was higher when the experiment was performed at low rotational speed compared to high rotational speed for all tested materials. A less pronounced protein degradation in an environment with faster moving spheres again puts the mechanism of shear induced protein degradation in free solution into doubt. Furthermore, this behavior resembles protein degradation inside the SiC sliding bearing, where the amount of protein degradation per rotation declined above a rotational speed of 50 rpm. An additional incubation of the fast rotated samples was performed in a static position to obtain an equal experimental time as in the experiment at slow rotation. The idea behind this set-up was to reveal a time dependent protein degradation mechanism, which is independent of abrasion of adsorbed proteins but nevertheless related to friction. Touching of spheres lead to abrasion of the material itself in form of micro- and nanoparticles (single particle optical sizing, data not shown), which can induce protein aggregation (Bee et al., 2009a). However, as no additional protein degradation could be observed during incubation, a time related protein degradation mechanism could be excluded.

Protein degradation was significantly more pronounced for stainless steel spheres compared to SiC, glass and PTFE spheres, which had very comparable degradation rates. This behavior does not correlate with the hydrophobicity of the surfaces and may be influenced by other factors such as surface roughness. Therefore, the absolute protein degradation should not be compared between different materials but between different formulations in combination with the same material. Assuming abrasion of adsorbed proteins as prevailing degradation mechanism in the test system, the degradation rate should be related to the extent of protein adsorption to the spheres. For this reason, PS80 was added to the samples to reduce protein adsorption. As the amount of adsorbed protein could not directly be determined experimentally using the spheres, a system with a large surface area was used that facilitated adsorption analysis by solution depletion: micro-powders. Again, as the exact surface area of the micro-powders was not known, only a relative comparison of protein adsorption between a surfactant-containing and surfactant-free sample for the same material can be done. The reduction in adsorption by the addition of PS80 correlated to the reduction in protein degradation in the test system for the materials SiC and glass and is given as PS80 factor in both cases (see Table 2). The slightly higher protective effect in the test system can be explained by the presence of small air bubbles, which can't be totally avoided and which could be responsible for additional protein degradation by air/liquid interfacial effects in the absence of a surfactant. The combination of a surfactant-containing IgG1 solution with PTFE spheres gave almost no monomer loss, which confirmed findings of the experiment with the PTFE sliding bearing.

In contrast to the other materials, the addition of PS80 had no effect on protein degradation by stainless steel spheres, although protein adsorption was significantly lowered. Therefore, further investigations of the stainless steel samples were performed and it could be shown that Fe^{3+} ions were introduced into the sample solution by contact sliding of the spheres, which caused considerable monomer loss. Degradation of IgG1 in the presence of Fe^{3+} was reproduced in spiking experiments. Thereby, the presence of PS80 was amplifying protein degradation. It is known that Fe^{3+} ions can induce autooxidation of PS80 which leads to the formation of peroxy radicals in solution at room temperature (Harmon et al., 2006). Oxidation of IgG1 by Fe^{3+} ions could have caused subsequent aggregation and particle formation (Mirzaei and Regnier, 2008) which eventually masked the effect of protein degradation by abrasion of adsorbed proteins in the test system with stainless steel spheres.

Finally, it has to be mentioned that a small percentage of the protein degradation resulted from contact sliding between the spheres and the glass vial. However, based on the results of the glass and PTFE spheres in combination with and without surfactant, the impact is very small. The addition of a surfactant could almost totally prevent monomer loss in combination with PTFE spheres, whereas there was still significant monomer loss in combination with glass spheres. If a high percentage of monomer loss would be caused by abrasion of adsorbed protein from the glass vial, PTFE spheres in combination with surfactant would also show more pronounced monomer loss.

4.3.2. rhGH sample solution—monomer loss due to particle formation and aggregation

Compared to the IgG1 antibody, rhGH is with 22 kDa a relatively small and globular protein. The secondary structure of IgG1 consists mainly of β-sheets, whereas rhGH is a mainly alpha helical

Table 2
For better comparison of the protective effect of PS80, a “PS80 factor” was calculated by dividing the monomer loss of the sample solution without surfactant by the monomer loss of the surfactant-containing sample solution. The PS80 factor is a dimensionless number.

Material	IgG1–PS80 Factor		rhGH–PS80 Factor	
	Test System	Adsorption	Test System	Adsorption
Stainless Steel	1.0	7.0	3.1	4.5
SiC	1.8	1.5	1.8	1.8
Glass	1.4	1.1	no monomer loss	8.0
PTFE	45.8	n.d.	9.3	n.d.

protein, which might show a different response to mechanical stress. Furthermore, formulated at a pH of 7.0, rhGH has a negative net charge, whereas IgG1 has a positive net charge at pH 6.5. Therefore, the experiment with rotating spheres in vials was repeated using rhGH to investigate the behavior of a smaller protein with a different conformation and net charge. Again, the effect of non-protein particles (abraded sphere material) was tested by analyzing the samples of the experiment at 25 rpm directly after 8 h of rotation and after an additional 32 h of incubation in a static position.

In general, rhGH showed higher stability against friction-related physical protein degradation compared to IgG1. Therefore, a higher number of total rotations were applied to rhGH in the test system to facilitate the analysis. The adsorption of rhGH to SiC and glass micro-powder was significantly lower compared to IgG1. Thus, the lower amount of adsorbed protein could explain the overall decreased protein degradation by abrasion in the test system. Especially, protein degradation by glass spheres was almost negligible even in the absence of a surfactant. As observed for IgG1 samples, the addition of PS80 could reduce protein adsorption to micro-powder and protein degradation in the test system to the same extent.

The adsorption to stainless steel micro-powder was almost identical for rhGH and IgG1. However, protein degradation in the test system cannot be compared, as additional degradation by Fe^{3+} ions masked the effect of abrasion of adsorbed IgG1. The effect of Fe^{3+} ions on rhGH samples was tested but was negligible.

Different to IgG1, rhGH showed an increase in HMW variants in rotated stainless steel samples. Additional static incubation of the rotated stainless steel sample without surfactant allowed even further aggregation of rhGH. This indicates the presence of another degradation mechanism which is time dependent. As Fe^{3+} ions had almost no effect, it is very likely that the aggregation was induced by nano/micro-particles of stainless steel, which could act as aggregation seeds.

Summing up, the good correlation between IgG1/rhGH adsorption and monomer loss during contact sliding strongly supports the hypothesis of abrasion of adsorbed molecules as prevailing protein degradation mechanism.

4.3.3. Characterization of IgG1 and rhGH particles by FTIR spectroscopy

Abrasion of adsorbed proteins was assumed as underlying mechanism of protein degradation inside of sliding bearings and the test system. The test system was able to reproduce the results of the bearings regarding the protective effect of the addition of a surfactant on monomer loss. Nevertheless, another experiment was performed in order to confirm an identical degradation pathway in both systems. Thus, degradation products of various stresses were compared by their ATR-FTIR spectra. Besides the shape of the amide I and amide II bands that is defined by the secondary structure composition of the protein (particles), differences in the ratio of the intensity of the amide I and amide II band are attributable to secondary and tertiary structure alterations (Ishida and Griffiths, 1993; Kong and Yu, 2007). An identical degradation pathway should result in degradation products with similar secondary and tertiary structure, whereas a different pathway could lead to different unfolding products (Kishore et al., 2012).

Initially, a comparison of degradation products of IgG1 was performed that were induced by distinctive stresses such as heat, sulfuric acid precipitation and interfacial stress. Clear differences in shape and intensity ratios of amide I and amide II (Fig. 10a) could be observed. Therefore, it was first assumed that the respective degradation products can be distinguished from each other. In another analytical comparison FTIR spectra of friction-related degradation products from ceramic surfaces proofed to be highly similar to each other and to the spectrum of a product that was created by air/liquid interfacial stress. In general, all degradation products from stress conditions which are associated with interfacial effects showed comparable FTIR spectra with only minor differences in amide I to amide II intensity ratios (data not shown). Even though there is the possibility that analysis by FTIR is not sensitive enough to pick up all dissimilarities of the degradation products, an essential difference in the physical protein degradation mechanism inside the test system and the sliding bearing can be excluded.

Also rhGH showed distinctive differences in the FTIR spectra of the native, heat treated, sulfuric acid precipitated and air/liquid interfacial stressed samples (see Fig. 11a). As for IgG1, degradation products of samples which have been exposed to stress at ceramic surfaces were very similar to each other and to the air/liquid interface sample (see Fig. 11b).

Summarizing, the high similarity in the FTIR-spectra of the degradation products supports the assumption of a similar degradation mechanism during rotational movement of the sliding bearing and in the test system. Furthermore, also the degradation products that were created by pumping with a piston pump (stainless steel and ceramic) showed similar spectra to these. As there is contact sliding happening inside a piston pump, it is very likely that also protein degradation inside a piston pump can be described by the mechanism of abrasion of adsorbed proteins.

5. Conclusion

Significant physical protein degradation could be shown for an IgG1 antibody within a SiC sliding bearing which can be found in compounding vessels with a magnetic bottom stirrer. Protein degradation was observed in form of monomer loss and particle formation. The extent of protein degradation was highly dependent on the material of the sliding bearing, the rotational speed and time as well as the buffer of the protein and its concentration. Based on our results, we could exclude heat, cavitation, heterogeneous nucleation on extrinsic particles and shear stress in free solution within the gap as the root cause of protein degradation inside the bearing. Our data show that the favored root cause of protein degradation and particle formation is abrasion of adsorbed protein at the surface of the sliding bearing and thereby strongly support the degradation mechanism recently published by Sediq et al. As protein degradation inside the sliding bearing was limited by adsorption and dependent on protein concentration, it could be described by a Michaelis-Menten-type kinetics.

Moreover, we established a test system that easily allowed to test for protein degradation by abrasion under various combinations of buffers with surface materials. An additional advantage of the test system is the ability to study the effect of foreign nano/micro particles (abraded sphere material) and any other friction-related effect on protein stability. For evaluation of the test system rhGH was included which is smaller, mainly alpha helical and had an opposite net charge to IgG1. Combination of a highly hydrophobic material (PTFE) with a surfactant containing protein solution was able to minimize IgG1 and rhGH degradation probably by strong preferential adsorption and steric displacement. This effect was significantly less pronounced for more hydrophilic materials such as glass and SiC. A characterization by ATR-FTIR of IgG1 and rhGH particles, which were created in the test system and inside the sliding bearing, showed a high similarity of the respective spectra. This supports the assumption of similar degradation mechanisms. Furthermore, a comparison of the FTIR spectra against samples which have been subjected to diverse stress conditions resulted in a high similarity of all spectra from interfacial stressed samples. Therefore, we conclude that abrasion

of adsorbed protein is a major root cause of physical protein degradation in form of particle formation during biopharmaceutical manufacturing steps such as compounding and pumping. Furthermore, unexpected side effects of contact sliding, such as the introduction of Fe^{3+} ions or steel particles into the sample solution, can significantly affect protein stability.

Funding

This work was funded by Sandoz GmbH's internal research funds.

Acknowledgement

The authors are grateful to the Biophysical Characterization group in Oberhaching (Sandoz) for providing measurement time and assistance at the FTIR spectrometer.

References

Ashton, L., Dusting, J., Imomoh, E., Balabani, S., Blanch, E.W., 2009. Shear-induced unfolding of lysozyme monitored in situ. Biophys. J. 96, 4231–4236.
Bee, J.S., Chiu, D., Sawicki, S., Stevenson, J.L., Chatterjee, K., Freund, E., Carpenter, J.F., Randolph, T.W., 2009a. Monoclonal antibody interactions with micro- and nanoparticles: adsorption, aggregation, and accelerated stress studies. J. Pharm. Sci. 98, 3218–3238.
Bee, J.S., Stevenson, J.L., Mehta, B., Svitel, J., Pollastrini, J., Platz, R., Freund, E., Carpenter, J.F., Randolph, T.W., 2009b. Response of a concentrated monoclonal antibody formulation to high shear. Biotechnol. Bioeng. 103, 936–943.
Bee, J.S., Schwartz, D.K., Trabelsi, S., Freund, E., Stevenson, J.L., Carpenter, J.F., Randolph, T.W., 2012. Production of particles of therapeutic proteins at the air–water interface during compression/dilation cycles. Soft Matter 8, 10329–10335.
Bekard, I.B., Asimakis, P., Bertolini, J., Dunstan, D.E., 2011. The effects of shear flow on protein structure and function. Biopolymers 95, 733–745.
Bekard, I.B., Asimakis, P., Teoh, C.L., Ryan, T., Howlett, G.J., Bertolini, J., Dunstan, D.E., 2012. Bovine serum albumin unfolds in Couette flow. Soft Matter 8, 385–389.
Brückl, L., Schröder, T., Scheler, S., Hahn, R., Sonderegger, C., 2016. The effect of shear on the structural conformation of rhGH and IgG1 in free solution. J. Pharm. Sci. 105, 1810–1818.
Brennen, C.E., 2013. Cavitation and Bubble Dynamics. Cambridge University Press.
Chang, B.S., Yeung, B., 2010. Physical Stability of Protein Pharmaceuticals. John Wiley & Sons, Inc., Hoboken, NJ, USA.
Chisti, Y., 1992. Assure bioreactor sterility. Chem. Eng. Progr. 88 80–80.
Denkinger, S.N., 2010. Modelle zur Simulation des Abfüllprozesses biologisch-pharmazeutischer Arzneimittel (Doctoral dissertation). Title, Universitäts-und Landesbibliothek, Bonn.
Gikanga, B., Chen, Y., Stauch, O.B., Maa, Y.-F., 2015. Mixing monoclonal antibody formulations using bottom-mounted mixers: impact of mechanism and design on drug product quality. PDA J. Pharm. Sci. Technol. 69, 284–296.
Harmon, P.A., Kosuda, K., Nelson, E., Mowery, M., Reed, R.A., 2006. A novel peroxy radical based oxidative stressing system for ranking the oxidizability of drug substances. J. Pharm. Sci. 95, 2014–2028.
Ishida, K.P., Griffiths, P.R., 1993. Comparison of the amide I/II intensity ratio of solution and solid-state proteins sampled by transmission, attenuated total reflectance, and diffuse reflectance spectrometry. Appl. Spectrosc. 47, 584–589.
Ishikawa, T., Kobayashi, N., Osawa, C., Sawa, E., Wakamatsu, K., 2010. Prevention of stirring-induced microparticle formation in monoclonal antibody solutions. Biol. Pharm. Bull. 33, 1043–1046.
Jaspe, J., Hagen, S.J., 2006. Do protein molecules unfold in a simple shear flow? Biophys. J. 91, 3415–3424.
Kerwin, B.A., 2008. Polysorbates 20 and 80 used in the formulation of protein biotherapeutics: structure and degradation pathways. J. Pharm. Sci. 97, 2924–2935.
Kim, J.-H., Yoon, J.-Y., 2002. Protein Adsorption on Polymer Particles. Marcel Dekker, Inc., New York (p. 4373).
Kishore, D., Kundu, S., Kayastha, A.M., 2012. Thermal, chemical and pH induced denaturation of a multimeric β-galactosidase reveals multiple unfolding pathways. PLoS One 7, e50380.
Kong, J., Yu, S., 2007. Fourier transform infrared spectroscopic analysis of protein secondary structures. Acta Biochim. Biophys. Sin. 39, 549–559.
Mahler, H.C., Friess, W., Grauschopf, U., Kiese, S., 2009. Protein aggregation: pathways, induction factors and analysis. J. Pharm. Sci. 98, 2909–2934.
Mirzaei, H., Regnier, F., 2008. Protein: protein aggregation induced by protein oxidation. J. Chromatogr. B 873, 8–14.
Mollmann, S., Elofsson, U., Bukrinsky, J., Frokjaer, S., 2005. Displacement of adsorbed insulin by Tween 80 monitored using total internal reflection fluorescence and ellipsometry. Pharm. Res. 22, 1931–1941.
Perevozchikova, T., Nanda, H., Nesta, D.P., Roberts, C.J., 2015. Protein adsorption, desorption, and aggregation mediated by solid-liquid interfaces. J. Pharm. Sci. 104, 1946–1959.
Putz, M.V., Lacrama, A.-M., Ostafe, V., 2006. Full analytic progress curves of enzymic reactions in vitro. Int. J. Mol. Sci. 7, 469–484.
Rabe, M., Verdes, D., Seeger, S., 2011. Understanding protein adsorption phenomena at solid surfaces. Adv. Colloid Interface Sci. 162, 87–106.
Rajniak, P., Tsinontides, S., Pham, D., Hunke, W., Reynolds, S., Chern, R., 2008. Sterilizing filtration—principles and practice for successful scale-up to manufacturing. J. Membr. Sci. 325, 223–237.
Rathore, N., Rajan, R.S., 2008. Current perspectives on stability of protein drug products during formulation, fill and finish operations. Biotechnol. Progr. 24, 504–514.
Sediq, A.S., van Duijvenvoorde, R., Jiskoot, W., Nejadnik, M.R., 2016. No touching! Abrasion of adsorbed protein is the root cause of subvisible particle formation during stirring. J. Pharm. Sci. 105 (2), 519–529.
Somiya, S., 2013. Handbook of Advanced Ceramics: Materials, Applications, Processing, and Properties. Academic Press.
Stalder, A., Kulik, G., Sage, D., Barbieri, L., Hoffmann, P., 2006. A snake-based approach to accurate determination of both contact points and contact angles. Colloids Surf. A: Physicochem. Eng. Asp. 286, 92–103.
Thomas, C., Geer, D., 2011. Effects of shear on proteins in solution. Biotechnol. Lett. 33, 443–456.
Tirrell, M., Middleman, S., 1975. Shear modification of enzyme kinetics. Biotechnol. Bioeng. 17, 299–303.
Tyagi, A.K., Randolph, T.W., Dong, A., Maloney, K.M., Hitscherich, C., Carpenter, J.F., 2009. IgG particle formation during filling pump operation: a case study of heterogeneous nucleation on stainless steel nanoparticles. J. Pharm. Sci. 98, 94–104.
Wang, W., Nema, S., Teagarden, D., 2010. Protein aggregation—pathways and influencing factors. Int. J. Pharm. 390, 89–99.